

UNCLASSIFIED

AD NUMBER

AD355505

CLASSIFICATION CHANGES

TO: unclassified

FROM: secret

LIMITATION CHANGES

TO:

Approved for public release, distribution unlimited

FROM:

Notice: Release only to Department of Defense Agencies is authorized. Other certified requesters shall obtain release approval from Director, Defense Atomic Support Agency, Wash.25, D. C. Release or announcement to foreign governments or their nationals is not authorized.

AUTHORITY

DSWA ltr., 27 Aug 1998; Same

THIS PAGE IS UNCLASSIFIED

SECRET
FORMERLY RESTRICTED DATA

AD 3 5 5 5 0 5 L

*Reproduced
by the*

DEFENSE DOCUMENTATION CENTER

FOR

SCIENTIFIC AND TECHNICAL INFORMATION

CAMERON STATION, ALEXANDRIA, VIRGINIA



FORMERLY RESTRICTED DATA
SECRET

NOTICE: When government or other drawings, specifications or other data are used for any purpose other than in connection with a definitely related government procurement operation, the U. S. Government thereby incurs no responsibility, nor any obligation whatsoever; and the fact that the Government may have formulated, furnished, or in any way supplied the said drawings, specifications, or other data is not to be regarded by implication or otherwise as in any manner licensing the holder or any other person or corporation, or conveying any rights or permission to manufacture, use or sell any patented invention that may in any way be related thereto.

NOTICE:

THIS DOCUMENT CONTAINS INFORMATION
AFFECTING THE NATIONAL DEFENSE OF
THE UNITED STATES WITHIN THE MEAN-
ING OF THE ESPIONAGE LAWS, TITLE 18,
U.S.C., SECTIONS 793 and 794. THE
TRANSMISSION OR THE REVELATION OF
ITS CONTENTS IN ANY MANNER TO AN
UNAUTHORIZED PERSON IS PROHIBITED
BY LAW.

SECRET

WT-1631

This document consists of 174 pages.

No. 16 of 235 copies, Serial A

3 5 5 5 0 5 L

HARDWARE

PROVIDE TO EXISTING EPG STRUCTURES (U)

NOV 1 1964
DEPT. OF DEFENSE
SUPPLY AGENT

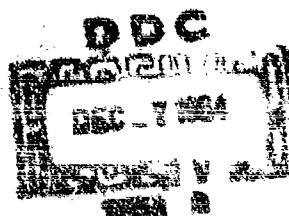
Release Date: October 27, 1964

HEADQUARTERS FIRST DIVISION
DEFENSE ATOMIC SUPPORT AGONY
SANDIA BASE, ALBUQUERQUE, NM 87160

RESTRICTED DATA

Approved for Release by NSA on 08-28-2013 pursuant to E.O. 13526

This report contains information affecting the defense of the United States within the meaning of the espionage laws, Title 18, U. S. C., Sec. 793 and 794, the transmission or revelation of which in any manner to an unauthorized person is prohibited by law.



05808

SECRET

SECRET

WT-1631

(2) *Ref. 1st*
OPERATION HARDTACK—PROJECT 37.

(6) DAMAGE *to* EXISTING EPG STRUCTURES (U) *(U)*

(1) *1st. 4-2-68*

W. J. Flathau W. J. Flathau, Project Officer
R. A. Cameron R. A. Cameron,

(3) ~~U.S.~~ Army Engineer Waterways
Experiment Station,
Vicksburg, Miss., ~~Mississippi~~

and

Holmes and Narver, Incorporated
Los Angeles, California

FORMERLY RESTRICTED DATA

Handle as Restricted Data in foreign dissemination. Section 144b, Atomic Energy Act of 1954.

This material contains information affecting the national defense of the United States within the meaning of the espionage laws, Title 18, U.S.C., Secs. 793 and 794, the transmission or revelation of which in any manner to an unauthorized person is prohibited by law.

EXCLUDED FROM AUTOMATIC
REGRADING; DOD DIR 5200.10
DOES NOT APPLY

SECRET

FOREWORD

This report presents the final results of one of the projects participating in the military-effects programs of Operation Hardtack. Overall information about this and the other military-effects projects can be obtained from ITR-1660, the "Summary Report of the Commander, Task Unit 3." This technical summary includes: (1) tables listing each detonation with its yield, type, environment, meteorological conditions, etc.; (2) maps showing shot locations; (3) discussion of results by programs; (4) summaries of objectives, procedures, results, etc., for all projects; and (5) a listing of project reports for the military-effects programs.

ABSTRACT

The purpose of this project was to document and evaluate the effects of blast forces, radiation, and water waves resulting from nuclear explosions on various support-type structures and previously exposed test structures located on the various islands of the Eniwetok Proving Ground. The major effort of the project, a joint Waterways Experiment Station and Holmes and Narver, Inc., effort, was concentrated on the early shots which were expected to yield the most significant information for this project. To cover any supplementary information from the later shots, because the project was to be a minimum effort of funds and personnel, arrangements were made with Holmes and Narver, Inc., for the project to receive appropriate additional data from the later shots from the damage survey normally conducted by that organization in the field. This report contains the general effects data for the stations investigated from all the shots of concern to this project.

No electronic recording was utilized; however, self-recording measurements of air overpressure and acceleration were made at several stations, along with some measurements of erosion due to water waves. The damage surveys were performed by visual inspection, photographs, and level surveys.

The curve used for predicting air overpressure, the most important parameter in determining blast damage, proved to be reliable. Observed pressure data obtained during this operation correlated well with the prediction curve, which was based on data obtained from previous operations.

The curve used for predicting acceleration for floor slabs of structures appears to give reasonable values. However, limited data was obtained, and the over-all reliability of the prediction curve is uncertain.

It was found that the path-of-least-resistance method for predicting radiation within structures proved adequate. The slant-thickness method did not give realistic values.

No structural damage was observed which was attributable to thermal radiation. Steel was observed for exposures up to $1,400 \text{ cal/cm}^2$; concrete surfaces showed minor spalling at 650 cal/cm^2 .

Structural damage, due to water waves, may be neglected for close-in structures designed to withstand air blast. At greater distances, where air blast is of no great consequence, water waves must be considered in structural planning.

Damage to camps (light, wood-frame type construction) was investigated. The damage data compared with and amplified the data contained in TM 23-200 (Reference 8) pertaining to wood-frame structures. Damage to antennas and radar reflectors correlated well with data in the referenced manual also. The curve of Reference 8 for predicting damage to three-story, blast-resistant buildings is also adequate.

Reinforcing steel in roofs of blast-resistant structures should be designed to provide more uniformity of strength. Positive reinforcement should be continuous extending over supports; at least one-half of the negative steel should be carried beyond the point of inflection a sufficient distance to develop the allowable stress in such bars or a distance equal to the depth of the member, whichever distance is greater.

A ground-surface 21,000-gallon water tank of $\frac{1}{8}$ -inch bolted steel plate, 8 feet high and 22 feet in diameter, suffered only light damage when exposed to pressures of 6.5 and 7.0 psi.

Heavily reinforced-concrete, earth-mounded structures (walls and roofs 5 to 6 feet thick with spans up to 5 feet) survived air overpressures up to 1,000 psi.

Objects located close behind earth mounds within a distance approximately equal to the height

of the mound received considerable protection from dynamic pressures at overpressures of 35 psi and lower.

Exposed standard 2-inch and 4-inch water pipes, including standard rising-stem valves, survived pressures up to 8 psi without any sign of damage.

The method used for predicting pressures at a zero angle of incidence on the front and rear faces of diffraction-type targets is satisfactory for both design and analysis purposes. At angles of incidence greater than zero however, the method is satisfactory for design purposes only. The predicted shape of overpressure-time curves for the roof of diffraction-type targets was not in close agreement with measured results.

PREFACE

This project was a joint, coordinated effort between the U. S. Army Engineer Waterways Experiment Station (WES), Vicksburg, Mississippi, and Holmes and Narver, Inc. (H&N), Engineers and Constructors, Los Angeles, California. This joint venture was made possible by the efforts of personnel from both the Armed Forces Special Weapons Project (AFSWP), and the Atomic Energy Commission (AEC). For WES, the project was under the general direction of E. P. Fortson, Jr., F. R. Brown, and G. L. Arbuthnot, Jr., with W. J. Flathau designated as the project officer. For H&N, the project was under the general direction of R. R. Alvy and S. B. Smith, with R. A. Cameron designated as the assistant project officer. Special recognition is given to Capt. E. S. Townsley, of WES, who prepared the appendix on radiation. Also contributing to this project were Sp2 R. P. Andrew, Pfc. C. W. Denzel, and Pfc. D. G. Brown, of WES. The cooperation received from personnel of the Los Alamos Scientific Laboratory (LASL), the University of California Radiation Laboratory (UCRL), the Stanford Research Institute (SRI), and the Ballistic Research Laboratories (BRL) greatly assisted this project in meeting its objective.

CONTENTS

FOREWORD	4
ABSTRACT	5
PREFACE	7
CHAPTER 1 INTRODUCTION	19
1.1 Objective	19
1.2 Background	19
1.2.1 Previous Damage Surveys	19
1.2.2 Conclusions from Ivy Damage Survey (1952)	21
1.2.3 Conclusions from Castle Damage Survey (1954)	27
CHAPTER 2 PROCEDURE	28
2.1 Shot Participation	28
2.2 Instrumentation	28
2.3 Data Requirements	30
CHAPTER 3 RESULTS: BIKINI ATOLL	33
3.1 Site Able	33
3.1.1 Item 1, Station 1341, Castle	33
3.1.2 Item 2, Station 80.01, Redwing	33
3.1.3 Item 3, Stations 152.01 and 153.01, Redwing	38
3.1.4 Item 4, Station 1519, Redwing	44
3.2 Site Charlie	44
3.2.1 Item 5, Station 78.01, 1319 Redwing	44
3.2.2 Item 6, Station 1200, Castle	44
3.3 Sites Fox and George	44
3.3.1 Items 7, 8, and 9, Stations 2410.01, -.02, and -.03	48
3.3.2 Item 10, Stations 50.01, -.02, -.03, -.04, -.05, and -.06	48
3.3.3 Item 11, Station 1810, 1830 Redwing	54
3.4 Sites Sugar and Tare	54
3.4.1 Item 12, Stations 2200 and 2250	55
3.4.2 Item 13, Station 2210	57
3.4.3 Item 14, Station 2270	57
3.4.4 Item 15, Station 2230.01	64
3.4.5 Item 16, Station 2230.02	64
3.4.6 Item 17, Station 630.01	64
CHAPTER 4 RESULTS: ENIWETOK ATOLL	65
4.1 Sites Gene, Helen, and Irene	65
4.1.1 Item 18, Station Complex	65
4.1.2 Item 19, Station 1525	65
4.1.3 Item 20, Station 1311	75
4.1.4 Item 21, Stations 1211 and 1410	76

4.1.5 Item 22, Station 3.4, Castle-----	83
4.1.6 Item 23, Generators-----	83
4.1.7 Item 24, Helicopter Pad-----	86
4.2 Site Janet-----	86
4.2.1 Item 25, Station 1312-----	86
4.2.2 Item 26, Station 3.1.1, Greenhouse-----	88
4.2.3 Item 27, Station 3.1.3, Greenhouse-----	101
4.2.4 Item 28, Stations 20A, B, C, D, E and F, Greenhouse-----	101
4.2.5 Item 29, Station 77.02-----	110
4.2.6 Item 30, Landing Pier-----	110
4.2.7 Camp-----	110
4.3 Site Yvonne-----	114
4.3.1 Item 31, Station 1130-----	114
4.3.2 Item 32, Station 1220.01-----	119
4.3.3 Item 33, Station 1216-----	119
4.3.4 Item 34, Station 1612-----	119
4.3.5 Item 35, Stations 1523.01 to 1523.04-----	119
4.3.6 Item 36, Station 1310-----	119
4.3.7 Item 37, Water Tank-----	119
4.3.8 Yvonne Camp-----	128
CHAPTER 5 DISCUSSION-----	133
5.1 Prediction Curves-----	133
5.1.1 Air Overpressure-----	133
5.1.2 Floor-Slab Acceleration-----	133
5.2 Radiation and Water Waves-----	133
5.2.1 Nuclear Radiation-----	133
5.2.2 Thermal Radiation Damage-----	133
5.2.3 Water Waves-----	135
5.3 Damage-Distance Relationships-----	135
5.3.1 Camp and Wood-Frame Structures-----	135
5.3.2 Storage Tanks-----	135
5.3.3 Station 3.1.1 (Item 26, Three-story Blast-Resistant Buildings)-----	137
5.3.4 Station 1312 (Item 25, One-story, Reinforced-Concrete Building)-----	138
5.3.5 Gage Piers (Item 28)-----	138
5.3.6 Miscellaneous Damage-----	138
CHAPTER 6 CONCLUSIONS AND RECOMMENDATIONS-----	139
6.1 Conclusions-----	139
6.2 Recommendations-----	140
APPENDIX A NUCLEAR RADIATION-----	141
A.1 Introduction-----	141
A.2 Theory of Radiation-----	141
A.3 Structural Shielding-----	141
A.4 Prediction Methods-----	142
A.4.1 Slant Thickness-----	142
A.4.2 Path of Least Resistance-----	142
A.5 Results-----	142
A.5.1 Station 563.01 (Item 2)-----	142
A.5.2 Station 76.01-----	144
A.5.3 Station Complex-----	144

A.5.4 Station 3.4	144
A.6 Discussion and Conclusions	145
A.7 Recommendations	145
APPENDIX B DIFFRACTION LOADING OF STATION 1312	146
B.1 Prediction Methods	146
B.2 Results and Discussion	146
B.3 Conclusions	146
APPENDIX C RESPONSE OF GAGE PIERS TO BLAST LOADS	152
C.1 Structural Analysis Using Design Strengths	152
C.2 Behavior of Concrete Section Under Dynamic Loads	155
C.2.1 Flexural Behavior at Yield	155
C.2.2 Flexural Behavior at Ultimate	156
C.2.3 Moment-Curvature Relation	158
C.2.4 Shear-Compression Mode	158
C.3 Dynamic Analysis	158
C.3.1 Determination of Load on Piers	158
C.3.2 Natural Period of Vibration	158
C.3.3 Dynamic Analysis of Pier	158
C.4 Discussion and Conclusions	163
C.5 Notations	163
APPENDIX D WATER-WAVE DAMAGE	165
D.1 Introduction	165
D.2 Background	165
D.2.1 Operation Castle	165
D.2.2 Operation Redwing	165
D.3 Theory	165
D.4 Wave Damage in Operation Hardtack	167
D.5 Discussion	167
D.6 Conclusions and Recommendations	169
REFERENCES	170
FIGURES	
1.1 Shot geometry with pressure contours for Bikini Atoll, Operation Castle	20
1.2 Shot geometry with pressure contours for Eniwetok Atoll, Operation Castle	20
1.3 Shot geometry with pressure contours for Bikini Atoll, Operation Redwing	22
1.4 Shot geometry with pressure contours for Eniwetok Atoll, Operation Redwing	22
2.1 General plan and shot geometry for Bikini Atoll	29
2.2 General plan and shot geometry for Eniwetok Atoll	29
2.3 Peak air overpressure for surface bursts	31
2.4 Positive-phase duration for a 1-kt surface burst	31
2.5 Reduced vertical ground acceleration 10 feet below ground surface for a 1-kt surface burst	31
3.1 Shot geometry with pressure contours for Site Able	36
3.2 Extent of inundation on Site Able after Shot Sycamore	37

3.3 Post-Fir, -Sycamore, -Aspen, and -Cedar, (Item 1) Station 1341 on Site Able, no additional damage -	37
3.4 Post-Poplar, (Item 1) Station 1341 -	38
3.5 Plan and elevation including film badge locations for (Item 2) Station 560.01, Site Able -	39
3.6 Preshot, (Item 2) Station 560.01, Site Able -	40
3.7 Preshot, (Item 2) Station 560.01 including earth berm, Site Able -	40
3.8 Post-Fir, (Item 2) Station 560.01 -	41
3.9 Post-Fir, (Item 2) Station 560.01 including earth berm -	41
3.10 Ground-surface profile between (Item 2) Station 560.01 and (Item 4) Station 1519 -	42
3.11 Post-Poplar, (Item 2) Station 560.01, complete destruction of station -	43
3.12 Post-Fir, (Item 3) Stations 152.01 and 153.01 -	43
3.13 Post-Poplar, (Item 3) Stations 152.01 and 153.01 -	43
3.14 Post-Fir, (Item 4) Station 1519 -	43
3.15 Shot geometry with pressure contours for Site Charlie -	46
3.16 Post-Fir, Site Charlie, extent of inundation -	47
3.17 Preshot, steel tower on Site Charlie -	47
3.18 Plan including accelerometer and film badge locations for (Item 5) Station 78.01, Site Charlie, Redwing Station 1319 -	48
3.19 Preshot, (Item 5) Station 78.01, Site Charlie -	48
3.20 Post-Fir, (Item 5) Station 78.01 -	49
3.21 Post-Poplar, (Item 5) Station 78.01 -	49
3.22 Preshot, (Item 6) Station 1200, Site Charlie looking toward surface zero -	49
3.23 Post-Fir, (Item 6) Station 1200 -	50
3.24 Shot geometry with pressure contours for Sites Fox and George -	51
3.25 Preshot, (Item 8) Station 2410.02, Site Fox -	52
3.26 Post-Maple, (Item 8) Station 2410.02 -	52
3.27 Plan and elevation for wave stations, (Item 10) Stations 50.01 through 50.05 -	53
3.28 Preshot, (Item 10) Stations 50.01, -.02, and -.03, Site Fox -	54
3.29(a) Post-Maple, (Item 10) Stations 50.01, -.02, and -.03 -	54
3.29(b) Post-Maple, (Item 10) Station 50.03 -	55
3.29(c) Post-Redwood, (Item 10) Station 50.03 -	55
3.30 Preshot, (Item 11) Station 1810, Site George -	57
3.31 Post-Maple, (Item 11) Station 1810 -	57
3.32 Shot geometry with pressure contours for Sites Tare and Sugar -	58
3.33 Post-Nutmeg, general view of Sites Sugar and Tare -	59
3.34 Preshot view of timber bulkhead and sand bags at west end of Site Tare -	60
3.35 Post-Nutmeg view of timber bulkhead and sand bags at west end of Site Tare -	60
3.36 Post-Juniper view of east end of Site Tare looking toward surface zero -	61
3.37 Post-Nutmeg, (Item 12) Stations 2200 and 2250 -	61
3.38 Preshot, (Item 13) Station 2210, Site Tare, prior to being covered with sand -	62
3.39 Preshot, (Items 14, 15, and 16) Stations 2270, 2230.01, 2230.02, Site Tare, prior to being covered with sand -	62
3.40 Post-Nutmeg, (Items 15 and 16) Stations 2230.01 and 2230.02 -	63

3.41 Plan and elevation including the location of self-recording accelerometers for (Item 16) Station 2230.02, Site Tare	63
3.42 Post-impact, (Item 16) Station 2230.02, close-up of damaged 42-inch corrugated metal pipe	64
4.1 Shot geometry with pressure contours and station locations for Sites Gene, Helen, and Irene	70
4.2 Post-Koa, typical impact crater, 4,800 feet from ground zero	71
4.3 Plan of station complex on Site Irene	72
4.4 Preshot, (Item 18) station complex, close-up of entrance and crack in wing wall, Site Irene	72
4.5 Post-Yellowwood, (Item 18) station complex, close-up of entrance and cracked wing wall	73
4.6 Post-Walnut, (Item 18) station complex, close-up of wing wall failure	73
4.7 Plan and elevations for (Item 19) Station 1525, Site Irene	74
4.8 Preshot, (Item 19) Station 1525, Site Irene	75
4.9 Post-Koa, (Item 19) Station 1525, face-on view	75
4.10 Post-Koa, (Item 19) Station 1525, side-on view	76
4.11 Post-Walnut, (Item 19) Station 1525, retaining wall failure	76
4.12 Plan and elevations for (Item 20) Station 1311, Site Irene	77
4.13 Preshot, (Item 20) Station 1311, face-on view of retaining wall, Site Irene	78
4.14 Post-Koa, (Item 20) Station 1311, face-on view of retaining wall	78
4.15 Post-Walnut, (Item 20) Station 1311, face-on view of retaining wall	79
4.16 Preshot, (Item 20) Station 1311, entrance, Site Irene	79
4.17 Post-Koa, (Item 20) Station 1311, entrance	80
4.18 Post-Koa, (Item 20) Station 1311, 24-inch steel pipes pushed inward 2 1/4 inches	80
4.19 Post-Koa, (Item 20) Station 1311, crack pattern in floor	81
4.20 Preshot, (Item 21) Stations 1211 and 1410, view of side wall facing surface zero, Site Irene	81
4.21 Post-Walnut, (Item 21) Stations 1211 and 1410, view of exposed side wall	82
4.22 Preshot, pipeline to ground zero, Site Irene	82
4.23 Post-Koa, pipeline to ground zero	82
4.24 Plan including film badge locations for (Item 22) Station 3.4, Site Irene	84
4.25 Preshot, (Item 22) Station 3.4, side view, Site Irene	85
4.26 Post-Walnut, (Item 22) Station 3.4, side view showing scouring action of water wave; dark area represents original earth cover contact area	85
4.27 Preshot, (Item 23) generators, Site Irene	85
4.28 Post-Koa, (Item 23) generators	87
4.29 Post-Koa, (Item 23) close-up of damaged generator	87
4.30 Post-Koa, (Item 24) helicopter pad	88
4.31 Shot geometry with pressure contours for Site Janet	89
4.32 Plan including locations for air-overpressure gages and accelerometers for (Item 25) Station 1312, Site Janet	90
4.33 Post-Walnut, (Item 25) Station 1312, erosion adjacent to foundation	91
4.34 Over-all perspective for (Item 26) Station 3.1.1, Site Janet	91
4.35 Preshot, (Item 26) Station 3.1.1, Site Janet	92

4.36 Preshot, (Item 26) Station 3.1.1, Column 13C, concrete frame building, Site Janet -----	92
4.37 Preshot, (Item 26) Station 3.1.1, crack in ceiling adjacent to Column Line 10 of the shear wall building looking away from surface zero, Site Janet -----	93
4.38 Preshot, (Item 26) Station 3.1.1, crack in ceiling adjacent to north wall of the shear-wall building looking away from from surface zero, Site Janet -----	93
4.39 Post-Yellowwood, (Item 26) Station 3.1.1 -----	93
4.40 Post-Walnut, (Item 26) Station 3.1.1 -----	95
4.41 Post-Walnut, (Item 26) Station 3.1.1, aerial view -----	95
4.42 Post-Walnut, (Item 26) Station 3.1.1, close-up of Building 5, a reinforced-concrete frame structure -----	96
4.43 Post-Walnut, (Item 26) Station 3.1.1, front column of Building 5 -----	96
4.44 Post-Walnut, (Item 26) Station 3.1.1, second row of columns of Building 5 -----	97
4.45 Post-Walnut, (Item 26) Station 3.1.1, third row of columns of Building 5 -----	97
4.46 Post-Walnut, (Item 26) Station 3.1.1, Column 13C, second floor of Building 5 -----	98
4.47 Post-Walnut, (Item 26) Station 3.1.1, Column 8A, third floor of Building 3 -----	98
4.48 Post-Walnut, (Item 26) Station 3.1.1, Column 7B, third floor of Building 3 -----	99
4.49 Post-Walnut, (Item 26) Station 3.1.1, Column 5C, first floor of Building 2 -----	99
4.50 Post-Walnut, (Item 26) Station 3.1.1, roof slab damage, Building 6 -----	100
4.51 Post-Walnut, (Item 26) Station 3.1.1, crack in ceiling adjacent to Column Line 10 of the shear-wall building looking away from surface zero -----	100
4.52 Post-Walnut, (Item 26) Station 3.1.1, crack in ceiling adjacent to north wall of shear-wall building looking away from surface zero -----	102
4.53 Post-Elder, (Item 26) Station 3.1.1, front view -----	102
4.54 Post-Elder, (Item 26) Station 3.1.1, rear view -----	103
4.55 Post-Elder, (Item 26) Station 3.1.1, close-up of Building 5, first floor collapsed -----	103
4.56 Post-Elder, (Item 26) Station 3.1.1, close-up of Buildings 1, 2, and 3 -----	104
4.57 Post-Elder, (Item 26) Station 3.1.1, Columns 7 and 8B, first floor of Building 3 -----	104
4.58 Post-Elder, (Item 26) Station 3.1.1, Columns 7 and 8B, second floor of Building 3 -----	105
4.59 Post-Elder, (Item 26) Station 3.1.1, Columns 7 and 8B, third floor of Building 3 -----	105
4.60 Post-Elder, (Item 26) Station 3.1.1, Column 8D and crack in rear wall, first floor of Building 3 -----	106
4.61 Post-Elder, (Item 26) Station 3.1.1, destroyed roof section of Building 6 and damaged area to roof at south end of Building 4 -----	106
4.62 Post-Elder, (Item 26) Station 3.1.1, outside view of punched-in roof section at north end of Building 4 -----	106

4.63 Post-Elder, (Item 26) Station 3.1.1, inside view of punched-in roof section, north end of Building 4	107
4.64 Post-Elder, (Item 26) Station 3.1.1, close-up of punched-in roof section, north end of Building 4	107
4.65 Post-Dogwood, -Olive, and -Pine, (Item 26) Station 3.1.1, aerial view	108
4.66 Post-Dogwood, -Olive, and -Pine, (Item 26) Station 3.1.1, underside of third floor along Column Line 11, and the front wall facing surface zero	108
4.67 Post-Dogwood, -Olive, and -Pine, (Item 26) Station 3.1.1, crack in third floor at intersection of front wall between Column Line 11 and south shear wall	109
4.68 Post-Walnut, (Item 27) Station 3.1.3, entrance filled with mud	109
4.69 Structural details and elevation views of (Item 28) Stations 20A, B, C, D, E, and F, Site Janet	110
4.70 Preshot, (Item 28) Station 20B, view of gage pier facing surface zero, Site Janet	111
4.71 Post-Walnut, (Item 28) Station 20B, view of toppled gage pier	111
4.72 Postshot, (Item 29) Station 77.02, recording station	112
4.73 Preshot, (Item 30) landing pier, Site Janet	112
4.74 Post-Walnut, (Item 30) landing pier	112
4.75 Post-Elder, (Item 30) landing pier	113
4.76 Postshot, Janet Camp	114
4.77 Shot geometry with pressure contours and test stations for Site Yvonne	115
4.78 Plan and elevation for (Item 31) Station 1130, reinforced-concrete bunker, Site Yvonne	116
4.79 Preshot, (Item 31) Station 1130, entrance, Site Yvonne	117
4.80 Postshot, (Item 31) Station 1130, entrance	117
4.81 Preshot, (Item 31) Station 1130, side-tunnel entrance, Site Yvonne	118
4.82 Post-Cactus, (Item 31) Station 1130, side-tunnel entrance	118
4.83 Post-Cactus, (Item 31) Station 1130, crack at intersection of tunnel and main structure	120
4.84 Preshot, (Item 32) Station 1220.01, cubicle, Site Yvonne	120
4.85 Preshot, (Item 33) Station 1216, Site Yvonne	121
4.86 Post-Cactus, (Items 32 and 33) Stations 1220.01 and 1216	121
4.87 Plan and elevation for (Item 34) Station 1612, Site Yvonne	122
4.88 Preshot, (Item 34) Station 1612, retaining wall, Site Yvonne	123
4.89 Post-Cactus, (Item 34) Station 1612, retaining wall and entrance to station	123
4.90 Post-Cactus, (Item 34) Station 1612, interior view	124
4.91 Preshot, (Item 35) Stations 1523.01 to 1523.04, Site Yvonne	124
4.92 Post-Cactus, (Item 35) Stations 1523.01 to 1523.04, foundation pit for towers	125
4.93 Post-Cactus, (Item 35) Stations 1523.01 to 1523.04, 48-inch metal corrugated pipe leading to ground zero	125
4.94 Preshot, (Item 36) Station 1310, concrete, earth-covered station, Site Yvonne	126
4.95 Post-Rose, (Item 36) Station 1310, concrete, earth-covered station	126
4.96 Post-Butternut, (Item 37) 21,000-gallon water tank	127

4.97 Post-Magnolia, (Item 37) 21,000-gallon water tank and Yvonne Camp area	127
4.98 Post-Cactus, camp damage, tents	128
4.99 Post-Cactus, camp damage, light timber construction	129
4.100 Post-Cactus, camp damage, latrine	129
4.101 Post-Butternut, telephone poles	130
4.102 Post-Butternut, radar reflector	130
4.103 Post-Butternut, helium bottles	131
4.104 Post-Magnolia, helium bottles	131
4.105 Postshot, fire hydrant	132
5.1 Peak air overpressure for a 1-kt surface burst, with observed points	134
5.2 Reduced vertical ground acceleration 10 feet below ground surface for a 1-kt surface burst, with observed points	136
5.3 Damage to wood-frame camp structures for a surface burst	136
5.4 Data for Structure 3.1.1 plotted on curves	139
B.1 Plan, elevation, and gage geometry for Station 1312, Site Janet	147
B.2 Measured and predicted pressures for Station 1312, Shot Yellowwood	148
B.3 Measured and predicted pressures for Station 1312, Shot Tobacco	149
B.4 Measured and predicted pressures for Station 1312, Shot Walnut	150
B.5 Measured and predicted pressures for Station 1312, Shot Elder	151
C.1 Stress-strain curve for reinforcing steel	153
C.2 Stress-strain curve for concrete	153
C.3 Assumed loading geometry for typical pier	154
C.4 Stress relationship for concrete section at design strength	155
C.5 Stress and strain relationships for concrete section at yield strength	156
C.6 Stress and strain relationships for concrete section at ultimate strength	157
C.7 Determination of deflection at ultimate capacity	159
C.8 Moment-curvature diagram for beam	159
C.9 Effective blast pressure on Station 20-D	160
C.10 Effective blast pressure on Station 20-F	161
C.11 Reflected pressures for Stations 20-D and 20-F	162
D.1 Wave action at the personnel pier from Shot Oak, Site Elmer	168
D.2 Transformer station prior to wave arrival	168
D.3 Transformer station, first wave striking the lagoon shore	168
D.4 Transformer station, first wave moving onshore; the start of inundation	168
D.5 Transformer station after wave action ceased and water subsided	169

TABLES

1.1 Observations of Gross Damage: Operation Castle, Bikini and Eniwetok Atolls	21
1.2 Observations of Gross Damage: Operation Redwing, Bikini Atoll	23
1.3 Observations of Gross Damage: Operation Redwing, Eniwetok Atoll	24
1.4 Damage Summary, Operation Hardtack	26
2.1 Schedule of Data Collection During and After Operation Hardtack	30
2.2 Summary of Self-Recording Instrumentation	32
3.1 Summary of Results at Bikini Atoll	34
3.2 Recorded Radiation Within Station 560.01 (Item 2)	50

3.3	Recorded Radiation Within Station 78.01 (Item 5) -----	56
3.4	Free-Field Air-Overpressure Measurements, Sites Charlie and Tare -----	56
4.1	Summary of Results at Eniwetok Atoll -----	66
4.2	Recorded Radiation Within Station Complex (Item 18) -----	71
4.3	Recorded Radiation Within Station 3.4 (Item 22) -----	83
4.4	Free-Field Air-Overpressure Measurements, Site Janet -----	88
4.5	Comparative Displacement of Columns -----	94
A.1	Predicted and Recorded Radiation Values for Station 560.01 -----	143
A.2	Predicted and Recorded Radiation Values for Station 78.01 -----	143
A.3	Predicted and Recorded Radiation Values for Station Complex -----	143
A.4	Predicted and Recorded Radiation Values for Station 3.4 -----	143
C.1	Predicted Pressures and Durations for Stations 20-A to 20-F -----	153
D.1	Observations of Wave Damage, Operation Castle -----	166

SECRET

Chapter 1 **INTRODUCTION**

1.1 OBJECTIVE

The objective of this project was to record and evaluate damage from blast, radiation, and water waves to selected pre-existent and new structures at the Eniwetok Proving Ground by examination and measurement before and after certain test detonations. The damage properly associated with shot geometries can provide valuable information to designers and planners of structures to resist the effects of nuclear weapons.

1.2 BACKGROUND

Many structures have been built in prior tests at the Eniwetok Proving Ground for the purpose of housing scientific instruments in extreme environments. Damage to these structures was reported, but their exposure to nuclear effects was only incidental to their function, and the opportunity to gain useful information from their behavior was not exploited. In addition, considerable effort and funds have been invested in prior operations for structural tests, per se. Some of these structures still exist in an undamaged or partially damaged condition. Since a number of these structures were supposed to be subjected to severe loading conditions during Operation Hardtack, an opportunity was afforded to obtain valuable information on structural response and damage with minimum additional effort. Therefore, this project was planned to exploit the opportunity to gain general information that would amplify and supplement existing design criteria and concepts.

The selection of pre-existent stations that were investigated was based upon an on-site survey of structures made in November 1957. Certain new test structures were also included where it was predicted that they would be subject to high pressure and temperature or destructive water-wave action.

1.2.1 Previous Damage Surveys. Damage surveys were performed for Operation Ivy (Reference 1), conducted in 1952, and for Shot 1 of Operation Castle (Reference 2), conducted in 1954. These surveys described damage from a total of three shots; for this reason, no overall discussion of damage-distance relationships as a function of shot yield was made in either report. In addition to the published reports (References 1 and 2), Holmes and Narver, Inc. (H&N) made damage observations and took numerous photographs of scientific stations during Operation Castle (1954) and Operation Redwing (1956). The postshot damage reports prepared by H&N were given only limited distribution within the JEC. Since no complete damage surveys are available for Operations Castle and Redwing, the H&N reports were reviewed, and a summary of the miscellaneous damage observations are tabulated in this report for the first time for a more general distribution.

Shot geometries with pressure contours for Operation Castle are shown in Figures 1.1 and 1.2 for Bikini and Eniwetok, respectively. Table 1.1 summarizes the blast damage observations for Shots 2, 3, 4, 5, and 6. Damage due to Shot 1 is thoroughly presented in Reference 2; however, pertinent results are presented in Chapter 3 of this report.

SECRET

FORMERLY RESTRICTED DATA

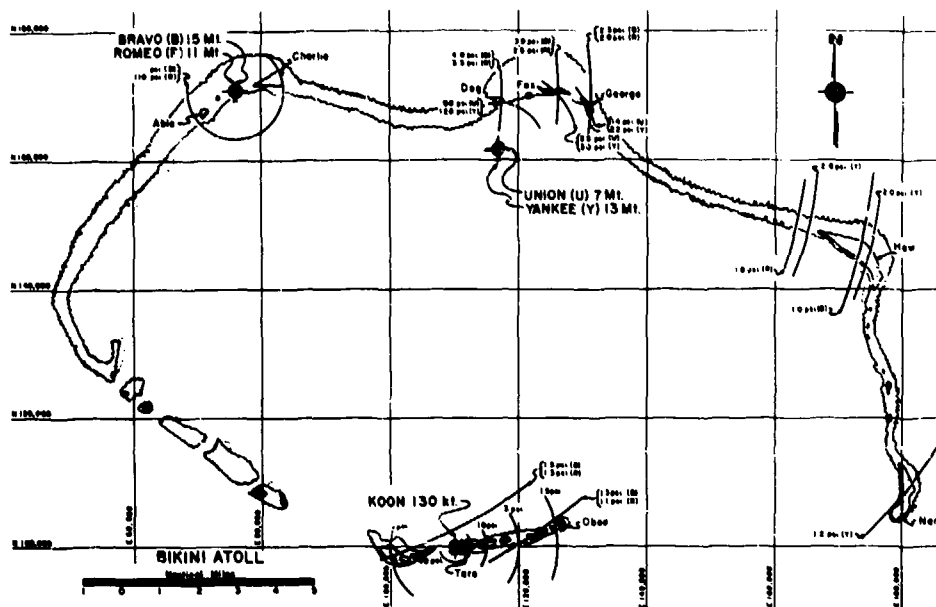


Figure 1.1 Shot geometry with pressure contours for Bikini Atoll, Operation Castle (1954).

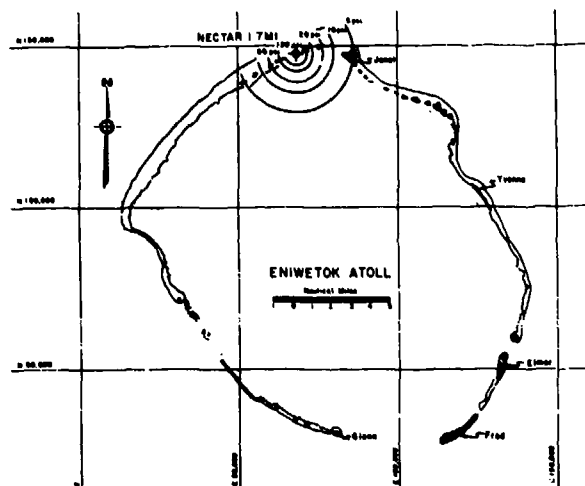


Figure 1.2 Shot geometry with pressure contours for Eniwetok Atoll, Operation Castle (1954).

Shot geometries with pressure contours for Operation Redwing are shown in Figures 1.3 and 1.4, and the summary of blast damage observations is shown in Tables 1.2 and 1.3.

The summary of blast damage observations for Operation Hardtack is shown in Table 1.4.

Salient conclusions reported during previous surveys (References 1 and 2) are given below.

1.2.2 Conclusions from Ivy Damage Survey (1952). (1) Exposed steel beams and pipes attached to structures were damaged or destroyed by overpressures of 11 psi and greater. (2) Small Build-

TABLE 1.1 OBSERVATIONS OF GROSS DAMAGE: OPERATION CASTLE*, BIKINI AND ENIWETOK ATOLLS

Description	Site	Shot Number	Code Name	Damage	Ground Range ft	Pressure psi
Concrete Structure:						
Station 1341; reinforced concrete, 3 story instrument shelter, above ground. Damaged and left in a weakened condition by Shot Bravo (Reference 2).	Able	2	Romeo	Severe damage; the third story was blown completely off.	7,500	9.5
Wood Framed Structure:						
Station 11: windowless, 16 feet to eaves; 3 1/4 inch x 3 1/4 inch x 1/4 inch steel angle studs at 48 inches o.c.; 1/4-inch exterior plywood.	George	1	Bravo	Moderate damage; plywood panels bowed in 1 to 2 feet; one panel ripped off.	56,400	2.4
Steel Framed Structure:						
Station 2210; steel framed with corrugated aluminum roofing and siding; exposed end-on to blast.	Sugar	3	Koon	Moderate damage; frame undamaged; roofing blown off; some siding blown off.	5,600	8.3
Storage Tanks:						
POL facility; four 1,000-barrel fuel storage tanks	Sugar	3	Koon	Severe damage; blast wave blew the top off one tank; all tanks damaged and leaked fuel; spilled fuel burned, severely damaging all tanks.	4,000	15
Towers:						
Timber water tower; 30 feet high; six 12-inch x 12-inch columns; guyed at the 30 foot level; 2 full 4,200 gallon water tanks in place.	Fox	1	Bravo	Undamaged	51,000	2.9
Station 80.01; antenna array of five 75-foot trylon towers; guyed at 3 levels; 3 guys at each guy level.	Nan	5	Yankee	Completely leveled	78,000	1.3
Station 1303.04; 75-foot, square, steel photo tower.	Janet	6	Nectar	Moderate damage; tower undamaged; cab frame was twisted and members bent; cab siding and rollup doors damaged beyond practical repair.	19,460	4.6
Field Generators and Fuel Tanks:						
Building DO-500; five 75-KW generators, 3 pontoon fuel tanks protected by high surrounding berm.	Dog	1	Bravo	Undamaged	40,000	4.2
Station 110.03; exposed generators.	Dog	1	Bravo	Damaged; extent unreported.	41,000	4.1
Utilities:						
Station 2221.02; exposed vacuum pump.	Sugar	3	Koon	Moderate damage	5,500	8.3

* Covers observations made subsequent to the Shot 1 damage survey reported in Reference 2

ings covered with thin sheet metal over diagonal wood sheathing generally withstood overpressures up to 5 and 8 psi. However, one structure of this type was badly damaged by an overpressure of 4.5 psi. (3) Lightly constructed wood-frame shacks sheathed with corrugated metal and located in regions with overpressures greater than 4 psi were completely destroyed. No structures of this type were located in regions subjected to less than 4-psi overpressure. (4) Palm trees were

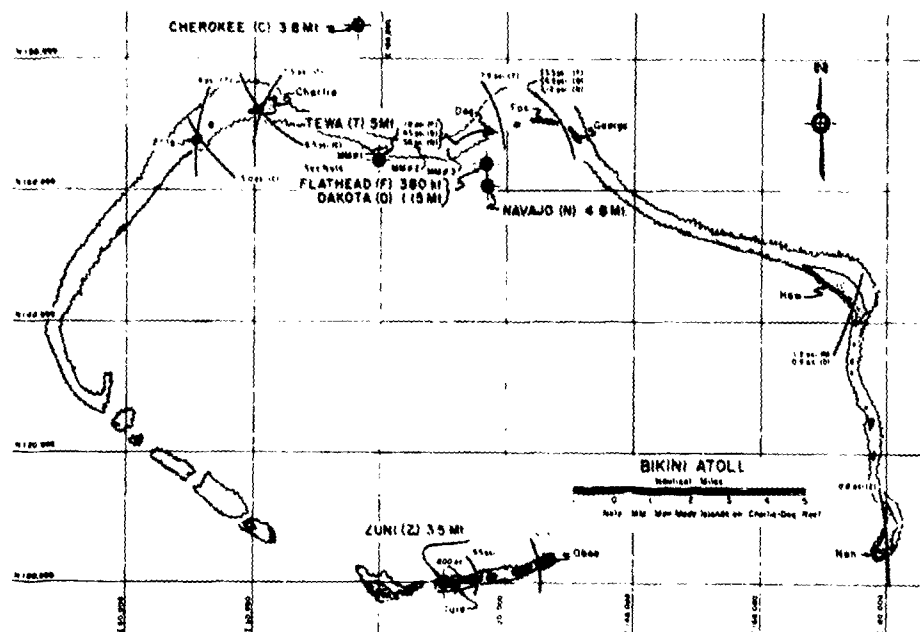


Figure 1.3 Shot geometry with pressure contours for Bikini Atoll, Operation Redwing (1956).

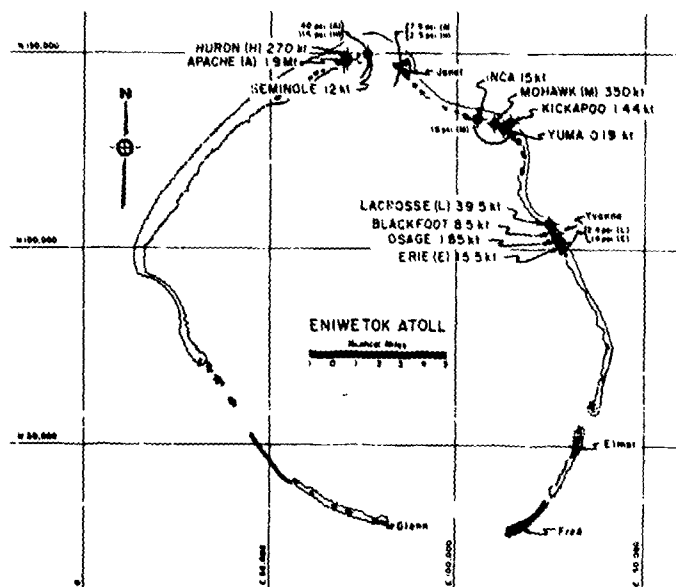


Figure 1.4 Shot geometry with pressure contours for Eniwetok Atoll, Operation Redwing (1956).

TABLE 1.2 OBSERVATIONS OF GROSS DAMAGE: OPERATION REDWING, BIKINI ATOLL

Description	Site	Shot	Damage	Ground Range ft	Pressure psi
Construction Camps: (8-man tents of typical construction over concrete slabs; light wood frame structures framed with 2 inch x 4 inch studs and trussed rafters 2 feet on centers, 1/4 inch exterior plywood siding, and corrugated aluminum roofing.)					
Tents, and light wood frame structures.	Fox	Cherokee	Complete destruction except for concrete floor slabs and some telephone poles; exposed wood surfaces were charred; there was evidence of several fires which apparently were extinguished by the shot air blast.	33,600	3.3
Tents, light wood frame structures, shop buildings, and hangars.	Nan	Zuni	Light damage was sustained; window screens broken; shutters broken; bulging walls; roof sheeting damaged at joints; a few rafters partially fractured; 2 inch x 10 inch studs in hangar building partially fractured and wall knocked inward 4 feet; carpenter shop shifted 5 inches.	70,600	0.6
Storage Tanks:					
Building 37: 21,000 gallon ground storage tank; 22 foot diameter; 8 feet high; 1/4 inch steel plate.	Fox	Cherokee	Apparently undamaged; tank was full at shot time.	33,600	3.3
		Flathead	Top of tank slightly dished in; no other apparent damage; water level in tank unknown.	12,200	3.9
		Dakota	Destroyed; the tank, probably empty, was blown 400 feet.	12,200	7.5
Towers:					
Station 1515: 75-foot, square, steel, photo tower.	William	Zuni	Tower undamaged; the cab shutters were moderately damaged.	32,000	2.6
Antennas:					
Station 312.02: TV antenna.	Man-Made Island No. 2	Cherokee	Broken off at the base.	20,750	7.0
Station 312.03: TV antenna.	Man-Made Island No. 3	Cherokee	Broken off at the base.	23,550	6.0
Station 74: Radio antenna.	Oboe	Zuni	Beet over; top broken off.	14,830	11.0
Field Generators and Fuel Tanks:					
Station 1519: 3 generators, side-on to blast.	Able	Cherokee	Generator nearer the blast was blown off its base and left leaning on the other; light charring of wood and paint.	30,350	3.7
Station 131.01: Generator; fuel tanks on wood rack.	Able	Cherokee	Generator housing driven against generator and bent; fuel tanks knocked down; wooden rack slightly charred.	31,190	3.5
Station 1319: 2 generators, end-on to blast	Charlie	Cherokee	Generator nearer the blast moved one foot; side panels driven against the generator and bent or broken off; paint charred on exposed surfaces.	19,540	8.0
Station 312.02: Generator.	Man-Made Island No. 2	Cherokee	Undamaged; generator end-on to blast; sand bags at base of generator charred.	20,750	7.0
Station 312.03: Generator, at 45 degrees to blast.	Man-Made Island No. 3	Cherokee	Generator housing slightly bent, generator at 45 degree to blast with one side protected by sand bags.	23,550	6.0
Castle Station 110: 2 generators behind retaining wall.	Uncle	Zuni	One generator blown on its side; the other upside down.	10,270	21.0
Station 74: Generator, fuel tank.	Oboe	Zuni	Undamaged.	14,830	11.0
Station 1319: Generator behind retaining wall; cylindrical fuel tank.	Sugar	Zuni	Generator badly damaged by the collapse of an adjoining concrete dividing wall; fuel tank was dished in.	5,140	98.0
Utilities and Ventilation Equipment:					
Station 1319: Exterior dehumidifier and compressor unit.	Charlie	Cherokee	Dehumidifier thrown against the compressor; the air intake fan was blasted against the intake.	19,540	8.0

TABLE 1.3 OBSERVATIONS OF GROSS DAMAGE: OPERATION REDWING, ENIWETOK ATOLL

Description	Site	Shot	Damage	Ground Range ft	Pressure psi
Concrete Structures:					
Station 1311.04; massive, semiburied; walls, roof and floor 8 feet thick; heavily reinforced; earth cover 1 foot deep.	Yvonne	LaCroese	Undamaged; earth cover almost completely blown away.	520	1,100
Station 1310; above ground; 5 x 9 feet blast door exposed (on-on to blast wave); door consisted of 1/4 inch cover-plate, 6 x 1/4 inch horizontal stiffeners at 13 inches o.c. with 8 x 1/4 inch flanges on the stiffeners.	Yvonne	Erie	Structurally undamaged; blast door severely damaged; door locking handles sheared off; door hinge was bent so that it was impossible to open the door.	1,420	35
Station 7304; Above ground cubical, 11 by 11 feet by 9 feet high; walls and roof 1 foot 6 inches thick; 9.4 percent reinforcement each way, each face, in walls and roof.	Irene	Seminole	Completely destroyed; only the base slab remained.	1,680	18
Construction Camps: (8-man tents of typical construction over concrete slabs; light wood frame structures framed with 2 x 4 inch studs and trussed rafters 2 feet on center; 1/4 inch exterior plywood siding, and corrugated aluminum roofings).					
Tents.	Yvonne	LaCroese	Wood frames failed; tents collapsed.	5,200	2.3
Light wood frame structures.	Yvonne	LaCroese	Severe damage; sides of buildings caved in; roofs blown off; lower walls of boiler house was undamaged.	5,200	2.3
Tents and light wood frame structures.	Yvonne	and	Complete destruction; the site was leveled leaving only the floor slabs.	2,300	13
Light wood frame structures.	Urula	Kickapoo	Light damage; several plywood panels were forced off the rear wall of shade; aluminum roof panel blown off one roof.	5,600	0.75
Tents and light wood frame structures.	Urula	Mohawk	Complete destruction; only electrical power poles and concrete floor slabs were reusable.	5,600	7.0
Tents and light wood frame structures.	Goss	Seminole	Complete destruction except for concrete floor slabs.	3,900	4.1
Wood Framed Structures:					
Station 1309; essentially windowless; 2 x 4 inch studs 2 feet o.c. and 2 x 6 inch rafters 2 feet o.c.; 1/4 inch exterior plywood siding.	Yvonne	LaCroese	Moderate damage; end wall, facing blast was pushed inward; side walls were pushed inward; several panels caved in completely.	5,000	2.4
Station 1308; rehabilitated to as-built condition after LaCroese shot.	Yvonne	Erie	Completely destroyed; walls were caved in; roof fell in.	2,100	15
Storage Tanks:					
Building 06; 21,000 gallon ground storage tank; 23 feet diameter, 8 feet high, 1/4 inch steel plate; full at shot time.	Yvonne	LaCroese	No damage.	5,120	2.4
Light Baffles: (Wood frame billboards with 1/4 inch plywood siding; facing blast; back stays at 45 degree support brace top of board; bottom of board is supported by a horizontal tie to the back stays).					
Station 1304; 8 feet high by 44 feet wide; four 4 x 10 inch posts; four 4 x 8 inch back stays.	Yvonne	LaCroese	Destroyed	7,500	2.7
Station 1303; 2 billboards, each 8 feet high by 12 feet wide; two 4 x 8 inch posts; two 4 x 8 inch back stays.	Yvonne	LaCroese	No apparent damage	7,500	2.5
Station 1302; 8 feet high by 20 feet wide; four 4 x 8 inch posts; four 4 x 8 inch back stays	Yvonne	Erie	Destroyed	1,900	16
Station 1301; 2 billboards, each 8 feet square; two 4 x 8 inch posts; two 4 x 8 inch backstays.	Yvonne	LaCroese	No apparent damage	7,985	2.4
		Erie	Destroyed	2,100	16
				5,040	2.4
				2,150	16

TABLE 1.3 CONTINUED

Description	Site	Shot	Damage	Ground Range ft	Pressure psi
Towers:					
Station 9; 300 foot shot tower, 20 feet square 6 inch steel box legs; guyed at 100 and 300 foot levels.	Yvonne	Erie	Moderate damage; tower assumed a curved shape; middle portion bent outward, however, cab remained in its original position, directly over tower base; elevation guide rails and outrigger were bent and twisted.	3,000	7.5
Building 88; timber water tower, 30 feet high, six 12 x 12 inch columns and double 2 x 6 inch bracing.	Yvonne	LaCrosse	No apparent damage; water tanks were removed prior to the shot.	3,150	2.3
Building 101; timber water tower, 30 feet high, eight 12 x 12 inch columns and double 2 x 6 inch bracing.	Ursula	Mohawk	Overturned; columns broken and fractured; water tanks were removed prior to shot.	3,000	7.0
Wood Pile Piers:					
Yvonne personnel pier	Yvonne	LaCrosse	Undamaged	3,000	4.6
		Erie	Destroyed; many piles broken at or near the water line.	300	150
Oose personnel pier	Oose	Seminole	Undamaged	3,000	2.7
		Apache	Completely destroyed.	1,000	> 1,000
Radar Reflectors:					
Station T411.01	Sally	Yuma	Undamaged	1,350	3.5
		Kichapoo	Knocked off its base.	1,340	9.0
Field Generators and Fuel Tanks:					
Central Yvonne area; 2 generators	Yvonne	LaCrosse	Overturned; reused after major overhaul	1,000	45
Station 1011; two 75-KW generators	Irene	Seminole	Overturned	1,350	27
Station 1011; two 75-KW generators;	Irene	Apache	Overturned; piston tank walls dished in.	7,250	26
3 Navy piston fuel tanks					
Station 1011; two 75-KW generators;	Irene	Huron	Overturned; recovered and salvaged;	3,630	9.2
3 Navy piston fuel tanks.			piston tanks undamaged.		
Vacuum Pipelines:					
Station 1011; 101R; 16 inch OD steel vacuum pipe line roller supported 30 feet o.c.; oriented approximately radial to the blast.	Yvonne	LaCrosse	Completely destroyed at less than 1,300 feet; undamaged beyond 1,300 feet.	1,300	70
				1,600	45
Station 1011; 101R; pipes tangential to blast.	Yvonne	Blackfoot	Undamaged beyond 1,100 feet.	1,100	40
Utilities and Ventilation Equipment:					
Building 76; Powerhouse	Yvonne	LaCrosse	Air intake dust burst when butterfly valve failed to close.	3,150	2.4
Station 2211; Powerhouse	Sally	Yuma	Piston chamber exploded when butterfly valve failed to close.	355	0.0
Building 100; Powerhouse	Ursula	Kichapoo	Piston chamber burst.	3,000	9.0
Building 76; Powerhouse	Yvonne	Erie	Outside fuel lines broken off leading into fuel storage tanks; fuel lines leading into powerhouse broken at entry.	2,200	15
Miscellaneous; water closets, urinals, washbowls, underground utilities	Yvonne	LaCrosse	Plumbing fixtures undamaged; underground utilities undisturbed except that exposed fixtures moved by the blast severed piping connections to the main lines (camp area)	3,000	2.2
Airport Runway:					
Asphalt paved runway	Yvonne	Erie	Moderate damage; asphalt broke into small pieces; exposed wood lagging in bulkhead burned away.	300 to 500	1,000 to 500

TABLE 1.4 DAMAGE SUMMARY, OPERATION HARDTACK

Description	Maximum Overpressure	Maximum Damage	Item Number	Special Remarks
Reinforced-Concrete Structures:				
Station 1541, Castle. Photo bunker. Three stories high. Damaged from Shot Bravo and Romeo of Operation Redwing. No damage from Operation Redwing.	350	Severe damage.	1	
Station 509.01, Redwing. Concrete shelter. No damage from Operation Redwing.	1,200	Completely destroyed.	2	Interior radiation measurement. Wave action.
Station 1519, Redwing. Reinforced-concrete photo bunker.	1,700	Completely destroyed.	4	Wave action.
Station 76.01. Concrete timing station. No damage from Operation Redwing.	50	No damage.	5	Interior radiation measurement. Wave action.
Station 1506, Castle. Concrete support structure. Damaged from Shot Bravo; no additional damage from Shot Romeo of Operation Castle. No damage from Operation Redwing.	32	Light damage.	6	
Station 1516. Coastal connector pit. Underground reinforced-concrete structure.	450	No damage.	12	
Station 1576. Connector pit, concrete box, earth-mounded.	1,400	No damage.	14	
Station 1530.01. Concrete bunker.	1,050	No damage.	15	
Station 1530.05. Concrete bunker.	1,000	No damage.	16	
Station 630.01. Buried concrete structure. Instrumentation pit for radiation effects.	500	No damage.	17	
Station Complex. A concrete shelter, addition to 1511 Redwing (combination of Stations 1534, 1535, and 1511). No damage to interior of station from Shot Domingo, Apache, or Huron of Operation Redwing.	42	Retaining wall failed.	18	Interior radiation measurement. Wave action.
Station 1535. A reinforced-concrete pier station.	42	Severe damage to retaining wall.	19	Thermal radiation. Wave action.
Station 1511. A concrete detector station mounded with earth.	42	Light damage.	20	Thermal radiation.
Station 1410 and 1511. A reinforced-concrete structure and terminus of pipeline.	42	No damage.	21	
Station 3 4. A reinforced-concrete signal terminal pit.	24	No damage.	22	Interior radiation measurement. Wave action.
Station 1313. A reinforced-concrete recording station.	50	No damage.	25	Blast diffraction study (Appendix B). Thermal radiation. Wave action.
Station 3.1.1. Three-story, multi-compartment test structure: concrete frame, steel frame, and concrete shear wall construction.	20	From light damage to collapse, depending on type of structure.	26	These structures were subjected to repeated loadings in the 10 psi to 7. psi (overpressure) range.
Station 20-B. Reinforced-concrete gage pier.	25	Severe damage, failure at base of stem.	28	Structural response study (Appendix C).
Station 77.02. A reinforced-concrete, earth-mounded timing station.	17	No damage.	29	
Station 1130. A reinforced-concrete bunker with a side tunnel.	450	Light damage to tunnel only.	31	Thermal radiation, 650 cal/cm ² .
Station 1215. A reinforced-concrete terminal for a pipeline.	450	No damage.	33	
Station 1515. A reinforced-concrete, earth-mounded Trivet station.	1,200	Severe damage to retaining wall. Light damage to structure.	34	
Station 1510. A large, massive, reinforced-concrete, earth-mounded structure.	16	No damage.	36	
Steel Structures:				
Stations 152.01 and 153.01, Redwing. Steel beams and pressure-gage mounts.	1,200	Completely destroyed.	3	
Stations 50.01 through 50.05. Water-wave gages.	340	50.01, 50.02 destroyed; 50.03 damaged.	10	Maximum total thermal radiation 2,000 cal/cm ² .
Station 3.1.1. Three-story, multi-compartment test structure: concrete frame, steel frame, and concrete shear wall construction.	20	From light damage to collapse, depending on type of structure.	26	These structures were subject to repeated loadings in the 10-psi and 20-psi overpressure range.

TABLE 1.4. CONTINUED

Description	Maximum Overpressure	Maximum Damage	Item Number	Special Remarks
Station 1220 f. Cable mounted on a structural-steel platform.	150	Severe damage.	32	
Stations 1523.01 to 0.04. Four steel-pipe towers encased by plywood covering.	450	Complete destruction.	35	
Wood Frame Structures:				
Station 2410.01. Wooden shelter earth-mounded.	385	Completely destroyed.	7	
Station 2410.02. Wooden shelter earth-mounded.	145	Completely destroyed.	8	
Station 2410.03. Wooden shelter earth-mounded.	76	Completely destroyed.	9	
Station 1510. Plywood construction between Stations 1530 and 1030.	21	Plywood room destroyed.	11	
Construction camp.	0.2	No damage from any of the shots.	None	
Construction camp.	1.1	Severe damage.	Other	
Construction camp.	5.2	Complete destruction.	Janet	
Construction camp.	6.6	Complete destruction.	Yvonne	
Miscellaneous Structures:				
Station 2250. 130 ft tower on top of concrete photo tank.	0.4	No damage.	12	
Generators. Four, 75-kva, diesel-driven units.	38	Severe damage.	23	
Helicopter pad. Steel landing mats.	44	Complete destruction.	24	
Station 3.1.3. Underground test structure.	29	No damage.	29	
Landing pier.	30	Light damage.	30	Wave action.
Water tank. A 21,000-gallon tank of 1/4-inch steel plate, 8 feet high, and 10 feet 10 inches in radius.	7	Light damage.	37	

destroyed by air-blast overpressures of 4 to 5 psi and greater; none were destroyed by overpressures less than 4 psi.

1.2.3 Conclusions from Castle Damage Survey (1954). (1) The blast wave of a 15.0-Mt surface burst caused considerable damage to light wood-frame structures out to a radius of about 16 miles from ground zero. (2) Trussing and knee bracing was effective in decreasing the severity of damage to light wood-frame buildings at great distances. (3) Heavily reinforced-concrete, above-ground, shelter-type structures subjected directly to the blast wave received significant damage as far away as 1.5 miles. It was not known how much farther this damage would have extended. (4) Earth cover appeared to provide a considerable degree of protection from air shock to reinforced-concrete, shelter-type structures. The addition of the earth cover appeared to be beneficial, primarily due to decreasing the blast loading by improving the aerodynamic shape, which in turn reduced reflection factors. Also, there was a possibility of slight attenuation of pressure incident on the structure, depending on the depth and condition of the earth cover.

Chapter 2 PROCEDURE

2.1 SHOT PARTICIPATION

The objective dictated that this project (a joint WES-H&N effort) adequately document information from nearly all the Operation Hardtack shots. The major effort of the project was concentrated on the early shots which were expected to yield the most significant information for this project. Some supplementary information of interest, however, was also expected from the later shots. Therefore, because this project was to be a minimum effort using limited funds and personnel, arrangements were made with H&N to receive the damage survey normally conducted by its field organization. In addition, it was planned to have a project representative visit the test site after the operation to obtain additional data regarding the later shots. The schedule of observation of effects from the various shots by the project during the operation and by the project representative after the operation is shown in Table 2.1.

The general layout and planned shot geometry for Operation Hardtack events, including the code name of the shot, site (island), and stations investigated, are shown in Figures 2.1 and 2.2 for Bikini and Eniwetok, respectively.

2.2 INSTRUMENTATION

Eleven self-recording, air-overpressure gages and six self-recording accelerometers were located as shown in Table 2.2. The locations were selected to provide the most useful data, taking into account shot geometries with respect to structures, and the available instrumentation. The exact location, as well as the results obtained with these gages, appear in Chapters 3 and 4 under the section pertaining to the structure in which or near which the gage was actually located. The gages were furnished, calibrated, and read by personnel from the Ballistics Research Laboratory (BRL).

The self-recording pressure gage consisted of a precisely governed, battery-operated motor that rotated a silvered-glass disk placed in operation by a fast-rising light pulse or thermal radiation from the detonation. A stylus attached to a compact metal-bellows element traced on the rotating disk a record of the dilations of the bellows produced by the pressure of the blast wave. In this way, a time-dependent record of the blast pressure was impressed on the disk.

The self-recording accelerometer was similar to the self-recording pressure gage, except that the sensing element was a cantilever spring with a mass attached at the free end. A recording stylus was mounted on this mass. A second element was mounted at a right angle to the other so that the two styluses recorded acceleration in two planes on a single glass disk. For a more detailed description of these two types of self-recording gages, including methods of installation and calibration, see WT-1612.

Dosimeter Film Packets, Type 559 (manufactured by E. I. du Pont de Nemours and Co.) obtained from and processed by TU 7.1.6 were placed in various stations to determine total gamma radiation. The location of the film badges and the values obtained appear in Chapters 3 and 4 under the section pertaining to the appropriate structure in which the badges were placed. The film used had two ranges of sensitivity; one from 0 roentgens (r) to 10 r and the other from 2 r to 400 r.

Photographs were taken before and after the shots at each station so that a visual comparison of damage could be made.

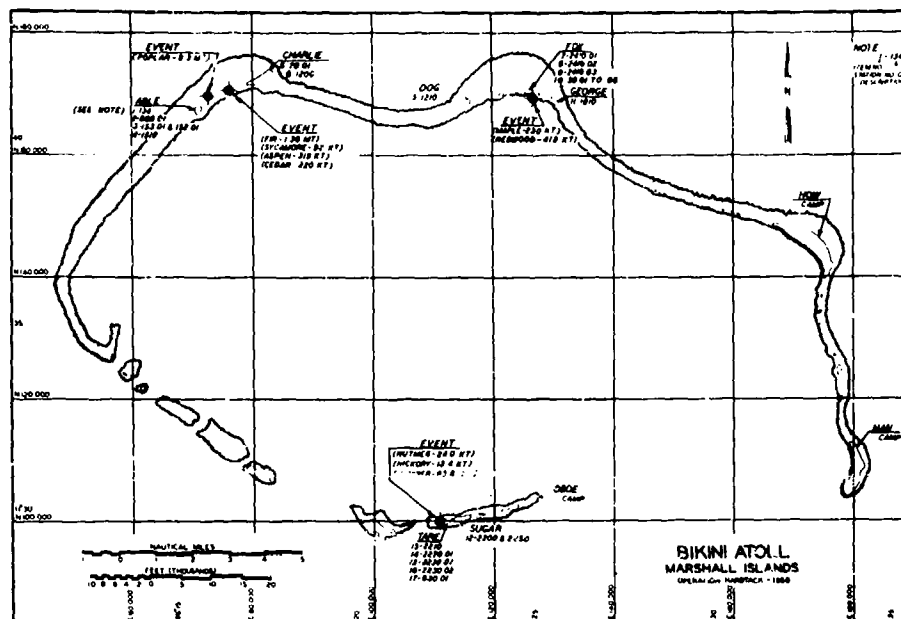


Figure 2.1 General plan and shot geometry for Bikini Atoll.

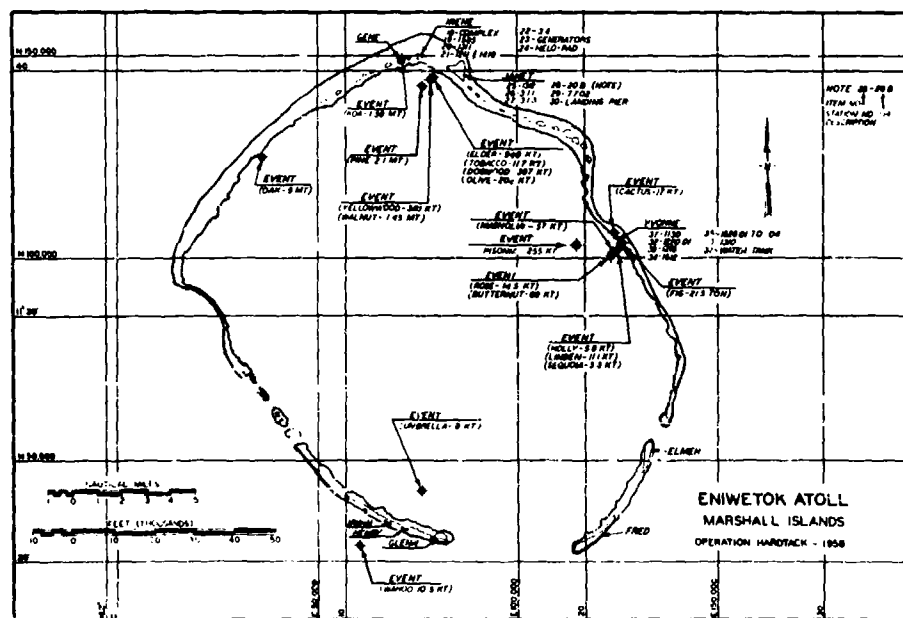


Figure 2.2 General plan and shot geometry for Eniwetok Atoll.

2.3 DATA REQUIREMENTS

Air overpressure was measured to correlate damage with pressure. The curves shown in Figures 2.3 and 2.4 were used for predicting values of air overpressure and positive-phase duration, respectively. Both curves are based on data found in References 3 and 4.

The geometry and position of Station 1312, a large, reinforced-concrete diagnostic station without earth cover (constructed for Operation Hardtack on Site Janet), offered the opportunity to obtain loading information for a large diffraction-type target. To obtain this information, two pressure gages were placed in the front face, two on the roof, and one on the back face of

TABLE 2.1 SCHEDULE OF DATA COLLECTION DURING AND AFTER OPERATION HARDTACK

Site	Shot	
	Effects Observed by Project During Operation	Effects Observed by Project Representative Postoperation
Bikini Atoll		
Abie	Fir	Cedar
	Sycamore	Poplar
	Aspen	
Charlie	Fir	Cedar
	Sycamore	Poplar
	Aspen	
Fox and George	Maple	Redwood
Tare and Sugar	Nutmeg	Hickory
		Juniper
Eniwetok Atoll		
Gene, Helen, and Irene	Koa	Dogwood
	Yellowwood	Olive
	Tobacco	Pine
	Walnut	
	Elder	
Janet	Koa	Dogwood
	Yellowwood	Olive
	Tobacco	Pine
	Walnut	
	Elder	
Yvonne	Cactus	Linden
	Butternut	Sequoia
	Holly	Fig
	Magnolia	Pisonia
	Rose	

the station. The results of this work are presented in Appendix B.

Acceleration measurements were obtained to assist in relating the response of a structural system with pressure and, also, to determine whether or not the acceleration was of such magnitude as to possibly cause physiological damage to personnel. For the purpose of predicting accelerations, a curve (Figure 2.5) was drawn from data contained in References 5, 6, and 7. The reference data indicated that the vertical acceleration of the floor slab approximated the vertical acceleration of the soil mass at the same level. If it is assumed that the total weight of a buried structure is approximately the same as the weight of soil displaced, the acceleration

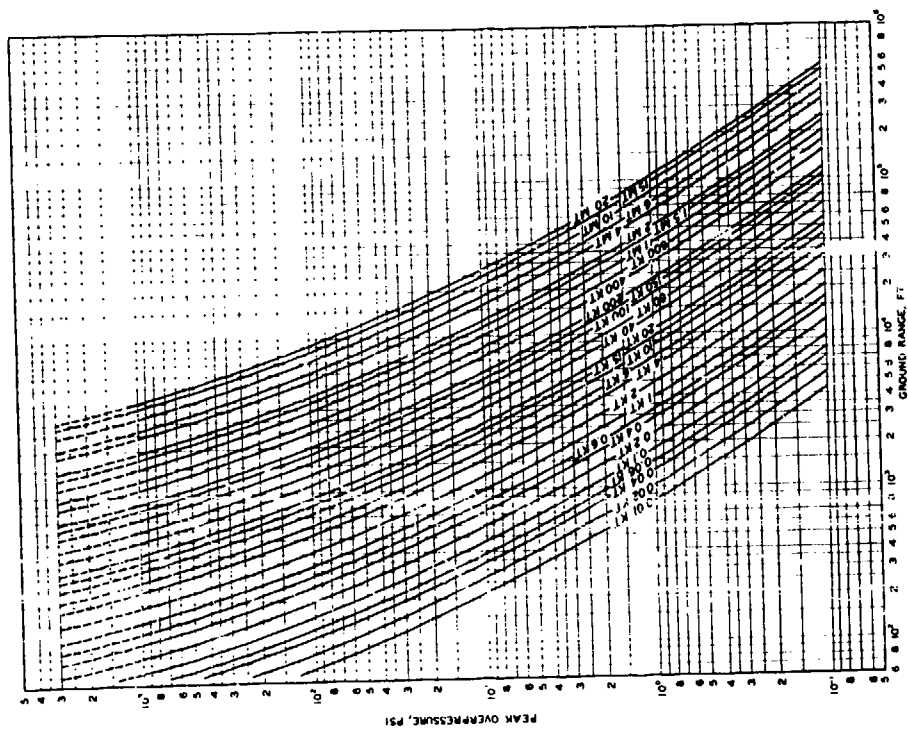


Figure 2.3 Peak air overpressure for surface bursts.

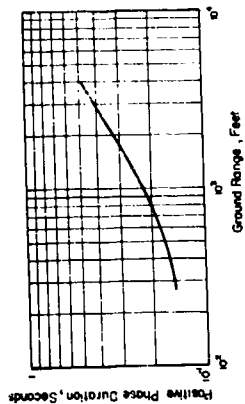


Figure 2.4 Positive-phase duration for a 1-kt surface burst.

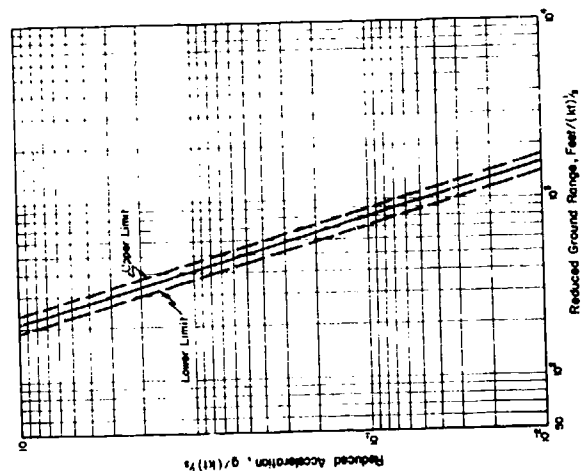


Figure 2.5 Reduced vertical ground acceleration 10 feet below ground surface for a 1-kt surface burst.

of the floor slab (at least in the downward direction) should approach the free-field value.

Radiation measurements were obtained to evaluate and compare actual with predicted values. The TM 23-200 (Reference 8) was used as the guide in making predicted radiation values, as well as in determining the attenuation factors for the various structures. A discussion of the method and calculations used for predicting radiation within the four structures that were radiologically evaluated is given in Appendix A to this report.

Water-wave predictions and wave-crest-height measurements were made by Project 50.1 (Scripps Institution of Oceanography). The data were used to study the relationship between wave action and land erosion. The results of this work are presented in Appendix D.

TABLE 2.2 SUMMARY OF SELF-RECORDING INSTRUMENTATION

Site	Station	Number of Gages	
		Air Overpressure	Acceleration
		psi	g
Charlie	78.01	2	2
Tare	2230.02	2	2
Janet	1312	6	2
	3.1.1	1	0

Level surveys were performed to determine the loss of earth cover over several mounded structures resulting from the effects of water waves and air blast.

The recorded damage from this operation and past operations, summarized in Chapter 1, was correlated with various curves of Reference 8. This project also utilized basic data from other Operation Hardtack projects to amplify the correlation.

An opportunity was afforded to compare predicted with observed response of reinforced-concrete gage piers which were located on Site Janet. This work is described in Appendix C.

Chapter 3

RESULTS: BIKINI ATOLL

For ease in interpretation of results and reference to various figures, the test results are presented in order according to atoll, then site (island), and then station. Where applicable to a particular station, a brief history relating effects from past operations is also included.

The general test results and descriptions of the stations investigated on Bikini are summarized in Table 3.1. Throughout this report, the terms severe, moderate, and light damage are used; for clarification the following definitions (Reference 8) are given:

Severe Damage. That degree of structural damage which precludes further use of a structure for the purpose for which it is intended without essentially complete reconstruction. Requires extensive repair effort before usable for any purpose.

Moderate Damage. That degree of structural damage to principal load-carrying members (trusses, columns, beams, and load-carrying walls) that precludes effective use of a structure for the purpose for which it is intended until major repairs are made.

Light Damage. That degree of damage which results in broken windows, slight damage to roofing and siding, blowing down of light interior partitions, and slight cracking of curtain walls in buildings.

3.1 SITE ABLE

The effects of Shots Fir (1.36 Mt), Sycamore (93 kt), Aspen (319 kt), Cedar (220 kt), and Poplar (9.3 Mt) were observed at Site Able. The shot geometry with pressure contours and test stations for this site is shown in Figure 3.1. The air blast and subsequent water wave from Shot Fir swept the island free of all vegetation. The extent of inundation from Shot Sycamore is shown in Figure 3.2. The effects from Shot Poplar which exposed the island to air blast pressures greater than 1,000 psi completely destroyed all man-made stations.

3.1.1 Item 1, Station 1341, Castle. A three-story, reinforced-concrete, photographic bunker, constructed during Operation Castle (1954), was designed for an incident air overpressure of 50 psi and a reflected pressure on the front face of 130 psi. A factor of safety of over 2 was used in the design; therefore structural failure at reflected pressures less than 260 psi would not be expected (Reference 2).

This station was severely damaged and left in a weakened condition as a result of Shot 1 (Bravo) of Operation Castle, which subjected it to about 130-psi air overpressure. A 95-psi overpressure from the Romeo shot (Operation Castle) caused additional damage, destroying nearly all of the previously damaged third story and making the station unsuitable for occupancy. No additional damage was inflicted during Operation Redwing (1956).

Figure 3.3 shows that blast effects from Shots Fir, Sycamore, Aspen, and Cedar inflicted no additional damage. However, the high overpressure level of 350 psi from Shot Poplar sheared the second floor from the structure, as shown in Figure 3.4.

3.1.2 Item 2, Station 560.01, Redwing. A reinforced-concrete shelter was constructed and not damaged during Operation Redwing (1956). The general plan and elevation for this structure, including film-badge locations, are shown in Figure 3.5.

This station was located in an estimated 30-, 6-, 12-, 10-, and 1,200-psi air-overpressure range from Shots Fir, Sycamore, Aspen, Cedar, and Poplar.

Pre- and post-Fir photographs (Figures 3.6 through 3.9) show the effect of water waves and

TABLE 3.1 SUMMARY OF RESULTS AT BIKINI ATOLL

Site	Item Number	Station Description	Shot	Yield	Ground Range to Ground Zero or Surface Zero	Predicted				Remarks
						Peak Overpressure	Duration	Initial Free-Field Gamma Radiation	Floor Slab Acceleration	
					ft	psi	sec	r/hr	g	
Abu	1	Station 1341, Cattle. Photo bunker. Three stories high. Damaged from Shot Bravo and Romeo of Operation Castle. No damage from Operation Redwing.	Fir	1.36 Mt	7,560	20	2.10	1,100	2.0	No additional damage
			Sycamore	93 kt	7,560	4.2	1.39	30	0.04	No additional damage
			Aspen	319 kt	7,560	8.5	1.66	150	0.2	No additional damage
			Cedar	220 kt	7,560	7.0	1.57	100	0.1	No additional damage
2			Poplar	9.3 Mt	4,400	350	3.16	1,000,000	210	Severe damage
		Station 560.01, Redwing. Concrete shelter. No damage from Operation Redwing.	Fir	1.36 Mt	6,030	30	1.92	7,000	4.2	No additional damage
			Sycamore	93 kt	6,030	6.0	1.20	210	0.1	No additional damage
			Aspen	319 kt	6,030	12	1.47	1,000	0.5	No additional damage
3			Cedar	220 kt	6,030	10	1.40	660	0.3	No additional damage
			Poplar	9.3 Mt	2,920	1,200	3.10	4,000,000	1,112	Completely destroyed
		Stations 152.01 and 153.01, Redwing. 8x8' beams and pressure gage mounts.	Fir	1.36 Mt	6,020	30	1.92	7,000	4.2	No damage
			Sycamore	93 kt	6,020	6.0	1.20	180	0.08	No damage
4			Aspen	319 kt	6,020	12	1.46	900	0.5	No damage
			Cedar	220 kt	6,020	10	1.39	600	0.3	No damage
			Poplar	9.3 Mt	2,820	1,200	3.10	5,000,000	1,020	Completely destroyed
		Station 1519, E. wing. Reinforced concrete photo bunker.	Fir	1.36 Mt	5,650	37	1.86	10,500	5.3	No damage, moved 11 feet horizontally
Charlie			Sycamore	93 kt	5,650	6.8	1.17	300	0.1	No damage
			Aspen	319 kt	5,650	14	1.45	1,400	0.6	No damage
			Cedar	220 kt	5,650	11	1.35	800	0.4	No damage
			Poplar	9.3 Mt	2,620	1,700	3.10	7,000,000	1,245	Completely destroyed
5		Station 78.01, Concrete timing station. No damage from Operation Redwing.	Fir	1.36 Mt	5,720	35	1.99	10,000	5.3	No damage
			Sycamore	93 kt	5,720	6.7	1.18	320	0.1	No damage
			Aspen	319 kt	5,720	14	1.45	1,500	0.6	No damage
			Cedar	220 kt	5,720	11	1.35	800	0.3	No damage
6			Poplar	9.3 Mt	9,190	50	3.42	10,600	17	No damage
		Station 1200, Cattle. Concrete superstructure. Damaged from Shot Bravo; no additional damage from Shot Romeo of Operation Castle. No damage from Operation Redwing.	Fir	1.36 Mt	7,550	20	2.10	1,150	2.0	Light damage
			Sycamore	93 kt	7,550	4.2	1.38	33	0.04	No additional damage
			Aspen	319 kt	7,550	8.3	1.66	150	0.2	No additional damage
7			Cedar	220 kt	7,550	7.0	1.57	90	0.1	No additional damage
			Poplar	9.3 Mt	11,020	32	3.63	3,500	8.6	No additional damage
		Station 5410.01, Wooden shelter, new.	Maple	220 kt	1,520	195	0.92	400,000	39	Completely destroyed
		Station 2410.02, Wooden shelter, new.	Redwood	412 kt	1,520	365	1.11	1,100,000	75	Completely destroyed
8			Maple	230 kt	2,125	85	0.95	200,000	12	Completely destroyed
			Redwood	412 kt	2,125	145	1.14	350,000	26	Completely destroyed

TABLE 3.1 CONTINUED

Site	Item Number	Station Number	Shot	Yield	Ground Range to Zero or Surface Zero	Predicted				Remarks
						Peak Overpressure	Duration	Free-Field Gamma Radiation	Floor Slab Acceleration	
					ft	psi	sec	r/hr	g	
George	9	Station 2410.03. Wooden shelter, new	Maple	230 kt	2,735	50	1.00	45,000	4.6	Completely destroyed
	10	Stations 50.01, 50.02, 50.03, 50.04, 50.05, and 50.06. Water-wave gage's.	Redwood	412 kt	2,735	76	1.17	120,000	12	No damage, see Section 3.3.2
			Redwood	412 kt	—	—	—	—	50.01 and 50.02 destroyed, 50.03 damaged	
George	11	Station 1810. Plywood construction between Stations 1830 and 1030.	Maple	230 kt	5,280	14	1.33	2,000	0.5	Plywood room destroyed
			Redwood	412 kt	5,260	21	1.46	4,000	1.1	No additional damage
Nas		Camp.	Maple	230 kt	82,500	0.1	5.8	0 ±	0	No damage from any of the shots
			Redwood	412 kt	92,500	0.2	6.4	0 ±	0	
Obse		Camp.	Nutmeg	24.0 kt	15,000	0.7	1.65	0 ±	0	No damage
			Hickory	13.4 kt	15,000	0.5	1.5	0 ±	0	No damage
			Poplar	9.3 kt	85,000	1.0	9.9	0 ±	0	No damage
			Plum	255 kt	11,000	3.8	1.95	1	0.04	Not known
			Juniper	63.8 kt	15,000	1.1	1.9	0 ±	0	No damage
Sugar	12	Station 2250. 150-foot tower on top of concrete photo bunker.	Nutmeg	24.0 kt	4,510	4.5	0.82	280	0.03	No damage
			Hickory	13.4 kt	4,510	3.5	0.76	170	0.01	No damage
			Juniper	63.8 kt	4,510	8.2	1.0	950	0.08	Severe damage
Tare	13	Station 2210. Conical connector pit. Underground and reinforced concrete structure.	Nutmeg	24.0 kt	785	170	0.43	260,000	12	No damage
			Hickory	13.4 kt	785	90	0.38	140,000	5.7	No damage
			Juniper	63.8 kt	785	430	0.60	700,000	50	No damage
14		Station 2270. Connector pit, concrete box, earth mounded.	Nutmeg	24.0 kt	550	490	0.42	400,000	47	No damage
			Hickory	13.4 kt	550	260	0.35	320,000	17	No damage
			Juniper	63.8 kt	550	1,490	0.59	1,300,000	181	No damage
15		Station 2230.01. Concrete bunker.	Nutmeg	24.0 kt	600	350	0.42	350,000	29	No damage
			Hickory	13.4 kt	600	200	0.35	220,000	14	No damage
			Juniper	63.8 kt	600	1,050	0.40	1,000,000	120	No damage
16		Station 2230.02. Concrete bunker.	Nutmeg	24.0 kt	635	320	0.42	300,000	24	No damage
			Hickory	13.4 kt	635	180	0.36	220,000	10	No damage
			Juniper	63.8 kt	635	1,000	0.61	1,000,000	108	No damage
17		Station 630.01. Buried concrete structure. Instrumentation pit for radiation effects.	Nutmeg	24.0 kt	725	210	0.42	300,000	15	No damage
			Hickory	13.4 kt	725	120	0.36	130,000	6.6	No damage
			Juniper	63.8 kt	725	560	0.60	700,000	65	No damage



Figure 3.2 Extent of inundation on Site Able after Shot Sycamore.



Figure 3.3 Post-Fir, -Sycamore, -Aspen, and -Cedar, (Item 1)
Station 1341 on Site Able, no additional damage. Pressure levels:
Fir, 20 psi; Sycamore, 4.2 psi; Aspen, 8.5 psi; and Cedar, 7.0 psi.

air blast on the immediate area. The telephone pole adjacent to the structure was broken at the roof line. Although the door of this structure could not be sealed tightly due to faulty seating, it is assumed that the pressure build-up within the station was slight. Three one-hundred-watt light bulbs fastened to the ceiling did not break, indicating that the pressure within the station was very low. Three inches of mud covered the floor and high water mark was noted 1 foot 8 inches above the floor. The sand bags were strewn about the entire area, the top of the berm was lowered 2 feet, and the earth mound in front of the station was reduced 7 feet in height. Indications were that at least 3 feet of water had been confined within the circular berm area. Pre-Fir, post-Fir, and post-Sycamore profiles of the island between Stations 560.01 and 1519 are shown in Figure 3.10.

Shots Sycamore, Aspen, and Cedar had no noticeable additional effects on this station as would be expected by observing the small overpressures resulting from these shots. It is also



Figure 3.4 Post-Poplar, (Item 1) Station 1341. Pressure level: Poplar, 350 psi.

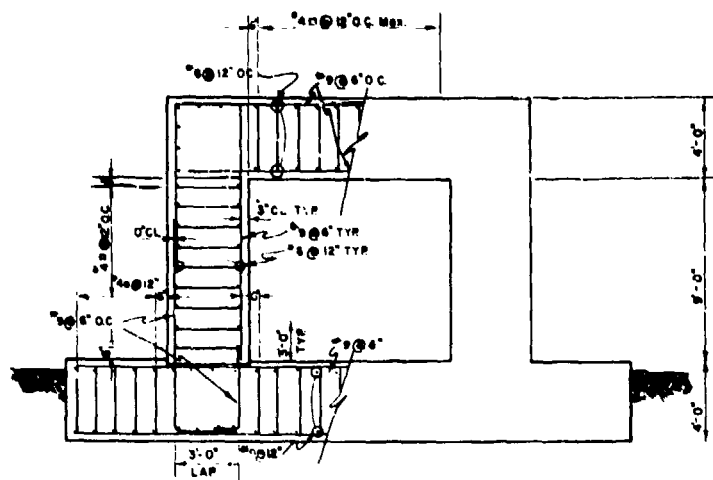
evident from Figure 3.10 that Shot Sycamore caused very little, if any, additional erosion.

The structure was completely destroyed from the effects of Shot Poplar. Figure 3.11 shows there was hardly a trace that the structure once existed and only a slight trace indicating the location of the circular earth berm that once surrounded the structure.

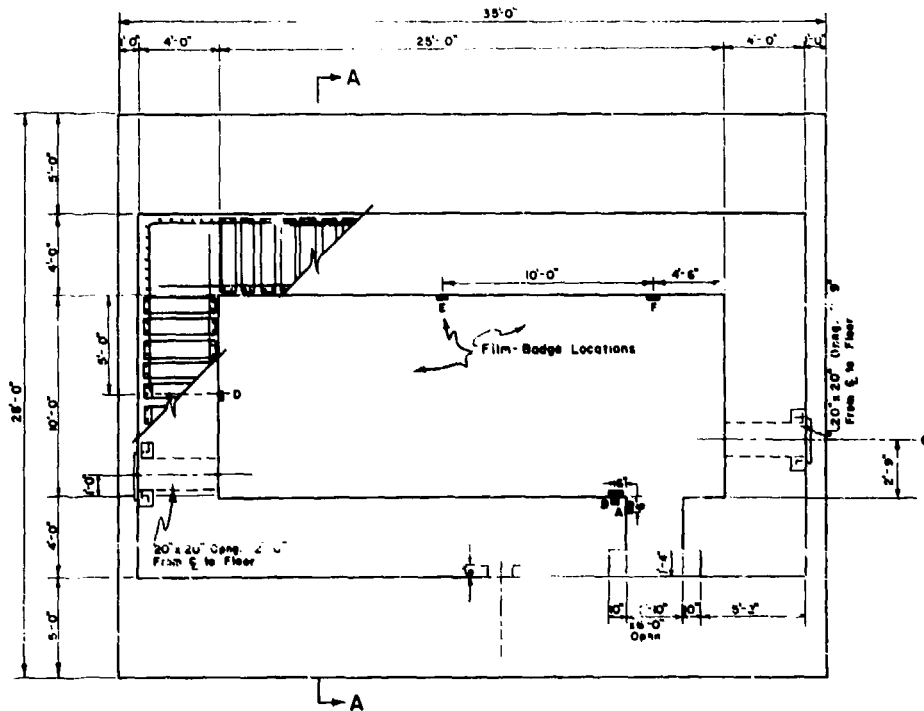
Radiation values within the structure for Shots Fir, Sycamore, and Aspen are listed in Table 3.2.

3.1.3 Item 3, Stations 152.01 and 153.01, Redwing. Two steel beams, one an 8-inch, 67-lb/ft, wide-flange beam, 10 feet 8 inches long, and the other an 8-by-8-inch, 56.9-lb/ft angle, 6 feet 8 inches long, were erected as test drag-type structures and were undamaged during Operation Redwing (1956).

These stations received an estimated air pressure of 30, 6, 12, 10, and 1,200 psi from Shots Fir, Sycamore, Aspen, Cedar, and Poplar, respectively. The stations were undamaged from the first four shots except for slight erosion of the soil around the concrete foundations, (Figure 3.12); however, the force from Shot Poplar destroyed the steel drag members, leaving only the concrete bases (Figure 3.13).



SECTION A-A



PLAN

Figure 3.5 Plan and elevation including film badge locations for (Item 2) Station 560.01, Site Able.

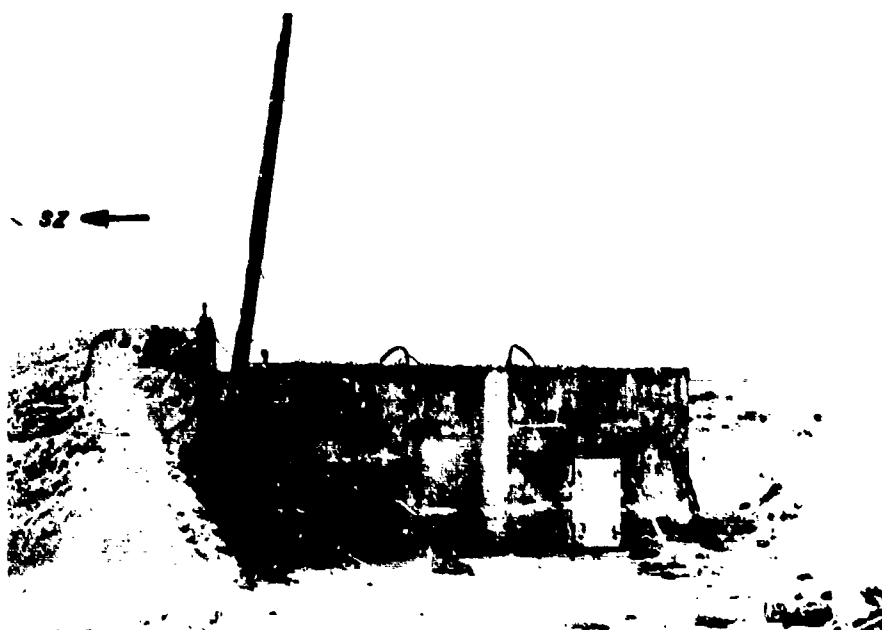


Figure 3.6 Preshot, (Item 2) Station 560.01, Site Able.

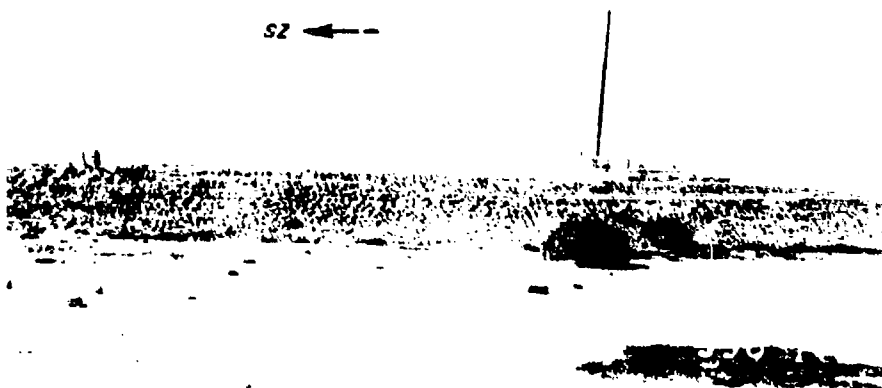


Figure 3.7 Preshot, (Item 2) Station 560.01 including earth berm, Site Able.



Figure 3.8 Post-Fir, (Item 2) Station 560.01. Pressure level: Fir, 30 psi.



Figure 3.9 Post-Fir, (Item 2) Station 560.01 including earth berm. Pressure level: Fir, 30 psi.

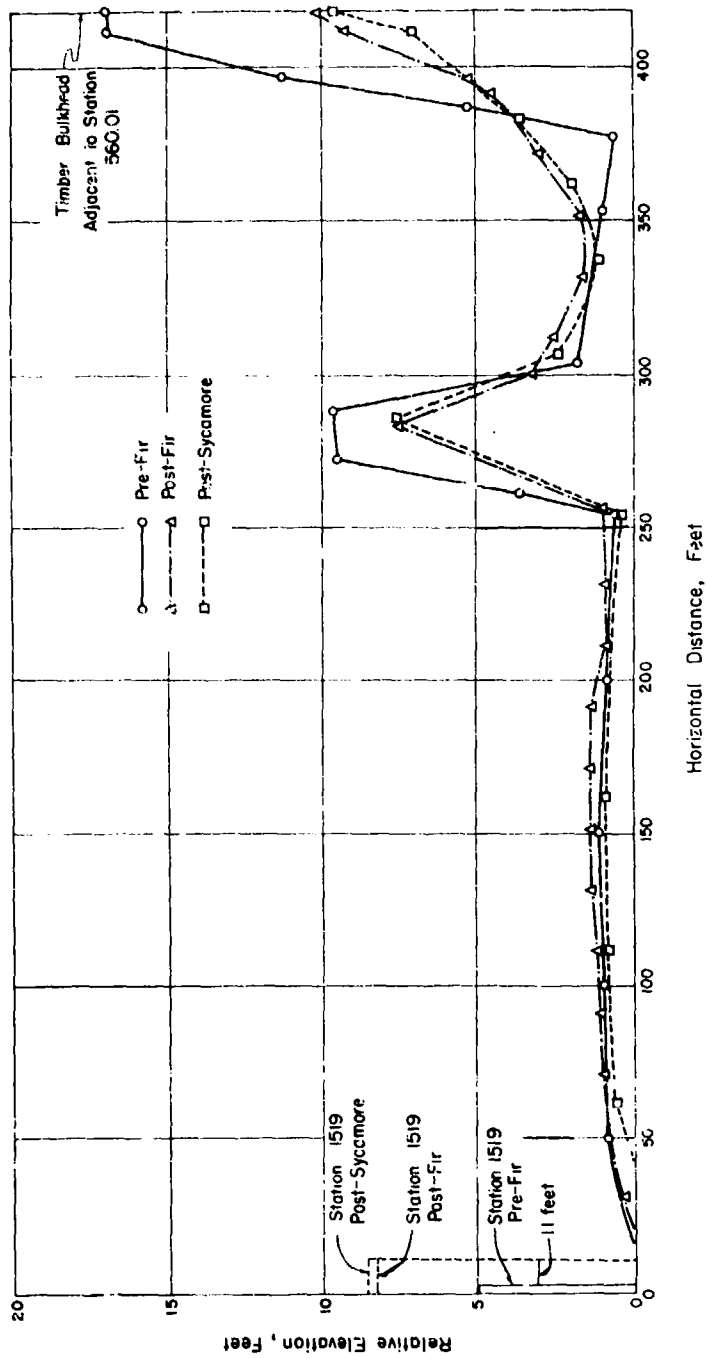


Figure 3.10 Ground-surface profile between (Item 2) Station 560.01 and (Item 4) Station 1519.

SECRET



Figure 5.11 Post-Poplar, (Item 2) Station 560.01, complete destruction of station. Station 1341 can be seen in background. Pressure level: Poplar, 1,200 psi.

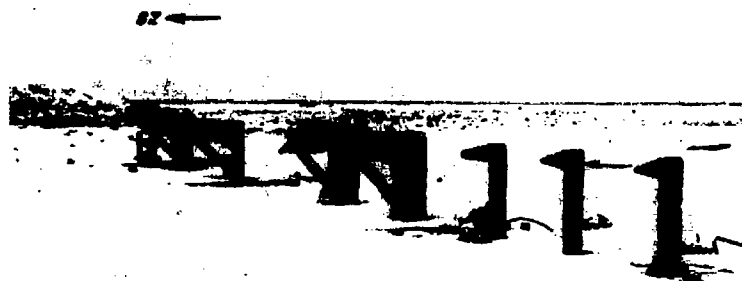


Figure 3.12 Post-Fir, (Item 3) Stations 152.01 and 153.01. Pressure level: Fir, 30 psi.

3.1.4 Item 4, Station 1519, Redwing. A reinforced-concrete, photographic station approximately 24 feet long, 9 feet wide, and 7 feet high and weighing 50 tons was constructed and undamaged structurally during Operation Redwing (1956).

This station was located in an estimated 37-psi overpressure range from Shot Fir and was displaced 11 feet horizontally away from surface zero. A post-Fir view is shown in Figure 3.14. The pressures of 6.8, 14, and 11 psi from Shots Sycamore, Aspen, and Cedar, respectively, caused no further damage or movement. The very-high overpressure of 1,700 psi from Shot Poplar completely destroyed this station.

3.2 SITE CHARLIE

The effects of Shots Fir (1.36 Mt), Sycamore (93 kt), Aspen (319 kt), Cedar (220 kt), and Poplar (9.3 Mt) were observed at this site. The shot geometry, with pressure contours and test stations, is shown in Figure 3.15.

The air blast and water wave from Shot Fir swept nearly all vegetation from the island. Inundation caused from Shot Fir extended past Station 78.01 as can be seen in Figure 3.16. A light steel tower, shown in Figure 3.17, was located in the 25-psi air-overpressure range of Shot Fir and was completely destroyed, leaving no trace of the structure.

3.2.1 Item 5, Station 78.01, 1319 Redwing. A reinforced-concrete timing station, constructed and undamaged during Operation Redwing (1956) was modified for use in Operation Hardtack (1958) by adding a new entranceway and mounding earth over the old entrance and retaining wall.

This station was located in an estimated 35-, 6.7-, 14-, 11-, and 50-psi air-overpressure range for Shots Fir, Sycamore, Aspen, Cedar, and Poplar, respectively. However, the structure apparently received no structural damage from any of the shots. The general plan including locations for accelerometers and film badges is shown in Figure 3.18 while the data obtained from the radiation measurements are shown in Table 3.3. The data obtained from the air-overpressure gages shown in Figure 3.15 are presented in Table 3.4. No records were obtained from the self-recording accelerometers located in this structure.

The structure, including the earth mound over the structure and light steel structural members used for guiding a guillotine-type gate over the entrance, is shown in Figure 3.19 prior to Shot Fir, in Figure 3.20 after Shot Fir, and in Figure 3.21 after Shot Poplar. For Shot Fir it appeared that the water-wave run-up on the side of the mound facing surface zero was 5 to 6 feet vertically (see Figure 3.20) and that the passing wave reached a height of 1 to 2 feet as observed by the water marks on the earth mound. A heavy, interior steel door was knocked off its pin and socket hinge from the shock effects of Shot Poplar.

3.2.2 Item 6, Station 1200, Castle. A reinforced-concrete, earth-mounded structure was constructed during Operation Castle (1954). The structure, situated in the 130-psi air-overpressure range, was damaged from Shot 1 (Bravo) of Castle; portions of the parapet and retaining walls at the rear of the structure were torn off by the blast. No additional damage was received during Operation Redwing (1956). The earth cover around this station was removed after Operation Redwing.

This station was located in the 20-psi air-overpressure range for Shot Fir and received slight additional damage. A retaining wall previously damaged was forced over, leaving only the reinforcing steel holding the cracked portion to the main section (Figures 3.22 and 3.23).

No additional damage as the result of Shots Sycamore and Aspen was observed. The station appeared intact as observed by distant observation after Shots Cedar and Poplar which caused pressures of 7 and 32 psi, respectively.

3.3 SITES FOX AND GEORGE

These sites were exposed to Shots Maple (230 kt) and Redwood (412 kt); however, the destructiveness of Shot Maple was such that no significant additional damage was inflicted by Shot Redwood. Site Fox was completely inundated by the water wave generated from Shot Maple while



Figure 3.13 Post-Poplar, (Item 3) Stations 152.01 and 153.01. Pressure level: Poplar, 1,200 psi.



Figure 3.14 Post-Fir, (Item 4) Station 1519. Pressure level: Fir, 37 psi.

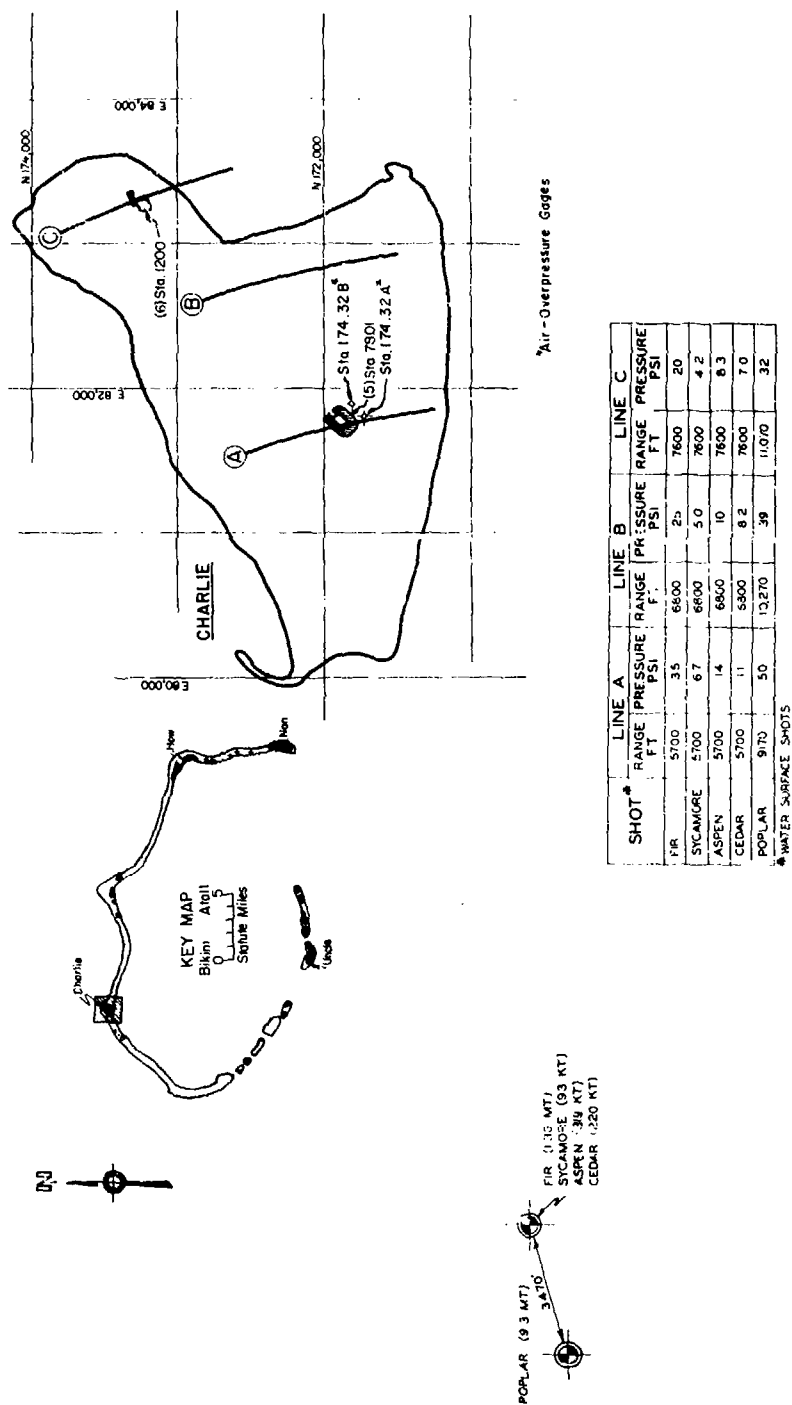


Figure 3.15 Shot geometry with pressure contours for Site Charlie.



Figure 3.16 Test Fir, Site Charlie, extent of inundation.

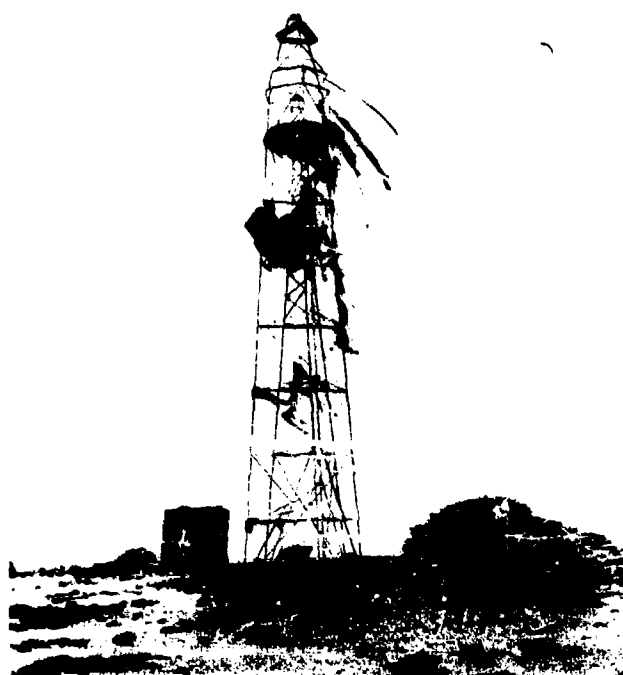


Figure 3.17 Preshot, steel tower on Site Charlie; completely destroyed by Shot Fir, 25 psi.

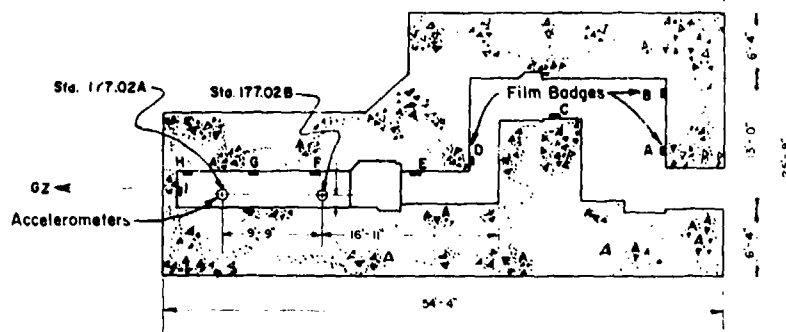


Figure 3.18 Plan including accelerometer and film badge locations for (Item 5) Station 78.01, Site Charlie, Redwing Station 1319.

Site George was partially washed over. The shot geometry with pressure contours and test stations for the two sites are shown in Figure 3.24.

3.3.1 Items 7, 8, and 9, Stations 2410.01, -.02, and -.03. Three identical timber shelters mounded over with earth were constructed during Operation Hardtack (1958). A typical preshot



Figure 3.19 Preshot. (Item 5) Station 78.01, Site Charlie.

view is shown in Figure 3.25 and typical post-Maple view (pressure level, 85 psi) in Figure 3.26. All three structures were completely destroyed and the earth mounds over the structures were washed away by the blast and water-wave forces of Shot Maple.

3.3.2 Item 10, Stations 50.01, -.02, -.03, -.04, -.05, and -.06. Six water-wave gages were constructed and located as shown in Figure 3.24. The structural details of a typical gage are shown in Figure 3.27.



Figure 3.20 Post-Fir, (Item 5) Station 78.01. Pressure level: Fir, 35 psi. Arrows indicate extent of inundation.



Figure 3.21 Post-Poplar, (Item 5) Station 78.01. Pressure level: Poplar, 50 psi.

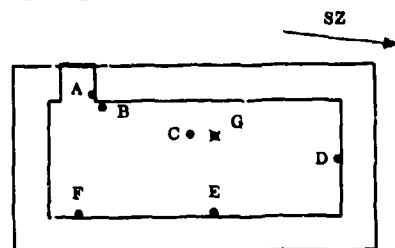


Figure 3.22 Preshot, (Item 6) Station 1200, Site Charlie looking toward surface zero.

TABLE 3.2 RECORDED RADIATION WITHIN STATION 560.01 (ITEM 2)

See Figure 3.5 for a detailed location of film badges.

Plan of Film-Badge Locations



- Film badge located 3 feet above floor
- ✕ Film badge located on ceiling

Shot	Radiation, r, at Film-Badge Locations														
	A		B		C		D		E		F		G		
	a*	b†	a*	b†	a*	b†	a*	b†	a*	b†	a*	b†	a*	c‡	d§
Fir	4.1	—	5.0	—	3.0	—	3.0	—	3.0	—	6.0	—	—	—	—
Sycamore	0.80	—	0.10	—	0.15	—	0.09	—	0.09	—	0.15	—	—	—	—
Aspen	20.0	22.0	4.8	4.8	3.4	—	2.3	—	3.2	—	5.2	4.4	2.5	2.6	2.2

* Plane of badge on surface of wall or ceiling.

† Plane of badge normal to both wall and ceiling.

‡ Plane of badge normal to ceiling and parallel to short wall.

§ Plane of badge normal to ceiling and parallel to long wall.



Figure 3.23 Post-Fir, (Item 6) Station 1200. Pressure level: Fir, 20 psi.

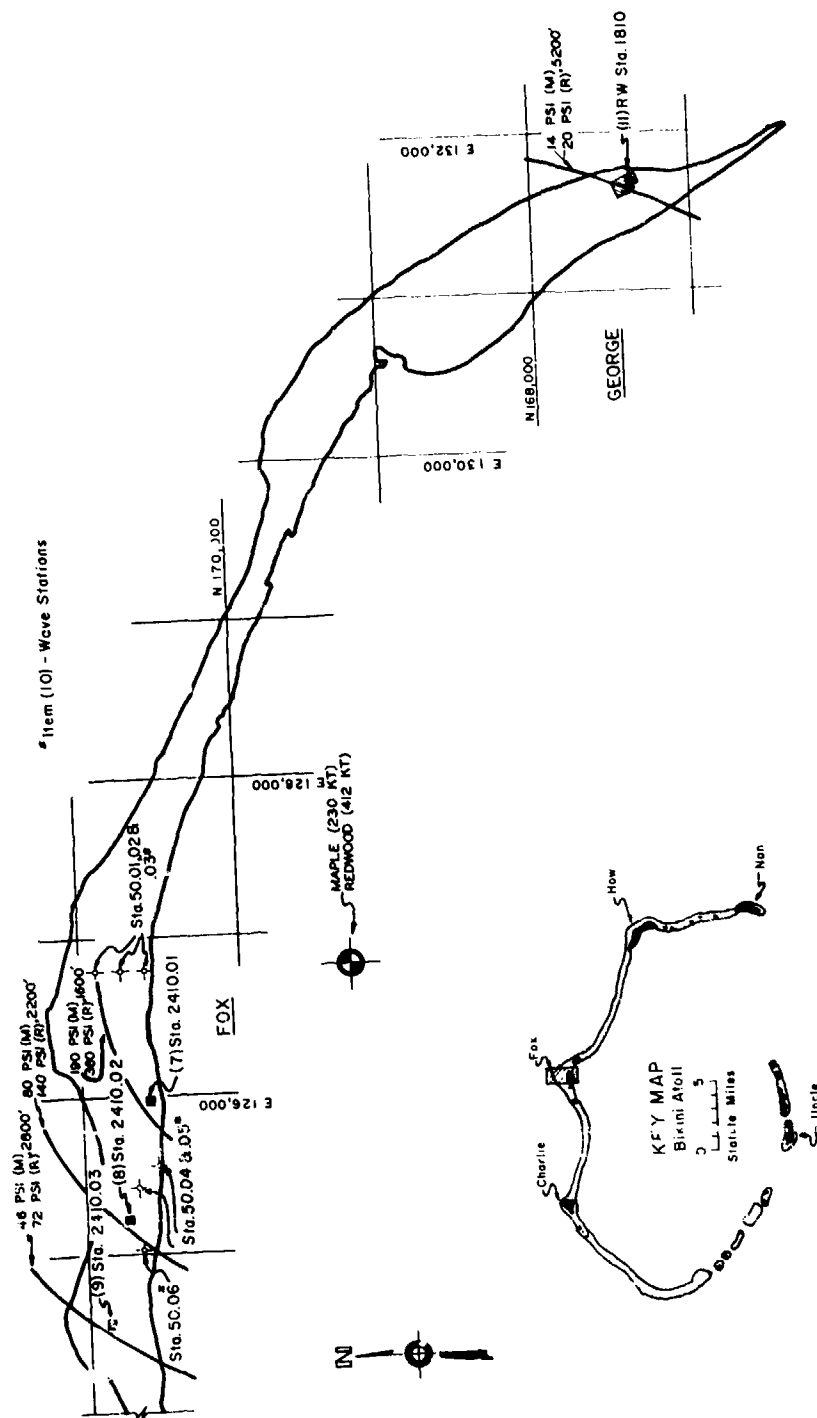


Figure 3.24 Shot geometry with pressure contours for Sites Fox and George.

All the wave stations survived the effects from air blast and water waves generated from Shot Maple; however, Station 50.04, which weighed about 10 tons, was thrown approximately 300 feet. The footing of Station 50.01 was cracked vertically. A preshot view of Stations 50.01, -.02, and -.03 is shown in Figure 3.28 and a post-Maple view in Figure 3.29(a). A large concrete block weighing approximately 15 tons (shown in the foreground of Figure 3.28) was thrown



Figure 3.25 Preshot, (Item 8) Station 2410.02, Site Fox.

approximately 150 feet by the force from the water wave generated by the shot. The final position can be seen in Figure 3.29(a). However, no structural damage was observed for this block which was located in the 340-psi range from Shot Maple.

These stations were subjected to thermal radiation with values ranging from 400 cal/cm² to 1,200 cal/cm² for Shot Maple without noticeable effects. Shot Redwood then subjected the stations to higher values of thermal radiation ranging from 800 cal/cm² to 2,000 cal/cm².



Figure 3.26 Post-Maple, (Item 8) Station 2410.02. Pressure level: Maple, 85 psi.

As a result of Shot Redwood, the two closest stations, 50.01 and 50.02, were destroyed. Station 50.03 was moderately damaged; the leeward pipe of the gage tower buckled laterally, leaving the whole tower tilting away from surface zero. Station 50.04, which had its base completely exposed (i.e., was not buried) was washed to the far side of the island. Stations 50.05 and 50.06 remained undamaged.

Station 50.03 which survived both shots is shown in Figures 3.29(b) post-Maple and 3.29(c) post-Redwood.

3.3.3 Item 11, Station 1810, 1830 Redwing. A reinforced-concrete shelter was rehabilitated for use in Operation Hardtack and a large plywood room added to the station between the existing structure (Redwing 1830) and Station 1030 (Redwing 1528).

A pre- and post-Maple view of the structure is shown in Figures 3.30 and 3.31. The blast



Figure 3.28 Preshot, (Item 10) Stations 50.01, .02, and .03, Site Fox.

effects (14 psi) destroyed the plywood room but caused no structural damage to the existing reinforced-concrete structures.

No additional damage was sustained as a result of Shot Redwood.

3.4 SITES SUGAR AND TARE

The effects of Shot Nutmeg (24 kt), Hickory (13.4 kt), and Juniper (63.8 kt) are reported



Figure 3.29(a) Post-Maple, (Item 10) Stations 50.01, .02, and .03. Pressure levels: Maple, 350 psi, 260 psi, and 190 psi, respectively.

herein. The shot geometry, with pressure contours and test stations for these sites, is shown in Figure 3.32. A post-Nutmeg picture, Figure 3.33, taken from above surface zero shows most of the test stations. A comparison of Figures 3.34 and 3.35 shows the damage to the timber bulkhead and sandbags located at the end of Tare before and after Shot Nutmeg. Severe shock from the first shot cracked the recording disks for both air-overpressure gages, the locations of which are shown in Figure 3.32. However, the records were pieced together and the recorded results for Stations 174.33A and B were 265 psi (estimated peak) and 310 psi, respectively, while

the predicted pressures for these two locations were 330 psi and 310 psi, respectively.

Shot Hickory had no appreciable effect on the island or any of the structures on the island.

The east end of Site Tare was severely washed by the effects of Shot Juniper as can be observed in Figure 3.36 showing that Items 14, 15, and 16 are now located in water, while Item 17 is now located on the high tide line. No structural damage was imparted to any of the structures.



Figure 3.29(b) Post-Maple, (Item 10) Station 50.03.
Pressure level: Maple, 190 psi; 800 cal/cm².

3.4.1 Item 12, Stations 2200 and 2250. Station 2200, a reinforced-concrete, photographic bunker was originally constructed and remained undamaged during Operation Castle (1954). The station was rehabilitated with additions for Operation Redwing (1956) and received damage only to several adjoining retaining walls. For Operation Hardtack (1958), the station was again re-

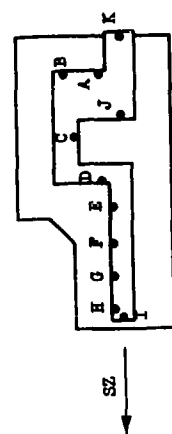


Figure 3.29(c) Post-Redwood, (Item 10) Station 50.03.
Pressure level: Redwood, 360 psi, 1,400 cal/cm².

habilitated with more additions. A 150-foot diagnostic tower designated as Station 2250 was erected atop Station 2200.

The stations were located in the 8.2-psi range from Shot Hickory and minor damage was received by the elevator cab of the tower. No damage was incurred from the other shots. A general postshot picture is shown in Figure 3.37.

TABLE 3.3 RECORDED RADIATION WITHIN STATION 78.01 (ITEM 5)
See Figure 3.18 for detailed location of film badges. All badges are located 3 feet above floor level.



Plan of Film-Badge Locations

Shot	Radiation, r. at Film-Badge Locations																	
	A			B			C			D			E			F		
	a*	b†	c‡	a*	b†	c‡	a*	b†	c‡	a*	b†	c‡	a*	b†	c‡	a*	b†	c‡
Fir	3.7	3.0	—	3.0	—	—	—	—	—	0	—	—	0	0	0	0	0	0
Sycamore	0.9	—	—	0	—	—	—	—	—	0	—	—	0	0	0	0	0	—
Maple	1.3	1.1	1.1	1.2	1.1	1.0	1.4	1.1	1.1	1.2	1.1	1.1	—	—	—	—	—	—
Aspen	1.6	1.6	1.7	1.1	1.1	1.1	0.8	0.8	0.8	0.6	0.6	0.6	0.5	0.5	0.5	0.5	0.5	2.3
																		23.0

* Plane of badge, on surface of wall.

† Plane of badge, normal to both wall and ceiling.

‡ Plane of badge normal to wall and parallel to ceiling.

TABLE 3.4 FREE-FIELD AIR-OVERPRESSURE MEASUREMENTS, SITES CHARLIE AND TARE

See Figure 3.13 for location of Stations 174.32A and B and Figure 3.32 for location of Stations 174.33A and B.

Shot	Site	Station 174.32A				Station 174.32B			
		Ground Range (d)	d/W ^{1/3} ft/kt ^{1/3}	Positive Duration sec	Maximum Overpressure psi	Ground Range (d)	d/W ^{1/3} ft/kt ^{1/3}	Positive Duration sec	Maximum Overpressure psi
Fir	Charlie	5,715	515	1.325	44.5	5,826	525	—	36.0
Sycamore		5,715	1,259	1.043	7.1	5,826	1,284	1.047	7.3
Aspen		5,715	836	1.720	14.5	5,826	852	1.535	12.6
		Station 174.33A				Station 174.33B			
Nutmeg	Tare	638	221	—	310.0	639	221	—	265*

* Partial record, peak overpressure was estimated.

3.4.2 Item 13, Station 2210. A reinforced-concrete, sand-mounded connector pit with the front wall sloping at $1\frac{1}{2}$ to 1 on the side facing the zero station was constructed during Operation Hardtack (1958). The walls (except the sloping front wall) were about the same size and configuration as those of the structure shown in Figure 3.41.

This structure was located in the estimated 170-, 90-, and 430-psi air-overpressure region

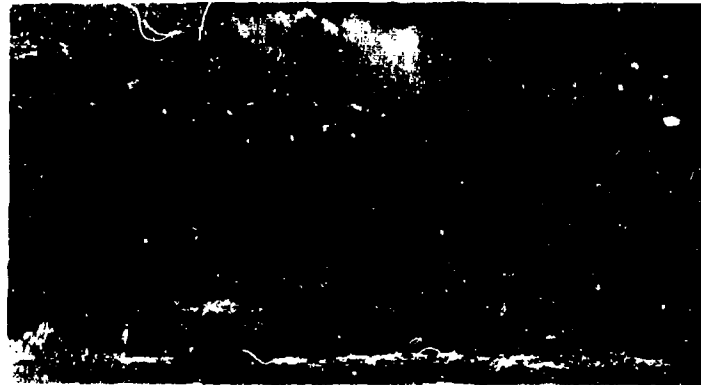


Figure 3.30 Preshot, (Item 11) Station 1810, Site George.

for Shots Nutmeg, Hickory, and Juniper, respectively, and was not damaged structurally by any of the shots. A view of this structure prior to being mounded with sand is shown in Figure 3.38. Sand was placed level with the roof of the structure.

3.4.3 Item 14, Station 2270. A small, reinforced-concrete connector pit mounded over with



Figure 3.31 Post-Maple, (Item 11) Station 1810. Pressure level: Maple, 14 psi.

sand was constructed during Operation Hardtack (1958). A preshot view of this station prior to being covered with sand is shown in Figure 3.39.

This station was located in the estimated 490-, 260-, and 1,400-psi overpressure range for Shots Nutmeg, Hickory, and Juniper, respectively. Even though the station was exposed to extremely high overpressures it was not damaged structurally. A post-Juniper view of this structure is shown in Figure 3.36.

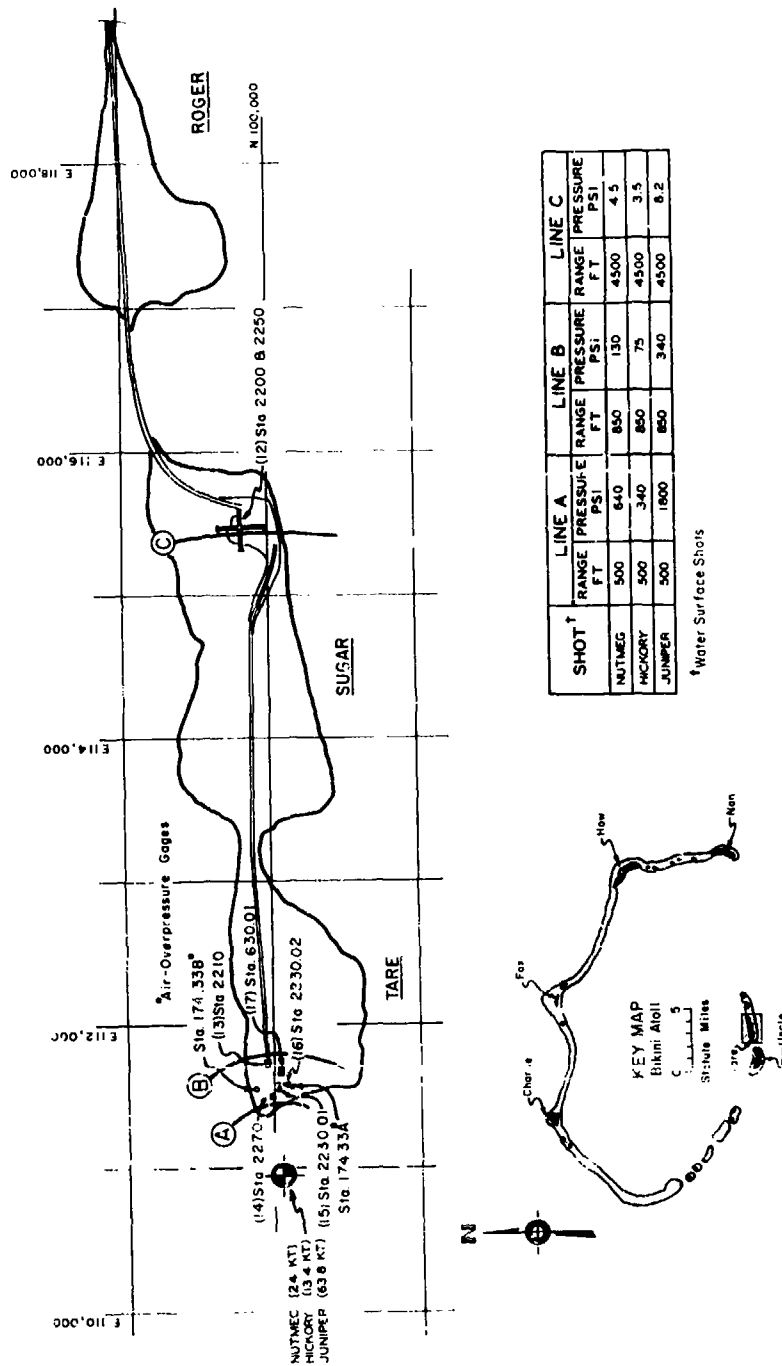


Figure 3.32 Shot Geometry with pressure contours for Sites Tare and Sugar.

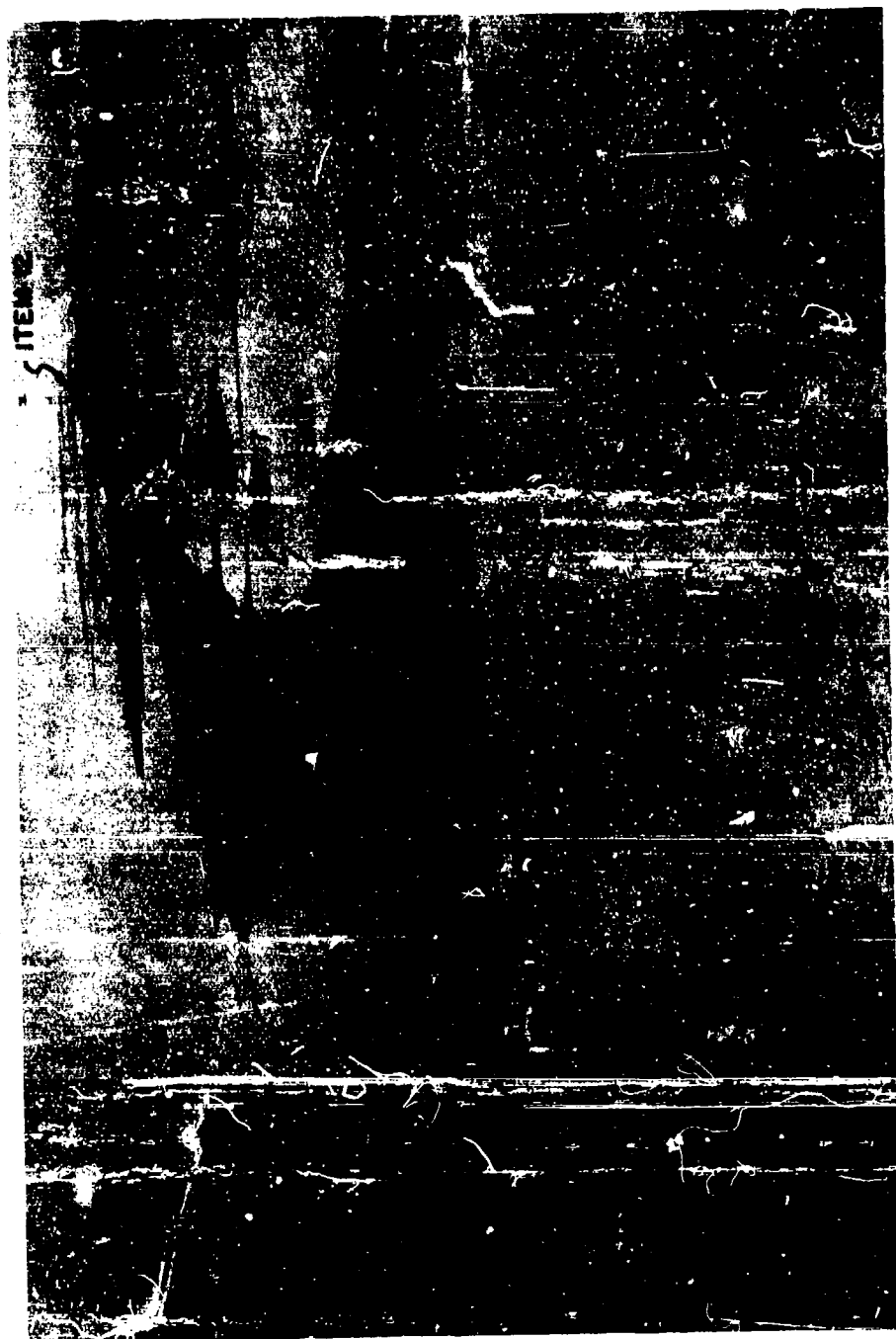


Figure 3.33 P. st-Nutmeg, general view of Sites Sugar and Tare.



Figure 3.34 Preshot view of timber bulkhead and sand bags at west end of Site Tare.

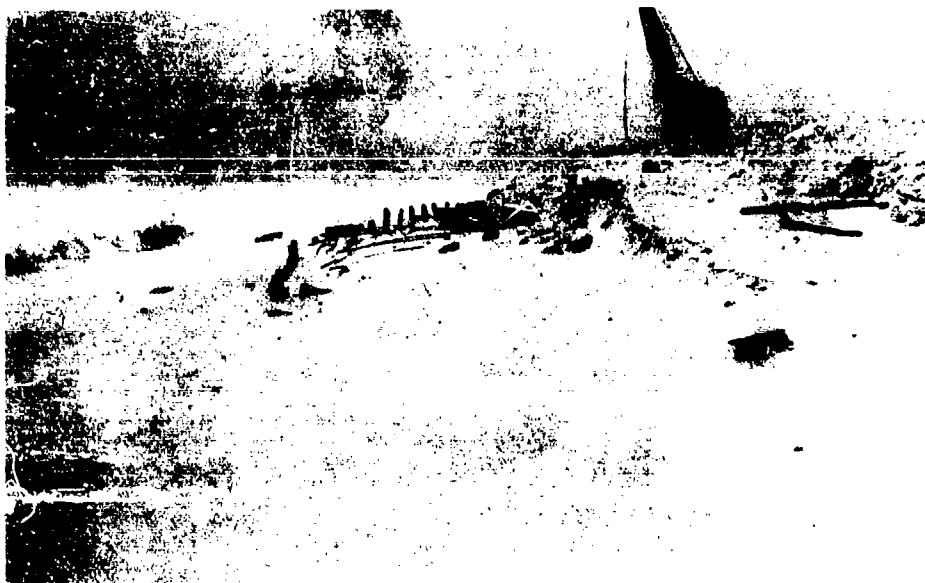


Figure 3.35 Post-Nutmeg view of timber bulkhead and sand bags at west end of Site Tare. Pressure level: Nutmeg, 650 psi.



Figure 3.36 Post-Juniper view of east end of Site Tare looking toward surface zero.

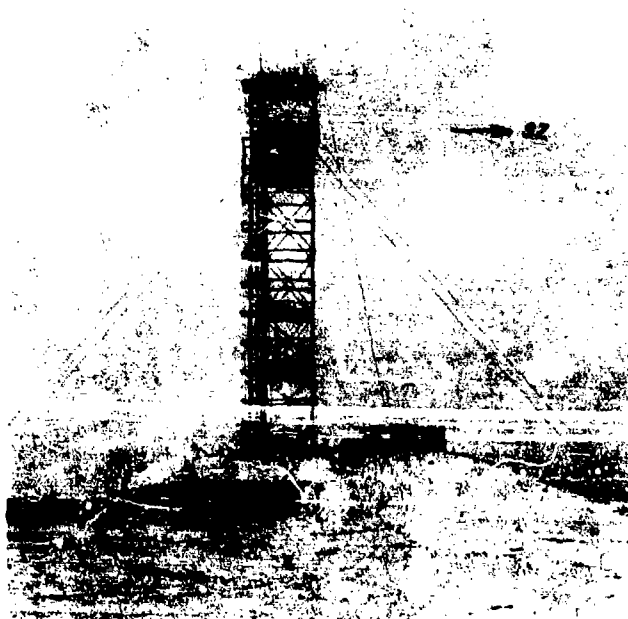


Figure 3.37 Post-Nutmeg, (Item 12) Stations 2200 and 2250.



Figure 3.38 Preshot, (Item 13) Station 2210, Site Tare, prior to being covered with sand.



Figure 3.39 Preshot, (Items 14, 15, and 16) Stations 2270, 2280.01, and 2280.02, Site Tare, prior to being covered with sand.



Figure 3.40 Post-Nutmeg, (Items 15 and 16) Stations 2230.01 and 2230.02. Pressure levels: Nutmeg, 350 and 320 psi, respectively.

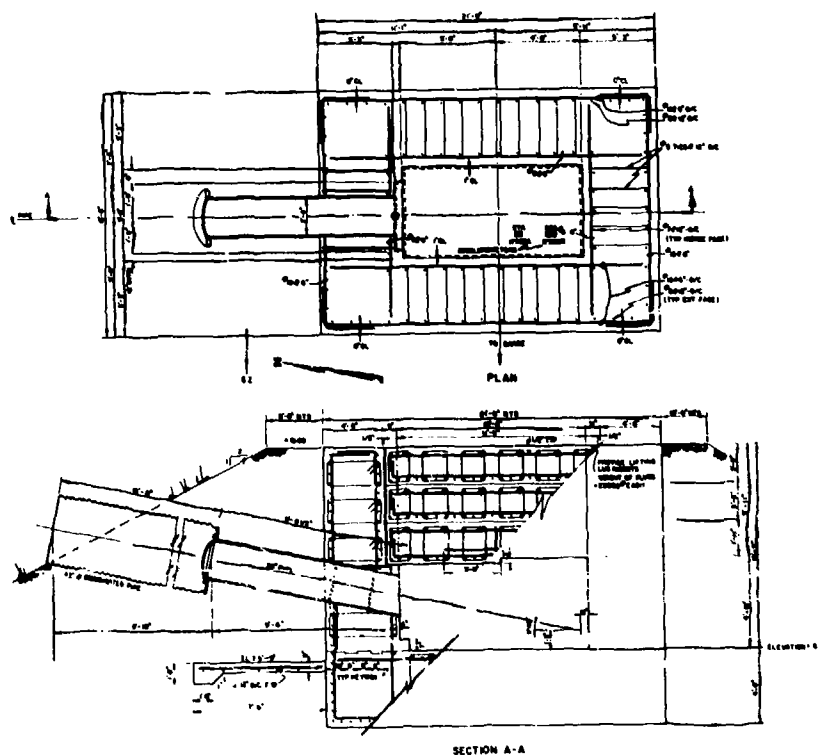


Figure 3.41 Plan and elevation including the location of self-recording accelerometers for (Item 16) Station 2230.02, Site Tare.

3.4.4 Item 15, Station 2230.01. A reinforced-concrete detector structure was constructed during Operation Hardtack (1958). For practical purposes the plans for this station were the same as those shown in Figure 3.41 for Station 2230.02 except that the walls were 6 inches greater in thickness.

This station was located in the estimated 350-, 200-, and 1,050-psi air-overpressure range for Shots Nutmeg, Hickory, and Juniper, respectively, and was undamaged. However, the structure settled 5 inches and moved 1.5 inches toward surface zero after Shot Nutmeg. Comparable measurements after the other two shots are not available. For a general preshot view of this structure prior to being mounded with sand, see Figure 3.39. A post-Nutmeg view, including the removed closure plugs, is shown in Figure 3.40.

3.4.5 Item 16, Station 2230.02. A reinforced-concrete detector structure was constructed during Operation Hardtack (1958). The plan and section for this structure, including the location

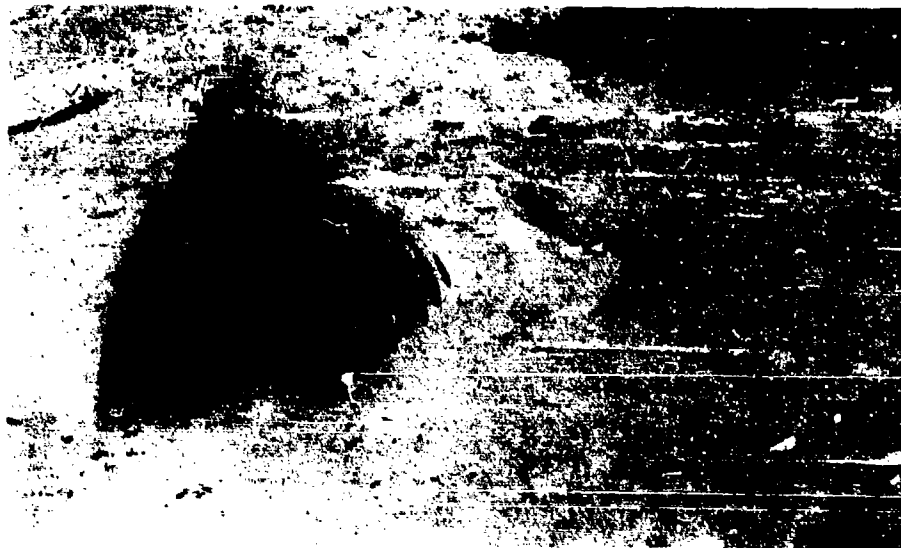


Figure 3.42 Post-Nutmeg, (Item 16) Station 2230.02, close-up of damaged 42-inch corrugated metal pipe. Pressure level: Nutmeg, 320 psi.

of self-recording accelerometers, are shown in Figure 3.41.

This station was located in the estimated 320-, 180-, and 1,000-psi air-overpressure range from Shots Nutmeg, Hickory, and Juniper, respectively, and was undamaged. However, sea water that leaked past the closure plugs into the structure as a result of the water wave from Shot Nutmeg corroded the recording disks of the accelerometers, thus causing a loss of the data. A general, preshot view of the structure and the attached 42-inch, round, corrugated-metal pipe, prior to being mounded with sand, is shown in Figure 3.39. Damage to the pipe after Shot Nutmeg is shown in Figures 3.40 and 3.42.

3.4.6 Item 17, Station 630.01. A reinforced-concrete instrumentation pit was constructed during Operation Hardtack (1958).

The station was situated in the estimated 210-, 120-, and 560-psi air-overpressure range from Shots Nutmeg, Hickory, and Juniper, respectively, and suffered no apparent damage.

Chapter 4

RESULTS: ENIWETOK ATOLL

This chapter pertains to the results obtained at the Eniwetok Atoll; however, the introductory remarks of Chapter 3 are applicable here as well.

The general test results and description of the stations investigated at Eniwetok, including estimated peak overpressure, duration, free-field gamma radiation, and floor-slab acceleration where applicable, are summarized in Table 4.1.

4.1 SITES GENE, HELEN, AND IRENE

The effects of Shots Koa (1.38 Mt), Yellowwood (340 kt), Tobacco (11.7 kt), Walnut (1.45 Mt), Elder (940 kt), Dogwood (397 kt), Olive (202 kt), and Pine (2.1 Mt), are reported at these sites. The shot geometry, with pressure contours and test stations, is shown in Figure 4.1. The detailed information concerning the effects on the various stations from each shot is presented in Table 4.1.

Small craters ranging from 30 to 60 feet in diameter and 6 to 10 feet deep dotted site Irene and were generally located near the long pipeline extending from Station 1410 to ground zero. It is believed that these craters were of the impact type (as indicated by wide, flat bottoms) and formed by missiles (possibly concrete blocks used for the pipeline foundation or pieces of coral) resulting from Shot Koa. A typical crater of this type is shown in Figure 4.2; the concrete block in the picture was one of the foundation blocks for the pipeline.

4.1.1 Item 18, Station Complex. A reinforced-concrete recording station was constructed during Operation Redwing (1956) and received no major damage during that operation. This station was rehabilitated for use in Operation Hardtack (1958), and various parts of it designated as Stations 73.01, 1314, 1524, and 1611. The general plan for the station complex and other adjoining stations is shown in Figure 4.3.

The highest overpressure received by the complex was an estimated 42 psi from Shot Koa. The interior of the station was not damaged by any of the shots. The reinforced-concrete wing wall located at the entranceway (Figure 4.4) was slightly cracked prior to any of the shots. The wing wall was not keyed to the structure nor was reinforcing steel used to tie the two together. The wall was side-on to the blast wave from Koa (40-psi range) but received no additional damage. The same wall was face-on to the blast from Yellowwood (11.5-psi range) and was cracked loose from the main structure. The vertical crack was approximately $\frac{3}{4}$ inch wide and extended the entire height of the wall (Figure 4.5). The wall failed from the face-on blast effects of Walnut (28-psi range) and cracked loose at the intersection of the ground surface behind the wall (Figure 4.6). The remaining shots had no additional effects.

The results obtained from the film badges located as shown in Figure 4.3 are shown in Table 4.2.

4.1.2 Item 19, Station 1525. A reinforced-concrete diagnostic station was constructed during Operation Hardtack (1958). The general location of this station is shown in Figure 4.3 and the detailed plan and elevations are shown in Figure 4.7.

This station received the highest estimated overpressure of 42 psi from Shot Koa. The retaining wall integral with the front wall of the structure was severely damaged by face-on air blast from Shot Koa but received no additional damage from Shots Yellowwood or Tobacco. However, one end of the wall was destroyed by Shot Walnut. A preshot view of the front wall with

TABLE 4.1 SUMMARY OF RESULTS AT ENWETOK ATOLL

Site	Item Number	Station Description	Shot	Yield	Ground Range to Ground Zero or Surface Zero	Predicted				Remarks
						Peak Overpressure	Duration	Free-Field Gamma Radiation	Floor Slab Acceleration	
					ft.	psi	sec	r/hr	g	
Irwin	18	Station Complex. A concrete shelter, addition to 1811 Station 1523, 1334, and 1311. No damage to interior of station from Huda Apache, Semihole, or Huda of Operation Redwing.	Koa	1.38 Mt	5,340	42	1.85	13,000	6.7	No damage
			Yellowwood	340 kt	6,210	11.5	1.55	800	0.4	Light damage to retaining wall
			Tobacco	11.7 kt	6,140	1.9	0.89	20	0	No additional damage
			Walnut	1.45 Mt	6,510	28	1.86	4,000	3.6	Retaining wall failed
			Elder	940 kt	6,140	23	1.80	4,100	2.3	No additional damage
			Dogwood	397 kt	6,140	13	1.55	1,300	0.7	No additional damage
			Olive	292 kt	6,140	9.5	1.38	369	0.2	No additional damage
			Pine	2.1 Mt	7,720	28	2.30	1,400	3.3	No additional damage
			Koa	1.38 Mt	5,300	42	1.85	13,000	6.9	Severe damage to retaining wall
			Yellowwood	340 kt	6,700	11	1.57	450	0.4	No additional damage
	19	Station 1825. A reinforced concrete floor station.	Tobacco	11.7 kt	6,240	1.3	0.91	14	0	No additional damage
			Walnut	1.45 Mt	6,700	27	2.00	3,000	3.2	Retaining wall failed
			Elder	940 kt	6,240	22	1.82	2,500	2.0	No additional damage
			Dogwood	397 kt	6,240	14	1.57	300	0.6	No additional damage
			Olive	292 kt	6,240	9	1.40	250	0.2	No additional damage
			Pine	2.1 Mt	7,890	26	2.32	1,100	3.2	No additional damage
			Koa	1.38 Mt	5,390	42	1.85	15,000	6.0	Light damage
			Yellowwood	340 kt	6,480	11	1.55	600	0.4	No additional damage
			Tobacco	11.7 kt	6,120	1.9	0.89	18	0	No additional damage
			Walnut	1.45 Mt	6,480	28	1.96	4,000	3.5	Additional light damage
	20	Station 1311. A concrete detector station mounted with earth.	Elder	940 kt	6,120	23	1.80	3,500	2.3	No additional damage
			Dogwood	397 kt	6,120	13	1.55	1,100	0.6	No additional damage
			Olive	292 kt	6,120	9.5	1.32	480	0.2	No additional damage
			Pine	2.1 Mt	7,870	27	2.30	1,300	3.5	No additional damage
			Koa	1.38 Mt	5,210	43	1.85	2,800	7.4	No damage
			Yellowwood	340 kt	6,710	11	1.57	450	0.5	No damage
			Tobacco	11.7 kt	6,360	1.8	0.91	14	0	No damage
			Walnut	1.45 Mt	6,710	26	2.00	3,000	3.2	No damage
			Elder	940 kt	6,380	21	1.82	2,500	2.0	No damage
			Dogwood	397 kt	6,380	13	1.57	830	0.6	No damage
	21	Stations 1410 and 1211. A reinforced concrete structure and terminals of pipelines	Olive	292 kt	6,380	9	1.40	270	0.2	No damage
			Pine	2.1 Mt	7,870	26	2.32	1,000	3.3	No damage
			Koa	1.38 Mt	5,340	42	1.85	13,000	6.7	No damage
			Yellowwood	340 kt	6,210	11.5	1.55	800	0.4	Light damage to retaining wall
			Tobacco	11.7 kt	6,140	1.9	0.89	20	0	No additional damage
			Walnut	1.45 Mt	6,510	28	1.86	4,000	3.6	Retaining wall failed
			Elder	940 kt	6,140	23	1.80	4,100	2.3	No additional damage
			Dogwood	397 kt	6,140	13	1.55	1,300	0.7	No additional damage
			Olive	292 kt	6,140	9.5	1.38	369	0.2	No additional damage
			Pine	2.1 Mt	7,720	28	2.30	1,400	3.3	No additional damage

TABLE 4.1 CONTINUED

Site	Item Number	Station Description	Shot	Yield	Ground Range to Zero or Surface Zero	Peak Overpressure	Duration	Predicted			Remarks
								Initial Gamma Radiation	Free-Field Acceleration	Floor Slab Acceleration	
					ft	psi	sec	r/hr	g	g	
Irene	22	Station 3.4. A reinforced concrete signal terminal pt.	Koa	1.38 Mt	5,850	34	1.90	7,000	4.9	No damage	
			Yellowwood	340 kt	6,130	13	1.50	1,000	0.5	No damage	
			Tobacco	11.7 kt	5,820	2.1	0.86	34	0	No damage	
			Walnut	1.45 Mt	6,130	32	1.93	6,700	4.4	No damage	
			Elder	940 kt	5,820	28	1.74	6,700	3.1	No damage	
	23	Generators. Four, 75-kva, diesel-driven units.	Dogwood	397 kt	5,820	16	1.48	2,500	0.9	No damage	
			Olive	202 kt	5,820	11	1.32	740	0.3	No damage	
			Pine	2.1 Mt	7,490	29	2.23	1,500	3.8	No damage	
			Koa	1.38 Mt	5,810	38	1.88	10,000	5.3	Severe Damage	
			Koa	1.38 Mt	5,590	38	1.88	10,000	5.3	Complete destruction	
Janet	24	Helicopter Pad. 8-wal landing concrete recording station.	Koa	1.38 Mt	12,100	8.8	2.63	8	0.4	No damage	
			Yellowwood	340 kt	6,000	13	1.46	1,000	0.6	No damage	
			Tobacco	11.7 kt	4,000	3.7	0.70	300	0.02	No damage	
			Walnut	1.45 Mt	6,000	33	1.93	6,500	4.8	No damage	
			Elder	940 kt	4,000	58	1.56	46,000	9.8	No damage	
	25	Station 3.1.1. Three story test structure.	Dogwood	397 kt	4,000	31	1.29	13,000	2.9	No damage	
			Olive	202 kt	4,000	21	1.12	7,500	1.0	No damage	
			Pine	2.1 Mt	8,520	22	2.40	580	2.3	No damage	
			Koa	1.38 Mt	15,450	5.6	3.01	3	0.2	No damage	
			Yellowwood	340 kt	8,460	7	1.79	60	0.2	No damage	
	26	Station 3.1.2. (n larground test structure.	Tobacco	11.7 kt	6,810	1.7	0.94	10	0	No damage	
			Walnut	1.45 Mt	8,460	16	2.20	450	1.5	Severe damage to Bldg 5; light damage to Bldg 4.	
			Elder	940 kt	6,810	20	1.85	2,000	1.8	Bldg 5 collapsed; wood-erase damage to Bldgs 4 and 6; light damage to Bldgs 2 and 3.	
			Dogwood	397 kt	6,810	12	1.60	610	0.5	No additional damage	
			Olive	202 kt	6,810	8.4	1.44	280	0.2	No additional damage	
27	Station 3.1.3. (n larground test structure.	Pine	2.1 Mt	10,870	13	2.65	70	70	1.1	No additional damage	
		Koa	1.38 Mt	14,250	6.4	2.86	1	0.3	No additional damage		
		Yellowwood	340 kt	7,450	8.6	1.63	190	0.3	No damage		
		Tobacco	11.7 kt	5,520	2.3	0.85	40	0	No damage		
		Walnut	1.45 Mt	7,450	21	2.09	1,400	2.2	No damage		
			Elder	940 kt	5,520	29	1.73	7,400	3.2	No damage	
			Dogwood	397 kt	5,520	17	1.47	2,300	0.9	No damage	
			Olive	202 kt	5,520	11	1.31	1,100	0.3	No damage	
			Pine	2.1 Mt	9,910	16	2.54	150	1.4	No damage	

TABLE 4.1 CONTINUED

Site	Item Number	Station Description	Shot	Yield	Ground Range to Ground Zero or Surface Zero	Predicted			Remarks
						Peak Overpressure	Duration	Initial Free-Field Gamma Radiation	Floor Slab Acceleration
					ft	psi	sec	r/hr	g
Janet	28	Station 20-B. 8 reinforced concrete gage pier.	Koa	1.38 Mt	13,920	6.6	2.84	24	0.3
			Yellowwood	340 kt	6,890	10	1.60	270	0.3
			Tobacco	11.7 kt	5,010	2.6	0.78	75	0.01
			Walnut	1.45 Mt	6,890	25	2.03	2,650	2.8
									Severe damage, failure at base of stem
29		Station 77.02. A reinforced concrete, earth mounded timing station.	Elder	940 kt	5,010	35	1.67	14,000	4.6
			Dogwood	387 kt	5,010	20	1.40	4,500	1.3
			Olive	202 kt	5,010	14	1.24	2,100	0.5
			Pine	2.1 Mt	9,400	77	2.49	300	1.8
			Koa	1.38 Mt	16,640	1.2	3.12	0.2	0.1
			Yellowwood	340 kt	6,790	7.6	1.81	36	0.2
			Tobacco	11.7 kt	7,200	1.6	0.96	5	0
			Walnut	1.45 Mt	8,790		2.24	280	1.3
			Elder	940 kt	7,200	17	1.91	1,000	1.4
			Dogwood	387 kt	7,200	10	1.67	360	0.4
			Olive	202 kt	7,200	7.2	1.53	110	0.1
			Pine	2.1 Mt	10,770	14	2.63	60	1.1
30		Landing Pier.	Koa	1.38 Mt	14,670	6.2	2.90	0.6	0.2
			Yellowwood	340 kt	7,200	9.5	1.83	250	0.3
			Tobacco	11.7 kt	5,400	2.3	0.83	45	0
			Walnut	1.45 Mt	7,200	23	2.06	1,500	2.5
			Elder	940 kt	5,400	30	1.71	8,400	3.7
			Dogwood	387 kt	5,400	17	1.45	3,000	1.0
			Olive	202 kt	5,400	12	1.29	1,100	0.4
			Pine	2.1 Mt	8,470	18	2.48	220	1.8
			Koa	1.38 Mt	16,200	5.2	3.10	0.7	0.1
			Cactus	17 kt	500	450	0.38	300,000	32
									Light damage to tunnel only
									Severe damage
Yvonne	31	Station 1130. A reinforced concrete bunker with a side tunnel.	Cactus	17 kt	500	450	0.38	300,000	32
	32	Station 1220.01. Cubicle mounted on a structural steel platform.	Cactus	17 kt	500	450	0.38	300,000	32
	33	Station 1216. A reinforced concrete terminal for a pipeline.	Cactus	17 kt	500	450	0.38	300,000	32
									No damage

TABLE 4.1. CONTINUED

Site	Item Number	Station Description	Shot	Yield	Ground Zero or Surface Zero	Peak Overpressure	Duration	Predicted			Remarks
								Initial Gamma Radiation	Floor Slab Acceleration	Free-Field Gamma Radiation	
Yvonne	34	Station 1812. A reinforced concrete, earth-mounded Trilux station.	Cactus	17 kt	330	1,400	0.38	650,000	120		Severe damage to retaining wall; light damage to structure.
	35	Stations 1822.0' to .04. Four steel-pipe towers enclosed by plywood covering.	Cactus	17 kt	500	450	0.38	300,000	32		Complete destruction
36		Station 1310. A large, massive, reinforced concrete, earth-mounded structure.	Cactus	17 kt	4,130	4.5	0.75	300	0.01		No damage
			Butternut	80 kt	4,130	12	0.57	2,200	0.3		No damage
			Holly	8.8 kt	2,130	7.6	0.44	2,800	0.04		No damage
			Magnolia	57 kt	3,130	16	0.80	5,700	0.4		No damage
			Rose	14.5 kt	4,130	4.2	0.74	300	0.02		No damage
			Lil. Jon	11.1 kt	2,720	12	0.50	5,500	0.1		No damage
			Sequoia	5.3 kt	2,130	7.3	0.44	2,800	0.04		No damage
			Fig	21.5 tons	1,100	1.1	—	1,360	0		No damage
			Pineola	255 kt	12,000	3.3	2.10	0	0		No damage
			Butternut	80 kt	5,510	6.5	1.13	350	0.08		Light damage
			Holly	5.8 kt	4,200	2.4	0.46	100	0		No additional damage
			Magnolia	57 kt	4,910	7	1.00	550	0.06		Additional light damage
			Rose	14.5 kt	5,910	2.5	0.86	42	0.02		No additional damage
37		Water tank. A 21,000 gal tank of 1/4-inch steel plate, 8 ft high, and 10 ft 10 in. in radius	Linden	11.1 kt	4,200	3.4	0.70	220	0.01		No additional damage
			Sequoia	5.3 kt	4,200	2.2	0.64	100	0		No additional damage
			Pineola	255 kt	14,400	2.6	2.15	0	0		No additional damage
			Cactus	17 kt	7,760	1.6	1.06	3.4	0		Severe damage
			Butternut	80 kt	5,530	6.8	1.13	300	0.02		Complete destruction
Yvonne Camp.											

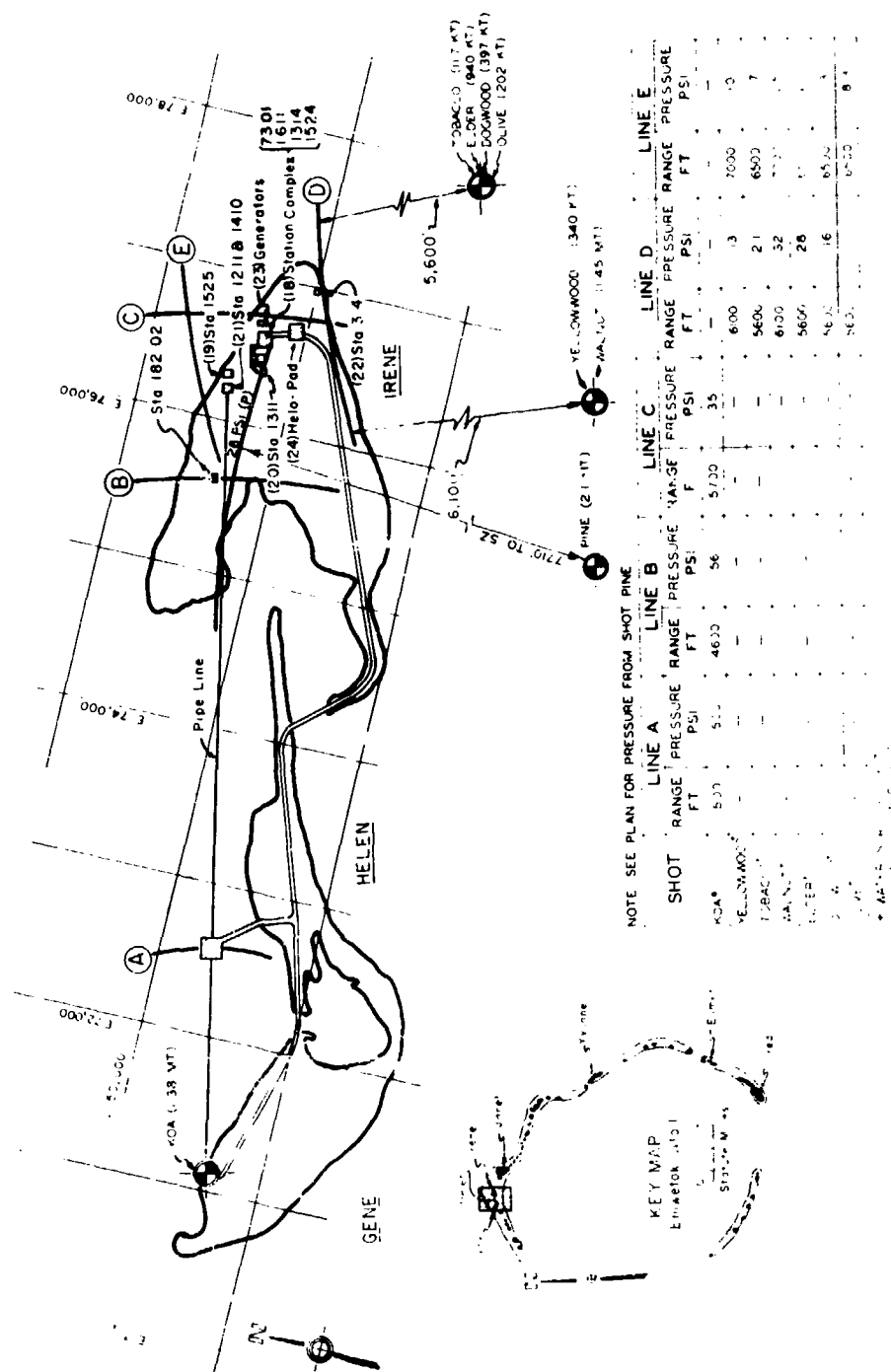
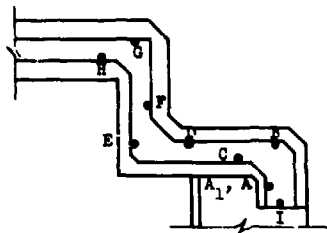


Figure 4.1 Shot geometry with pressure contours and station locations for Sites Gene, Helen, and Irene.

TABLE 4.2 RECORDED RADIATION WITHIN STATION COMPLEX (ITFM 18)

See Figure 4.3 for detailed location of film badges. All badges are located 3 feet above floor level with the plane of the badge on the surface of the wall except as noted.

Plan of Film-Badge Locations



Shot	Radiation, r, at Film-Badge Locations									
	A	A ₁ *	B	C	D	E	F	G	H	I†
Koa	90.0	—	46.0	4.90	1.02	0.52	0.17	0.12	0.11	—
Yellowwood	44.0	—	220.0	5.00	0.30	0.10	0	0	0	—
Walnut	800.0	—	950.0	130.0	7.85	1.80	0.77	—	—	—
Elder	700.0	700.0	610.0	44.0	10.2	1.80	—	—	—	830.0

* Plane of badge normal to both wall and ceiling.

† Plane of badge on back side of I-beam stiffener of blast door.



Figure 4.2 Post-Koa, typical impact crater, 4,800 feet from ground zero.

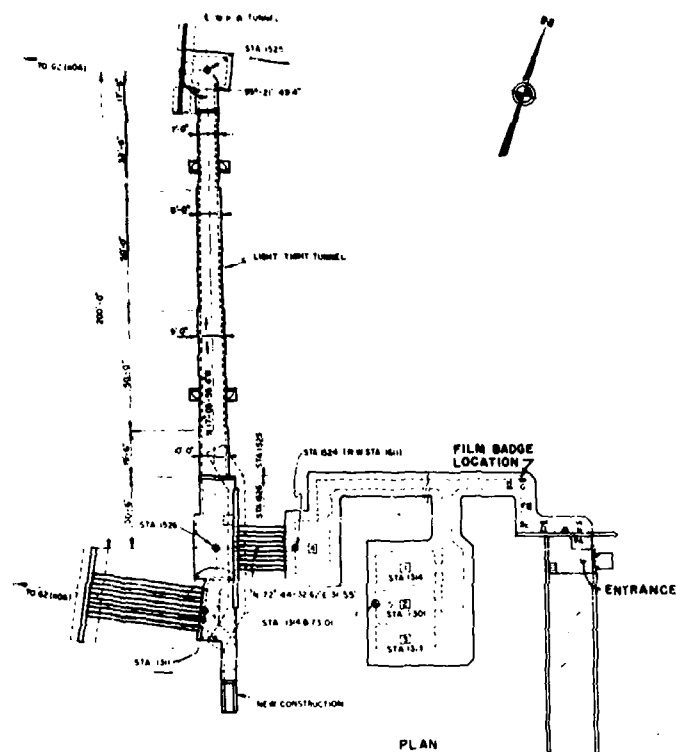


Figure 4.3 Plan of station complex on Site Irene.



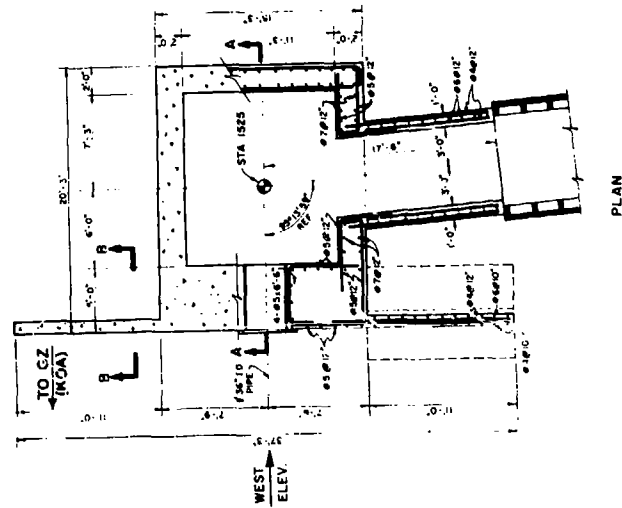
Figure 4.4 Preshot, (Item 18) station complex, close-up of entrance and crack in wing wall, Site Irene.



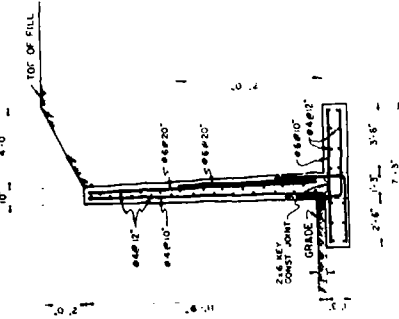
Figure 4.5 Post-Yellowwood, (Item 18) station complex, close-up of entrance and cracked wing wall. Pressure levels: Koa, 42 psi; Yellowwood, 11.5 psi; and Tobacco, 1.9 psi.



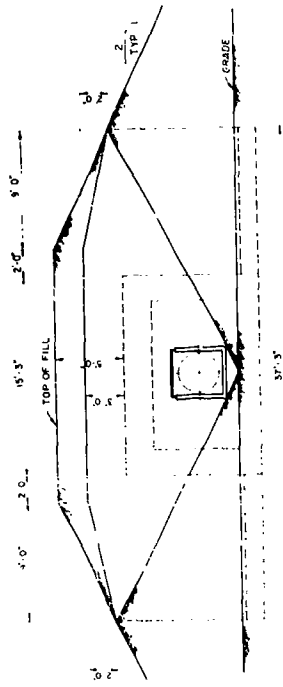
Figure 4.6 Post-Walnut, (Item 18) station complex, close-up of wing wall failure. Pressure level: Walnut, 28 psi.



SECTION A-A



SECTION 8-3.



WEST ELEVATION

Figure 4.7 Plan and elevations for (Item 19) Station 1525, Site Irene.

its painted surface is shown in Figure 4.8. The retaining wall cracked around the outline of the side walls and ceiling of the structure as shown in Figure 4.9. The diagonal cracks indicate the bending failure of the wall. A side view is shown in Figure 4.10. The damage from Shot Walnut is shown in Figure 4.11. No significant damage was observed from the remaining shots.

Thermal radiation burned the paint off the structure, as can be observed by comparing Figures

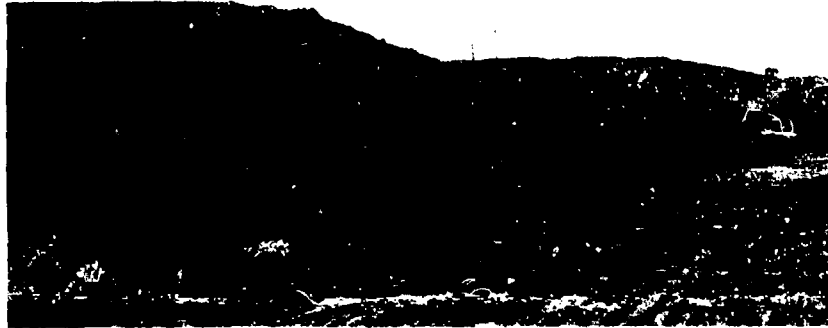


Figure 4.8 Preshot, (Item 19) Station 1525, Site Irene.

4.8 and 4.9; the total thermal radiation was approximately 350 cal/cm^2 .

4.1.3 Item 20, Station 1311. A reinforced-concrete detector station was constructed during Operation Hardtack (1958). The general location of this station is shown in Figure 4.3 and the detailed plan and elevations are shown in Figure 4.12.



Figure 4.9 Post-Koa, (Item 19) Station 1525, face-on view.
Pressure level: Koa, 42 psi; 350 cal/cm^2 .

The highest overpressure received at this station was an estimated 42 psi from Shot Koa. The station was structurally damaged mainly from the effects of Shots Koa and Walnut. A pre-shot view of the retaining wall for this station is shown in Figure 4.13, a post-Koa view is shown in Figure 4.14, and a post-Walnut view is shown in Figure 4.15.

The thermal radiation (and sand blast) had some surface effects on the retaining wall; the thermal radiation was approximately 350 cal/cm^2 .

The entrance to this station was nearly filled with sand as the result of Shot Koa, as shown by comparing Figures 4.16 and 4.17.

The plain-concrete floor of this station was badly cracked and the five 24-inch pipes entering this station were forced inward about $2\frac{1}{4}$ inches (Figure 4.18). The crack pattern (shown in Figure 4.19) indicates that the existing foundation underneath part of the floor gave additional support to that portion.



Figure 4.10 Post-Koa, (Item 19) Station 1525, side-on view.
Pressure level: Koa, 42 psi.

4.1.4 Item 21, Stations 1211 and 1410. A reinforced-concrete structure situated at the Irene terminus of a large pipeline from Gene was erected during Operation Hardtack (1958).

The highest pressure received by this station was an estimated 43 psi from Shot Koa. The structure was not damaged structurally by any of the shots. However, the earth cover on the



Figure 4.11 Post-Walnut, (Item 19) Station 1525, retaining wall failure. Pressure level: Walnut, 27 psi.

side of the structure facing surface zero for Shot Walnut was blown and washed away, exposing the concrete wall surface (Figures 4.20 and 4.21).

A preshot view of the 5,200-foot-long pipeline leading from this station to ground zero is shown in Figure 4.22. A postshot view is shown in Figure 4.23. Only about 800 feet of pipe farthest from ground zero remained in the area and connected in one piece after Shot Koa. This



Figure 4.13 Preshot, (Item 20) Station 1311, face-on view of retaining wall, Site Irene.



Figure 4.14 Post-Koa, (Item 20) Station 1311, face-on view of retaining wall. Pressure level: Koa, 42 psi; 350 cal/cm².



Figure 4.15 Post-Walnut, (Item 20) Station 1311, face-on view of retaining wall. Pressure level: Walnut, 28 psi.



Figure 4.16 Preshot, (Item 20) Station 1311, entrance, Site Irens.



Figure 4.17 Post-Koa, (Item 20) Station 1311, entrance.
Pressure level: Koa, 42 psi.

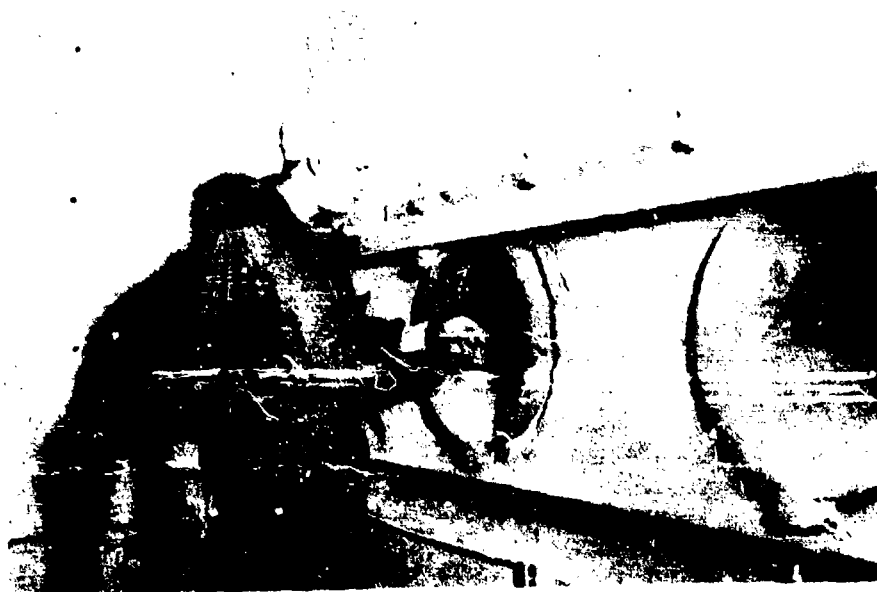


Figure 4.18 Post-Koa, (Item 20) Station 1311, 24-inch steel
pipes pushed inward $2\frac{1}{4}$ inches. Pressure level: Koa, 42 psi.

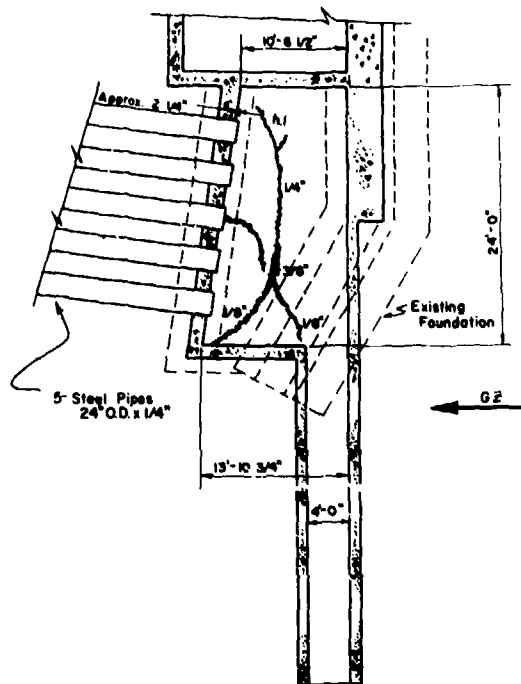


Figure 4.19 Post-Koa, (Item 20) Station 1311, crack pattern in floor. Pressure level: Koa, 42 psi.



Figure 4.20 Preshot, (Item 21) Stations 1211 and 1410, view of side wall facing surface zero, Site Irene.

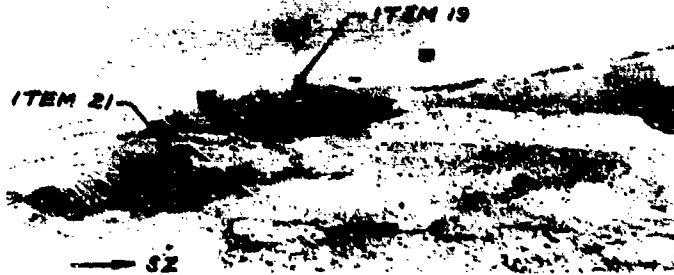


Figure 4.21 Post-Walnut, (Item 21) Stations 1211 and 1410, view of exposed side wall. Pressure level: Walnut, 26 psi.



Figure 4.22 Preshot, pipeline to ground zero, Site Irene.

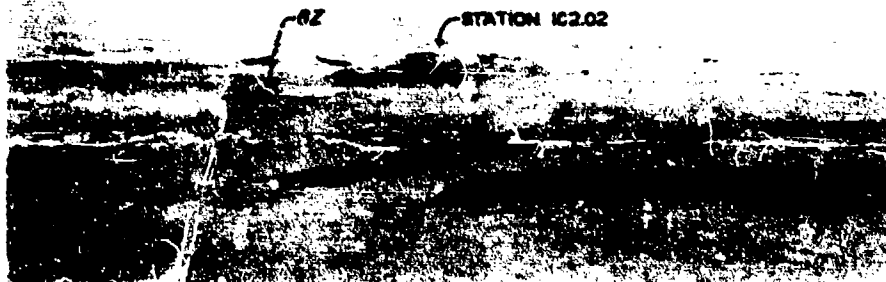


Figure 4.23 Post-Koa, pipeline to ground zero. Pressure level at near end: Koa, 45 psi.

portion was thrown from the concrete supports and was bent into a semicircular pattern with an approximate radius of 200 feet. The line of concrete supports is shown in the left portion of Figure 4.23. Most of the missing portions of the pipe were thrown into the area to the right in Figure 4.23.

4.1.5 Item 22, Station 3.4, Castle. A reinforced-concrete, signal terminal pit with a gravel floor was constructed and undamaged during Operation Castle (1954); neither was it damaged during Operation Redwing (1956).

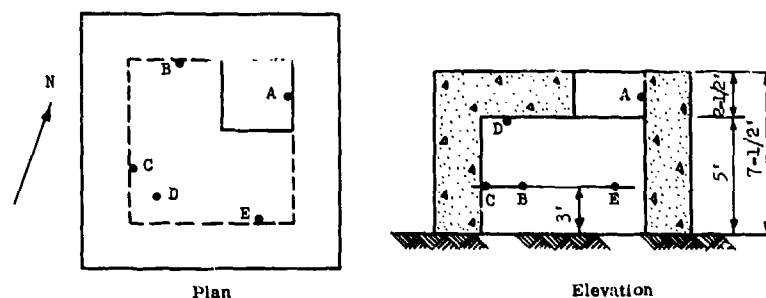
The highest estimated pressure received by this station was an estimated 34 psi from Shot Koa. The station was not damaged structurally from any of the shots. However, the hatch cover was not bolted down and the force from Shot Koa moved it horizontally $\frac{3}{4}$ inch away from ground zero.

The plan for this station, including the locations of film badges, is shown in Figure 4.24. The

TABLE 4.3 RECORDED RADIATION WITHIN STATION 3.4 (ITEM 22)

See Figure 4.24 for detailed location of film badges. All badges are positioned with the plane of the badge on the wall surface.

Film-Badge Locations



Shot	Radiation, r, at Film-Badge Locations				
	A	B	C	D	E
Koa	—	—	6.44	6.79	8.59
Yellowwood	6.29	1.77	0.68	0.67	0.65
Walnut	375.0	104.0	21.2	18.0	20.0
Elder	460.0	—	35.0	28.0	21.0

results of the film-badge readings are shown in Table 4.3. The water-wave action from Shot Walnut eroded the earth cover away from this structure, as shown in Figures 4.25 and 4.26. The dark area on the concrete walls represents the contact area of the preshot earth cover.

4.1.6 Item 23, Generators. Four 75-kva, diesel-driven generators (each 120 inches long, 37 inches wide, 78 inches high, and each weighing 6,700 pounds), located behind the station complex, were left in operation during Shot Koa.

The generators were located in the estimated 38-psi air-overpressure range for Shot Koa and were severely damaged. A preshot view of the generators is shown in Figure 4.27 along with standard, Navy, steel pontoon sections used as fuel tanks.

The earth mound approximately 15 feet above the ground surface for the station complex shielded the generators from the air blast to varying degrees. The generators were located approximately 40 feet from the intersection of the mound with the ground surface. The generator near the edge of the mound (least protected from air blast) was thrown 60 feet while the gen-



Figure 4.25 Preshot, (Rem 22) Station 3.4, side view, Site Irene.



Figure 4.26 Post-Walnut, (Rem 22) Station 3.4, side view showing scouring action of water wave; dark area represents original earth cover contact area. Pressure level: Walnut, 32 psi.



Figure 4.27 Preshot, (Rem 23) generators, Site Irene.

erator nearer the center of the mound (most protected) was moved 2 feet. The other two generators were thrown distances of 20 and 40 feet. A postshot view of the four generators is shown in Figure 4.28 and a close-up of one of the generators is shown in Figure 4.29. No additional damage to or movement of the generators occurred as the result of Shots Yellowwood (11.5 psi) or Tobacco (1.8 psi). The Na. / pontoon sections were not damaged from any of the shots; however, the air blasts from Shots Koa and Yellowwood moved the sections approximately 100 feet. Both the generators and pontoon sections underwent additional movement during Shot Walnut (28 psi). Movement from the remaining shots was not observed.

4.1.7 Item 24, Helicopter Pad. A helicopter pad approximately 100 by 100 feet, constructed of standard, interlocking, steel landing mat, was located near the station complex.

This station was subjected to an estimated air blast of 38 psi from Shot Koa, and was severely damaged. Individual pieces of landing mat were bent, broken, and scattered over a wide area. Both the negative and positive phase of the air blast scattered the mat. Pieces were found 400 feet from the original location away from ground zero; other pieces were moved a similar distance toward ground zero. A postshot view of the landing mat is shown in Figure 4.30. Because of the complete destruction resulting from Koa no further observations were made for the remaining shots.

4.2 SITE JANET

The effects of Shots Yellowwood (11.5 kt), Tobacco (11.7 kt), Walnut (1.45 Mt), Elder (940 kt), Dogwood (397 kt), Olive (202 kt), and Pine (2.1 Mt) were observed at Site Janet. Shot Koa had no real effect at this site. The shot geometry and pressure contours are shown in Figure 4.31. The thermal radiation from Yellowwood caused grass fires in scattered areas. Cracks on the ground surface apparently caused by ground shock from Shots Koa and Yellowwood were observed throughout the site.

4.2.1 Item 25, Station 1312. A large, 4-room, reinforced-concrete recording station was constructed during Operation Harotack (1958). The general plan for this structure, including the locations of the self-recording air-overpressure gages and accelerometers, is shown in Figure 4.32.

This station was located in an estimated 13-, 3.7-, 33-, 58-, 31-, 21-, and 22-psi air-overpressure range from Shots Yellowwood, Tobacco, Walnut, Elder, Dogwood, Olive, and Pine, respectively, and was not damaged by any of the shots.

The concrete face of the structure facing surface zero was pitted from the effects of Walnut and Elder. The total thermal radiation on the face of the structure was approximately 275 cal/cm² from Walnut and 450 cal/cm² from Elder. Since this station was very close to the shore line, the pitting of the front face must have been almost entirely the result of surface spalling of the concrete due to the thermal radiation. Steel surfaces exposed to this same radiation level on the face of the structure showed no structural effects.

The force of the water waves from Shot Walnut eroded the soil adjacent to the foundation of the structure to depths of 5 and 6 feet (Figure 4.33). Shot Elder had no additional effect.

The correlation of results of shock-tube tests on diffraction-type targets with similar results of full-scale tests are complicated due to the effects of precursor and dust loading in the field, which are not present in the shock tube. Because of the absence of precursor and dust effects the opportunity was afforded at Station 1312 to obtain data on the effect of a fast-rise-time pressure pulse on a diffraction-type structure, which could be more easily compared with similar results of shock-tube tests. Therefore, with the assistance of personnel of the Ballistics Research Laboratories, special efforts were made to obtain blast-diffraction data. For a detailed presentation of the diffraction study, see Appendix B.

The results of air-overpressure measurements are shown in Table 4.4. Due to malfunctions of the accelerometer gages no acceleration data was obtained.



Figure 4.28 Post-Koa, (Item 23) generators. Pressure level: Koa, 38 psi.



Figure 4.29 Post-Koa, (Item 23) close-up of damaged generator. Pressure level: Koa, 38 psi.

4.2.2 Item 26, Station 3.1.1, Greenhouse. A multistory, multicompartment structure was constructed during Operation Greenhouse (1951). During Greenhouse the structure was damaged due to a peak reflected air-blast overpressure of about 30 psi from Shot Easy (Reference 9). The air blast from Shot Item caused light damage. In general, the damage to the structure caused by the Mike shot of Operation Ivy (1952, Reference 1) was of the same order of magnitude as that caused by Shot Easy (Greenhouse). No additional damage was sustained by the structure during

TABLE 4.4 FREE-FIELD AIR-OVERPRESSURE MEASUREMENTS, SITE JANET

See Figure 4.31 for location of Stations 174.26 and 174.31.

Shot	Site	Ground Range (d) ft	d/W ^{1/3} ft/kt ^{1/3}	Positive Duration sec	Maximum Overpressure psi	Ground Range (d) ft	d/W ^{1/3} ft/kt ^{1/3}	Positive Duration sec	Maximum Overpressure psi
		Station 174.26 (near Station 1312)				Station 174.31 (near Station 3.1.1)			
Yellowwood	Janet	5,995	859	—	16.5	8,254	1,183	1.956	7.3
Tobacco		3,976	1,756	0.719	3.8	6,094	2,814	0.901	1.6
Walnut		5,995	829	1.708	43.0	8,254	729	2.087	15.0
Elder		3,996	407	—	71.0				

Operation Castle (1954, Reference 10) or Operation Redwing (1956, Reference 11). The overall perspective for this structure is shown in Figure 4.34.

This station was located in an estimated 7.0-, 1.7-, 16.0-, 20-, 12-, 8.4-, and 13-psi air-overpressure range for Shots Yellowwood, Tobacco, Walnut, Elder, Dogwood, Olive, and Pine, respectively. The effects from Tobacco were negligible and no further mention of that shot will



Figure 4.30 Post-Koa, (Item 24) helicopter pad.
Pressure level: Koa, 36 psi.

be made. An overall, pre-Hardtack view of this station is shown in Figure 4.35. A preshot view of typical damage to a first floor column (Col. 13C) in Building 5 is shown in Figure 4.36. Building 5, a reinforced-concrete structure with window openings, received more damage from previous operations than any other of the buildings. The other noticeable damage from previous

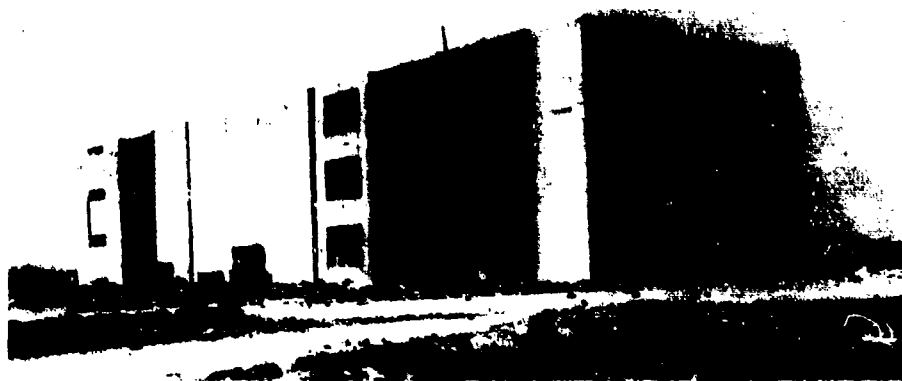


Figure 4.35 Preshot, (Item 26) Station 3.1.1, Site Janet.



Figure 4.36 Preshot, (Item 26) Station 3.1.1, Column 13C, concrete frame building, Site Janet.



Figure 4.37 Preshot, (Item 26) Station 3.1.1, crack in ceiling adjacent to Column Line 10 of the shear wall building looking away from surface zero, Site Janet.

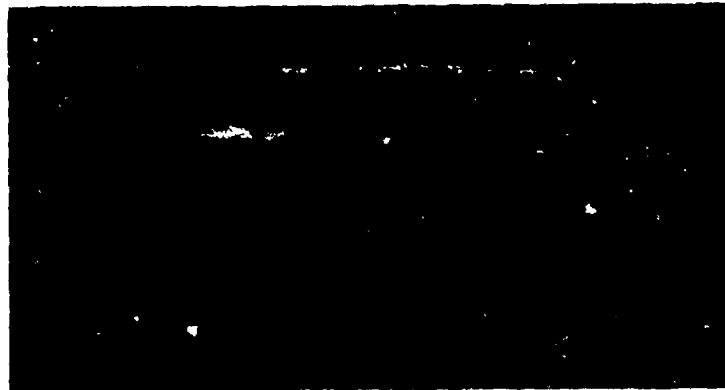


Figure 4.38 Preshot, (Item 26) Station 3.1.1, crack in ceiling adjacent to north wall of the shear-wall building looking away from surface zero, Site Janet.

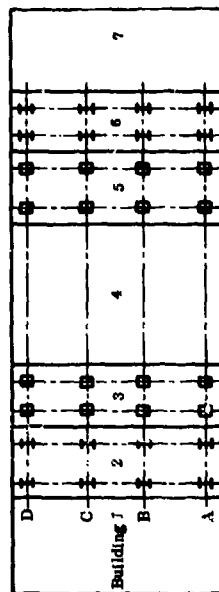


Figure 4.39 Post-Yellowwood, (Item 26) Station 3.1.1. Pressure level: Yellowwood, 7 psi.

TABLE 4.5 COMPARATIVE DEPLACEMENT OF COLUMNS

All measurements in feet.

Building Number	Column	Relative Displacement*											
		First Floor				Second Floor				Third Floor			
		Post-Ivy (1952)	Post-Koa	Post-Yellowwood	Post-Walnut	Post-Elder	Post-Olive, and -Pine	Post-Ivy (1952)	Post-Elder (1952)	Post-Olive, and -Pine	Post-Ivy (1952)	Post-Elder (1952)	Post-Olive, and -Pine
2	5A	0.129	0.094	0.104	0.115	0.156	0.135	0.240	0.333	0.271	0.236	0.323	0.281
	5B	0.092	0.09	0.089	0.104	0.135	0.125	0.232	0.313	0.266	0.237	0.313	0.271
	5C	0.091	0.115	0.104	0.115	0.156	0.135	0.247	0.292	0.260	0.233	0.281	0.266
	5D	0.091	—	—	—	—	0.125	0.244	—	—	0.230	—	—
	6A	0.091	0.104	0.099	0.115	0.146	0.115	0.241	0.313	0.276	0.252	—	—
	6B	0.107	0.104	0.099	0.104	0.135	0.125	0.238	0.313	0.266	0.252	—	—
3	6C	0.060	0.067	0.063	0.094	0.115	0.104	0.241	0.313	0.313	0.250	—	—
	6D	0.101	—	—	—	—	0.125	0.228	—	—	0.246	—	—
	7A	0.116	0.115	0.115	0.146	0.292	—	0.181	0.361	0.354	0.206	0.365	0.406
	7B	0.132	0.116	0.135	0.156	0.292	—	0.190	0.375	0.354	0.218	0.375	0.448
	7C	0.111	0.115	0.104	0.146	0.271	—	0.210	0.364	0.333	0.224	0.406	0.427
	8A	0.143	—	—	0.167	0.313	0.302	0.195	0.385	0.365	0.215	—	—
5	8B	0.129	0.135	0.094	0.156	0.292	0.292	0.180	0.365	0.354	0.205	—	—
	8C	0.110	0.125	0.104	0.135	0.271	0.271	0.174	0.344	0.333	0.218	0.365	0.417
	13A	0.248	0.219	0.230	1.063	Collapse	—	—	—	—	—	—	—
	13B	0.232	0.230	0.219	1.063	Collapse	—	—	—	—	—	—	—
	13C	0.200	0.219	0.208	1.196	Collapse	—	—	—	—	—	—	—
	14A	0.206	0.208	0.219	0.990	Collapse	—	—	—	—	—	—	—
6	14B	0.209	0.230	0.214	1.042	Collapse	—	—	—	—	—	—	—
	14C	0.217	0.219	0.208	1.104	Collapse	—	—	—	—	—	—	—
	15A	0.022	0.021	0.021	0.083	0.146	0.146	—	—	—	—	—	—
	15B	0.023	0.021	0.021	0.073	0.115	0.146	—	—	—	—	—	—
	15C	0.037	—	—	—	0.146	0.146	—	—	—	—	—	—
	16A	0.046	0.042	0.042	0.073	0.125	0.125	—	—	—	—	—	—
16	16B	0.032	0.031	0.031	0.063	0.083	—	—	—	—	—	—	—
	16C	0.030	—	—	—	0.083	0.089	—	—	—	—	—	—



* Total permanent displacement of top of column (away from surface zero) relative to bottom of column.

Figures 4.42 through 4.45. A pre- and post-Walnut view of Column 13C can be compared in Figures 4.36 and 4.45. The columns in the upper two floors of this building did not receive comparable damage as their first-floor counterparts (Figure 4.46). Evidently the first-floor columns took most of the moment and shearing forces while the second and third floors moved away from surface as a unit (Figure 4.42). The tops of the first-floor columns (Columns 13A, B, C and 14A, B, C) were displaced horizontally approximately 10 inches away from surface zero with respect to their bases (Table 4.5).



Figure 4.40 Post-Walnut, (Item 26) Station 3.1.1. Pressure level: Walnut, 16 psi.

The other three frame-type buildings (2, 3, and 5) underwent very little additional lateral movement (Table 4.5). It should be noted that the lateral movement as shown in Table 4.5 is the permanent displacement and not the peak transient deflection. Damage to columns in the third floor of Building 3 is shown in Figures 4.47 and 4.48. A typical column of Building 2 is shown in



Figure 4.41 Post-Walnut, (Item 26) Station 3.1.1, aerial view. Pressure level: Walnut, 16 psi.

Figure 4.49; this picture also shows the suspended plumb bob that was used in measuring column offsets. The roof in Building 6 lifted upward 3 to 4 inches, tapering to its normal position at a point 7 or 8 feet from the front wall (Figure 4.50). The cracked roof section in Building 4 opened considerably, being displaced a maximum of 10 inches at the center of the section adjacent to Column Line 10 and the north end of the building (Figures 4.51 and 4.52). The bottom bars (No. 4) of the slab failed in tension as was noted by the neck-down of the bars at the point of breakage.



Figure 4.42 Post-Walnut, (Item 26) Station 3.1.1, close-up of Building 5, a reinforced-concrete frame structure. Pressure level: Walnut, 16 psi.

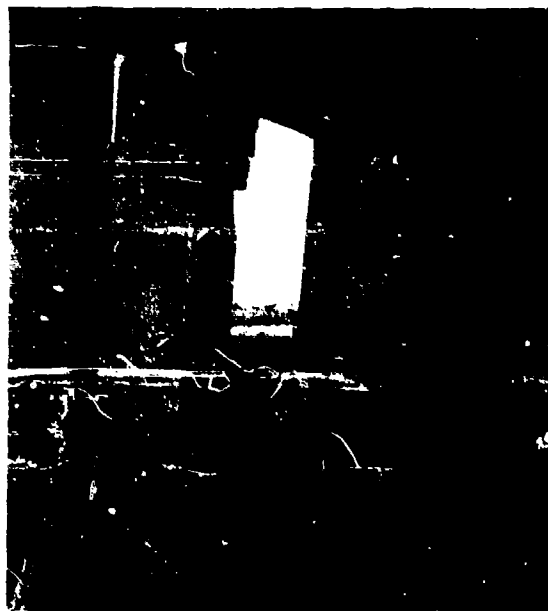


Figure 4.43 Post-Walnut, (Item 26) Station 3.1.1, front column of Building 5. Pressure level: Walnut, 16 psi.



**Figure 4.44 Post-Walnut, (Item 26)
Station 3.1.1, second row of columns
of Building 5. Pressure level: Walnut,
16 psi.**



**Figure 4.45 Post-Walnut, (Item 26)
Station 3.1.1, third row of columns of
Building 5. Pressure level: Walnut,
16 psi.**



Figure 4.46 Post-Walnut, (Item 26) Station 3.1.1, Column 13C, second floor of Building 5. Pressure level: Walnut, 15 psi.



Figure 4.47 Post-Walnut, (Item 26) Station 3.1.1, Column 8A, first floor of Building 3. Pressure level: Walnut, 16 psi.



Figure 4.48 Post-Walnut, (Item 26) Station 3.1.1, Column 7B, third floor of Building 3. Pressure level: Walnut, 16 psi.



Figure 4.49 Post-Walnut, (Item 26) Station 3.1.1, Column 5C, first floor of Building 2. Pressure level: Walnut, 16 psi.

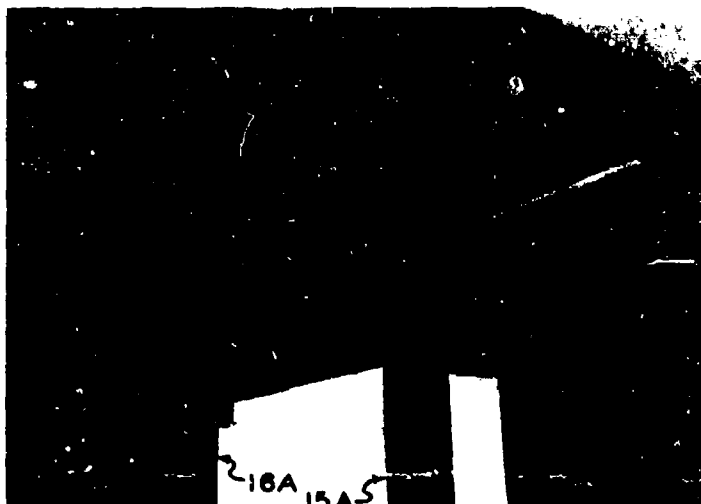


Figure 4.50 Post-Walnut, (Item 28) Station 3.1.1, roof slab damage, Building 6. Pressure level: Walnut, 16 psi.



Figure 4.51 Post-Walnut, (Item 28) Station 3.1.1, crack in ceiling adjacent to Column Line 10 of the shear-wall building looking away from surface zero. Pressure level: Walnut, 16 psi.

The top bars (No. 5) held the cracked roof section in place.

Shot Elder (pressure level of 20 psi) caused additional damage as can be compared by viewing Figures 4.53 and 4.54 with Figure 4.40. The shear resistance of the first-floor columns of Building 5, the concrete frame, drag structure, was overcome and the upper floors intact settled down with the second floor girders resting on the collapsed first floor columns (Figure 4.55). The column offset measurements for Buildings 2, 3, and 6 are shown in Table 4.5. A front view of Buildings 1, 2, and 3 is shown in Figure 4.56. Building 3, the reinforced-concrete (diffraction) structure underwent additional permanent lateral movement, but unlike its counterpart, Building 5 (drag-type structure), the columns on each floor displaced laterally approximately the same amount and showed signs of damage (Figures 4.57, 4.58, and 4.59). The rear wall of Building 3 cracked horizontally, evidently from bending (Figure 4.60). Buildings 2 and 6 deflected approximately $\frac{1}{2}$ inch away from surface zero. However, most of the roof section of Building 6 was blown upward by the blast and thrown to the ground surface to the rear of the structure (Figure 4.61). Channel shear keys welded to the roof girder are also visible in the picture as well as the damage to the roof at the south end of Building 4. The major damage to Building 4 occurred at the north end where the roof was punched inward and is supported by the cantilever effect of the reinforcing steel (Figures 4.62, 4.63, and 4.64).

The station was next investigated after Shots Dogwood, Olive, and Pine had been fired; the resulting estimated overpressure levels were 12, 8.4, and 13 psi, respectively. An overall postoperation view of the structure is shown in Figure 4.65. Little additional damage was observed for Buildings 2, 3, or 6. As shown in Table 4.5, the postoperation column displacements for Building 6 were approximately the same as those for post-Elder; the postoperation displacements for Buildings 2 and 3 were less than those for post-Elder, indicating that rebound for the buildings occurred at a slow rate.

Building 4 showed evidence of additional damage. However, the shear walls appeared sound and the damaged roof panels were in about the same condition as observed after Shot Elder. The third-floor slab underwent considerable bending. The maximum sag in the slab between the north shear wall and Column Line 10 was 6 inches, between Column Lines 10 and 11, 3 inches, and between Column Line 11 and the south shear wall, 12 inches. A view of the underside of the third floor along Column Line 11 and the front wall facing surface zero is shown in Figure 4.66. The rotation experienced by the third floor slab caused it to crack at the intersection of both shear walls. A crack, having a 3-inch differential vertical displacement, developed at the intersection of the third-floor slab and front wall between Column Line 11 and the south shear wall (Figure 4.67).

4.2.3 Item 27, Station 3.1.3, Greenhouse. A composite-type, semi-buried shelter was constructed during Operation Greenhouse (1951). No plastic deformations or damage were observed during that operation (Reference 9); however, earth blown by the blast from the Mike shot partially blocked the entrance. The structure consisted of four major parts: a cast-in-place, reinforced-concrete shelter; three precast, reinforced-concrete pipe sections; a corrugated-pipe section; and a cast-in-place, reinforced-concrete entrance (Reference 9). The structure suffered no major structural damage during Operation Ivy (1952, Reference 1); however, the blast doors were removed prior to the test and the woodframe air lock was destroyed by air blast (approximately 18 psi), and the painted surface of the vent pipe was charred on the side facing ground zero. No additional damage was inflicted to the structure during Operations Castle (1954, Reference 10) and Redwing (1956, Reference 11).

The maximum estimated overpressure received by this station was 29 psi from Shot Elder. The station received no additional damage from any of the shots; however, the water-wave effects from Shot Walnut filled the entranceway with 6 inches of mud and left water standing to a height indicated by the water marks shown in Figure 4.68.

4.2.4 Item 28, Stations 20A, B, C, D, E and F, Greenhouse. Reinforced-concrete gage piers were constructed and undamaged, except for Station 20A, during Operation Greenhouse (1951).



Figure 4.52 Post-Walnut, (Item 26) Station 3.1.1, crack in ceiling adjacent to north wall of shear-wall building looking away from surface zero. Pressure level: Walnut, 16 psi.



Figure 4.53 Post-Elder, (Item 26) Station 3.1.1, front view. Pressure level: Elder, 20 psi.



Figure 4.54 Post-Elder, (Item 26) Station 3.1.1, rear view. Pressure level: Elder, 20 psi.

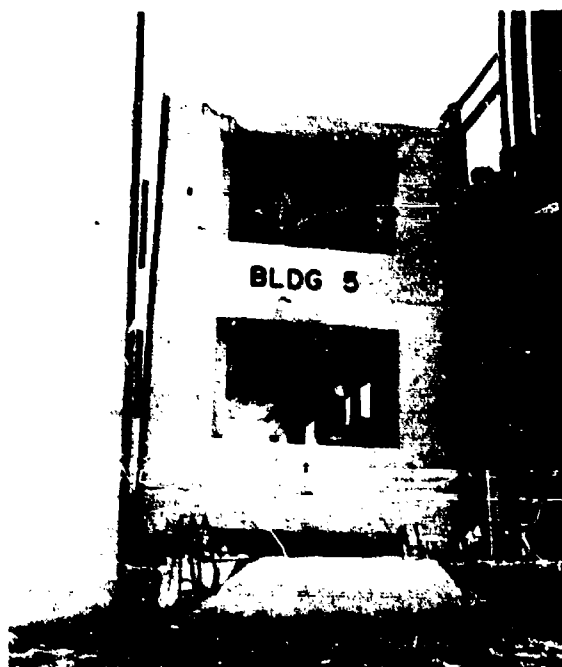


Figure 4.55 Post-Elder, (Item 26) Station 3.1.1, close-up of Building 5, first floor collapsed. Pressure level: Elder, 20 psi.

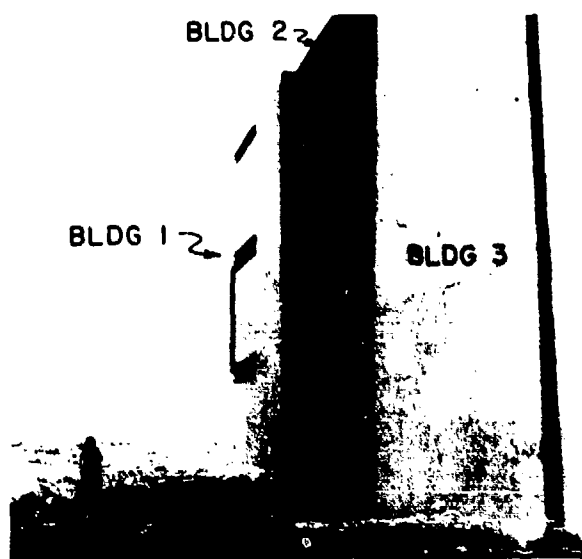


Figure 4.56 Post-Elder, (Item 26) Station 3.1.1, close-up of Buildings 1, 2, and 3. Pressure level: Elder 20 psi.

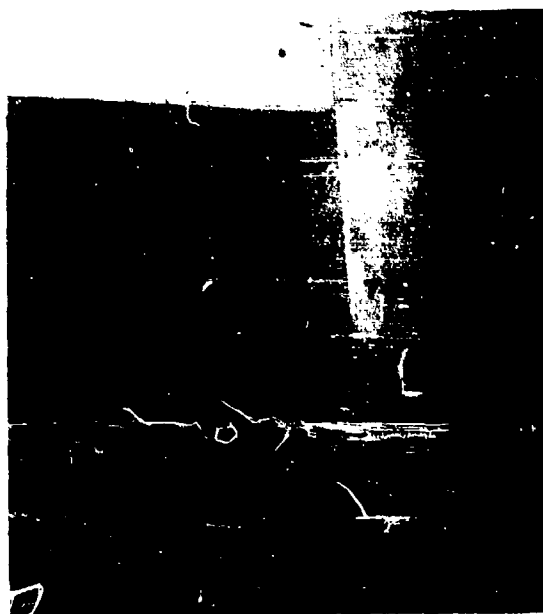


Figure 4.57 Post-Elder, (Item 26) Station 3.1.1, Columns 7 and 8B, first floor of Building 3. Pressure level: Elder, 20 psi.



Figure 4.58 Post-Elder, (Item 26) Station 3.1.1,
Columns 7 and 8B, second floor of Building 3.
Pressure level: Elder, 20 psi.

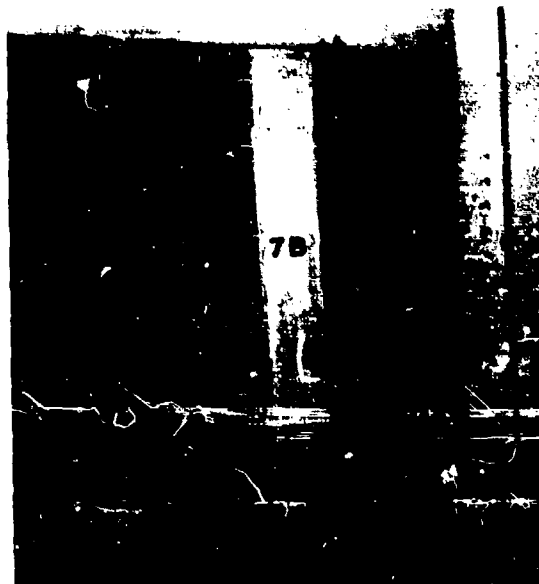


Figure 4.59 Post-Elder, (Item 26) Station 3.1.1,
Columns 7 and 8B, third floor of Building 3.
Pressure level: Elder, 20 psi.



Figure 4.60 Post-Elder, (Item 26) Station 3.1.1, Column 8D and crack in rear wall, first floor of Building 3. Pressure Level: Elder, 20 psi.

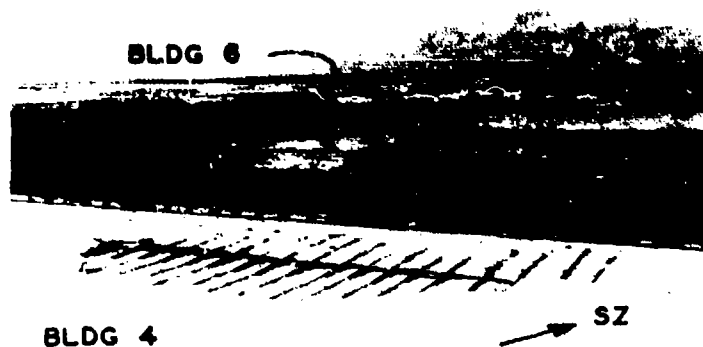


Figure 4.61 Post-Elder, (Item 26) Station 3.1.1, destroyed roof section of Building 6 and damaged area to roof at south end of Building 4. Pressure level: Elder, 20 psi.

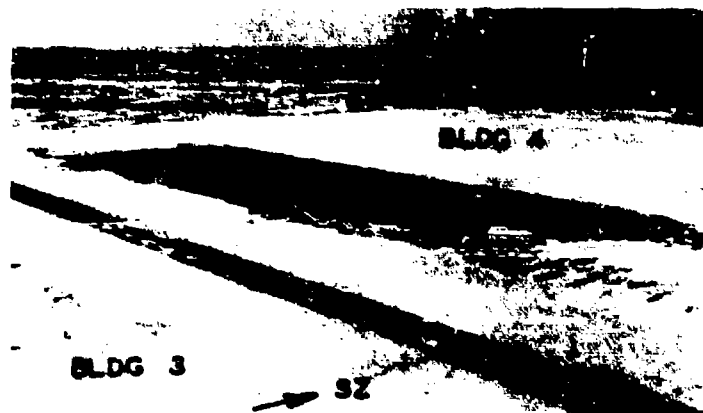


Figure 4.62 Post-Elder, (Item 26) Station 3.1.1, outside view of punched-in roof section at north end of Building 4. Pressure level: Elder, 20 psi.



Figure 4.63 Post Elder, (Item 26) Station 3.1.1, inside view of punched-in roof section, north end of Building 4. Pressure level: Elder, 20 psi.



Figure 4.64 Post-Elder, (Item 26) Station 3.1.1, close-up of punched-in roof section, north end of Building 4. Pressure level: Elder, 20 psi.

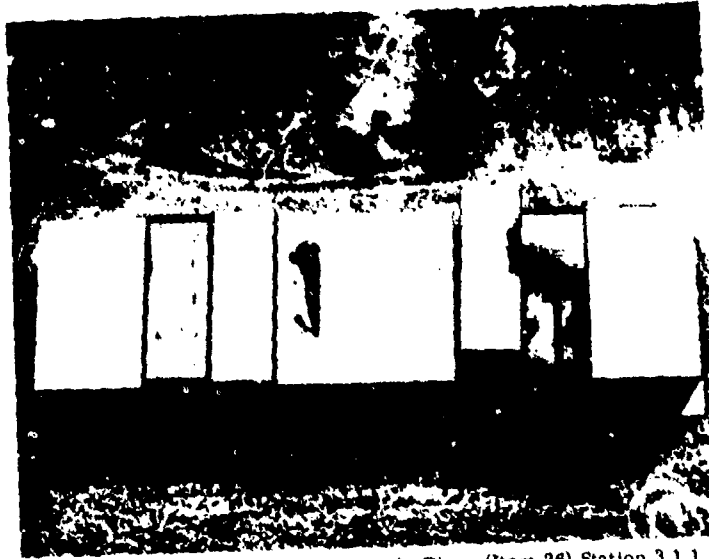


Figure 4.65 Post-Dogwood Olive, and -Pine, (Item 26) Station 3.1.1, aerial view. Pressure levels: Dogwood, 12 psi; Olive, 8.4 psi; and Pine, 13 psi.



Figure 4.66 Post-Dogwood, -Olive, and -Pine, (Item 26) Station 3.1.1, underside of third floor along Column Line 11, and the front wall facing surface zero. Pressure levels: Dogwood, 12 psi; Olive, 8.4 psi; and Pine, 13 psi.



Figure 4.67 Post-Dogwood, -Olive, and -Pine, (Item 26)
Station 3.1.1, crack in third floor at intersection of front
wall between Column Line 11 and south shear wall. Pres-
sure levels: Dogwood, 12 psi; Olive, 8.4 psi; and Pine,
13 psi.

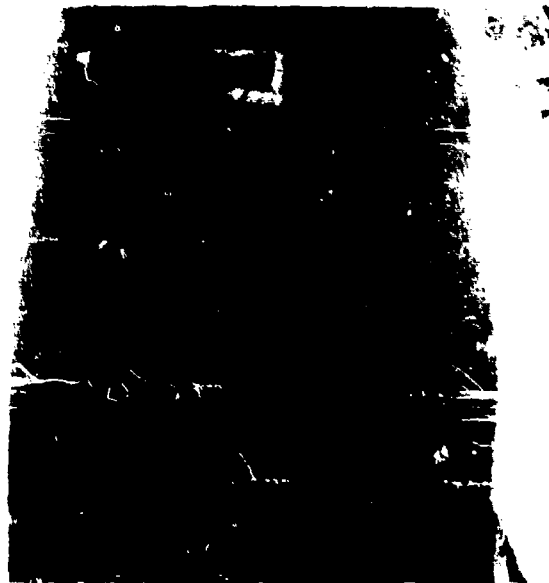


Figure 4.68 Post-Walnut, (Item 27)
Station 3.1.3, entrance filled with
mud. Pressure level: Walnut, 21 psi.

Station 20A was destroyed either during Operation Greenhouse or Operation Ivy.

The structural details and elevation views of this item are shown in Figure 4.69.

Stations 20B, C, D, and E were destroyed by the air-blast effects from Shot Walnut. Station 20F was not damaged by any of the shots. See Appendix C for a detailed analysis of the response of these piers to blast pressure.

Table C.1 lists the pressures sustained by the various piers and the subsequent damage. A typical preshot view of a pier (Station 20B) is shown in Figure 4.70 and a post-Walnut (pressure level, 25 psi) view of the same pier depicting typical damage, separation of the stem from the base, is shown in Figure 4.71.

4.2.5 Item 29, Station 77.02. A reinforced-concrete recording station was constructed during Operation Hardtack (1958).

This station was not damaged from any of the shots and received a maximum, estimated pres-

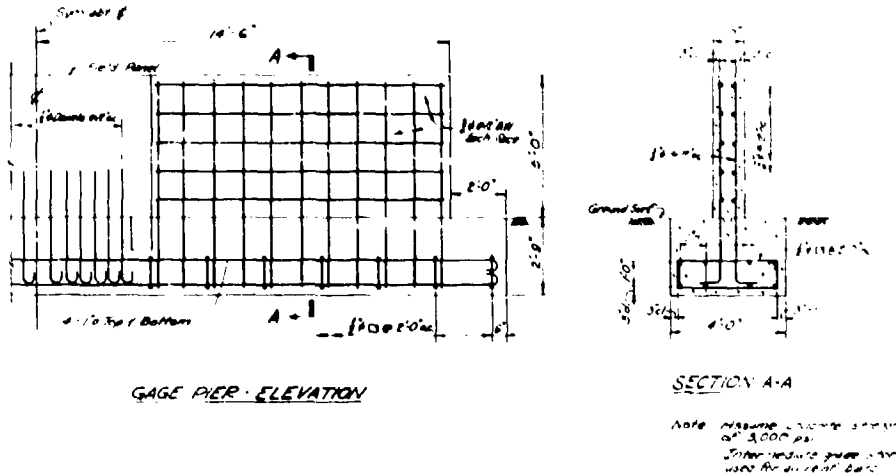


Figure 4.69 Structural details and elevation views of (Item 28) Stations 20A, B, C, D, E, and F, Site Janet.

sure of 17 psi from Shot Elder. The antenna and ventilating devices on top of this station (Figure 4.72) were removed prior to Shot Elder.

4.2.6 Item 30, Landing Pier. An earth-filled pier with reinforced-concrete side walls and concrete cubicles (5 by 5 by 5 feet with 6-inch walls and filled with sand) for additional stability received no damage from the first two shots, Yellowwood and Tobacco.

However, Shots Walnut and Elder caused considerable damage (compare Figures 4.73, 4.74, and 4.75). Two of the concrete cubicles were thrown 45 and 75 feet, respectively, the steel framework at the end of the pier was bent over, and the steel grill-type flooring was blown away from the effects of Walnut (Figure 4.74). The welded horizontal beams were fractured at the welds on the side adjacent to the columns; the columns tilted on a 3-to-1 (vertical to horizontal) slope away from surface zero. During Shot Elder the horizontal structural members of the steel framework were blown on shore and only the tilted legs remained in place (Figure 4.75). The two concrete cubes that were displaced from Walnut were moved only slightly; no additional cubes were displaced. No additional damage was observed from the other shots.

4.2.7 Camp. This camp was almost entirely dismantled prior to any of the shots; however, the wood frame for some buildings and tents were left in place.



Figure 4.70 Preshot (Item 28) Station 20B, view of gage pier facing surface zero, Site Janet.



Figure 4.71 Post-Walnut, (Item 28) Station 20B, view of toppled gage pier. Pressure level: Walnut, 25 psi.



Figure 4.72 Postshot, (Item 29) Station 77.02, recording station. Pressure level: Elder, 17 psi.



Figure 4.73 Preshot, (Item 30) landing pier, Site Janet.



Figure 4.74 Post-Walnut, (Item 30) landing pier. Pressure level: Walnut, 23 psi.

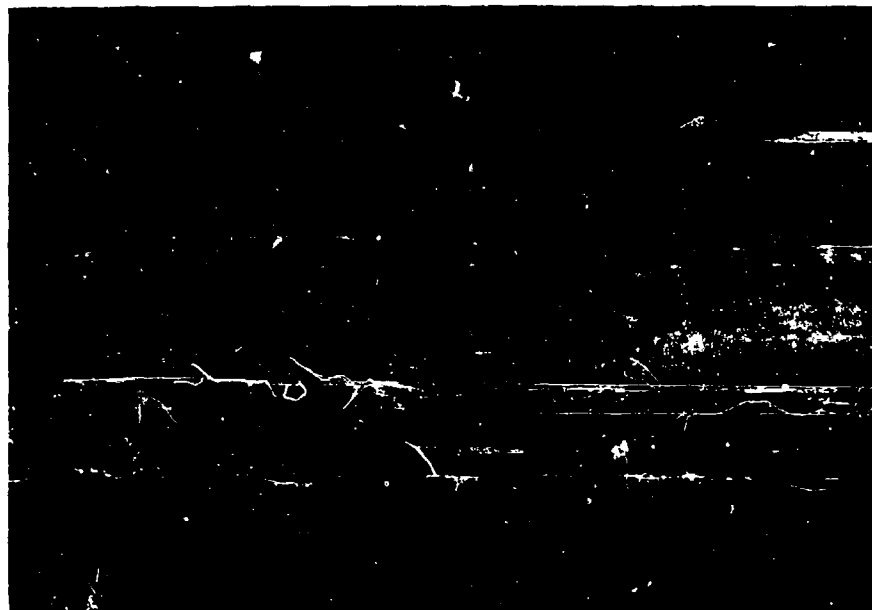


Figure 4.75 Post-Elder, (Item 30) landing pier. Pressure level: Elder, 30 psi.

The wood frames were destroyed by the effects from Shot Koa (pressure level of 5.2 psi). Shot Yellowwood (pressure level of 6.2 psi) scattered oil drums that had been previously scattered (Figure 4.76).

4.3 SITE YVONNE

The effects of Shots Cactus (17 kt), Butternut (86 kt), Holly (5.8 kt), Magnolia (57 kt), Rose (14.5 kt), Linden (11.1 kt), Sequola (5.3 kt), Pisonia (22.4 kt) and Fig (21.5 tons) were observed at Site Yvonne. The shot geometry, with pressure contours and test stations, is shown in Figure 4.77.

4.3.1 Item 31, Station 1130. A reinforced-concrete bunker was constructed during Operation Hardtack (1958). This structure was designed to resist a 470-psi air overpressure and a 3,270-



Figure 4.76 Postshot, Janet Camp. Pressure levels: Yellowwood, 6.2 psi; Tobacco, 1.5 psi.

psi reflected air overpressure. The plan and elevation for this structure are shown in Figure 4.78.

The structure was located in the 450-psi air-overpressure range for Shot Cactus and damaged only from that shot. The damage was confined to the side tunnel. A preshot view of the entrance (side away from ground zero) is shown in Figure 4.79 and a post-Cactus view is shown in Figure 4.80. Thermal radiation estimated to be 30 cal/cm² from Shot Butternut, which was fired after Shot Cactus, burned the black paint off the wall surface as can be seen by comparing Figures 4.79 and 4.80. A preshot view of the entrance to the side tunnel is shown in Figure 4.81. A post-Cactus view, Figure 4.82, shows the damaged entranceway. Apparently the blast wave that entered the tunnel-like entrance (side-on to the shock front) was reflected at the tunnel's end. The resulting increase in pressure caused the tunnel walls and roof to separate and crack as though an explosion had occurred inside the tunnel. An interior crack near the junction with main structure showing the "bulging" failure can be seen in Figure 4.83. The tunnel was not fastened with dowels to the main station but merely keyed.

Thermal radiation at this close range was estimated to be 650 cal/cm². Very little of the tunnel was directly exposed to this radiation as can be seen in Figure 4.81; however, the areas that were exposed showed remarkably little effect due to this exposure, Figure 4.82.

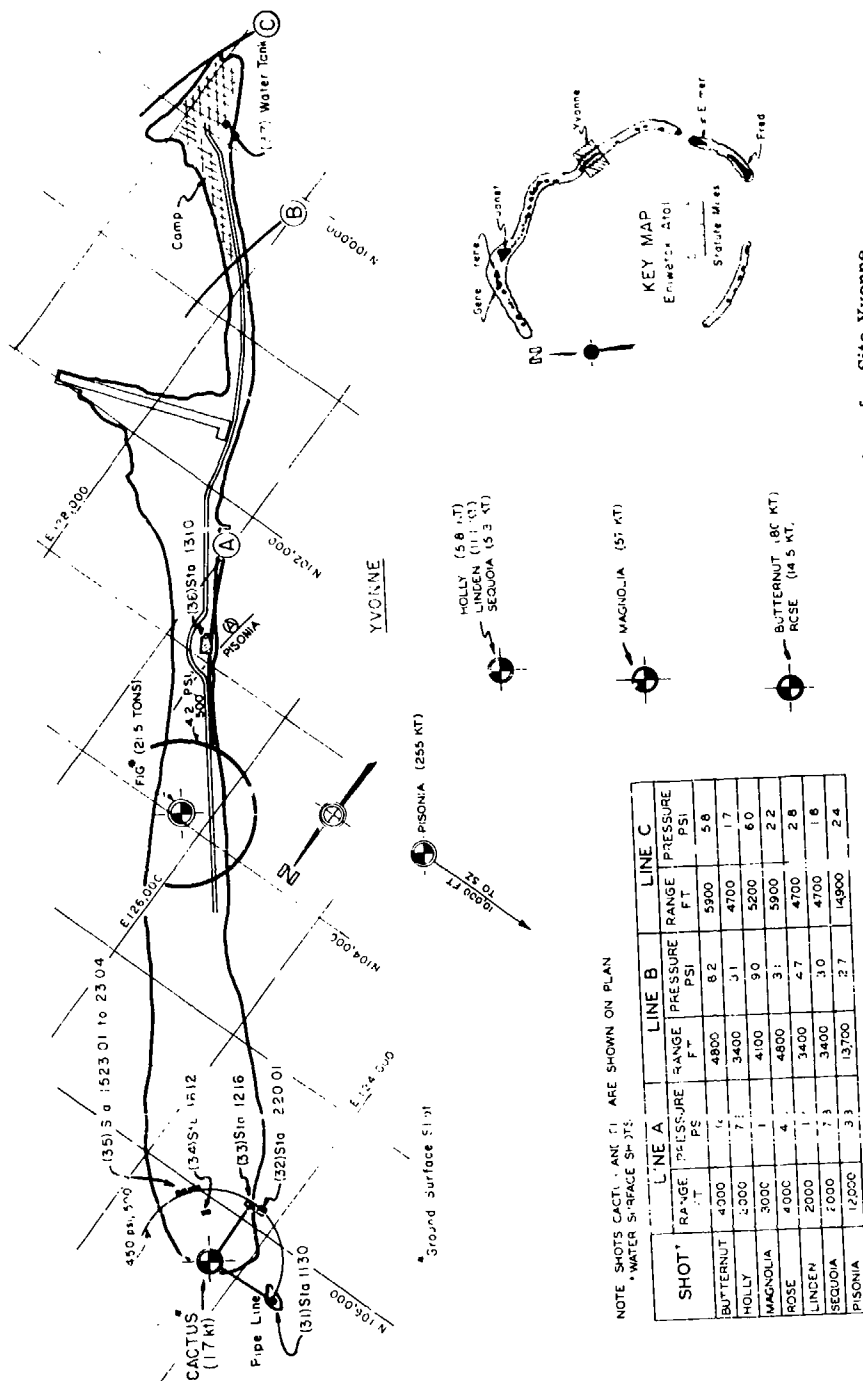
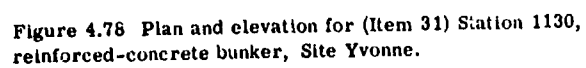


Figure 4.77 Shot geometry with pressure contours and test stations for Site Yvonne.



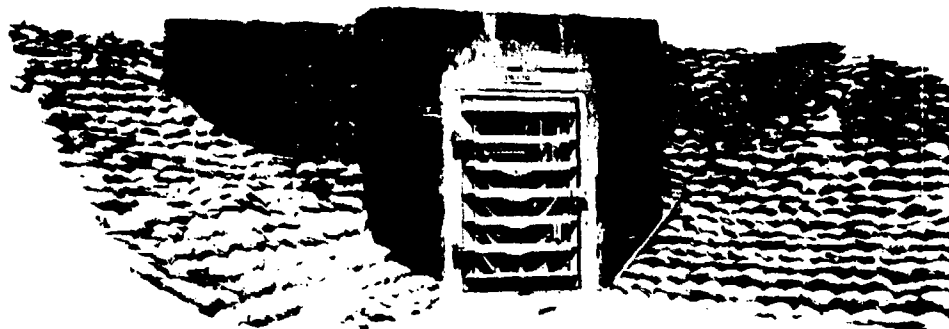


Figure 4.79 Preshot, (Item 31) Station 1130, entrance, Site Yvonne.

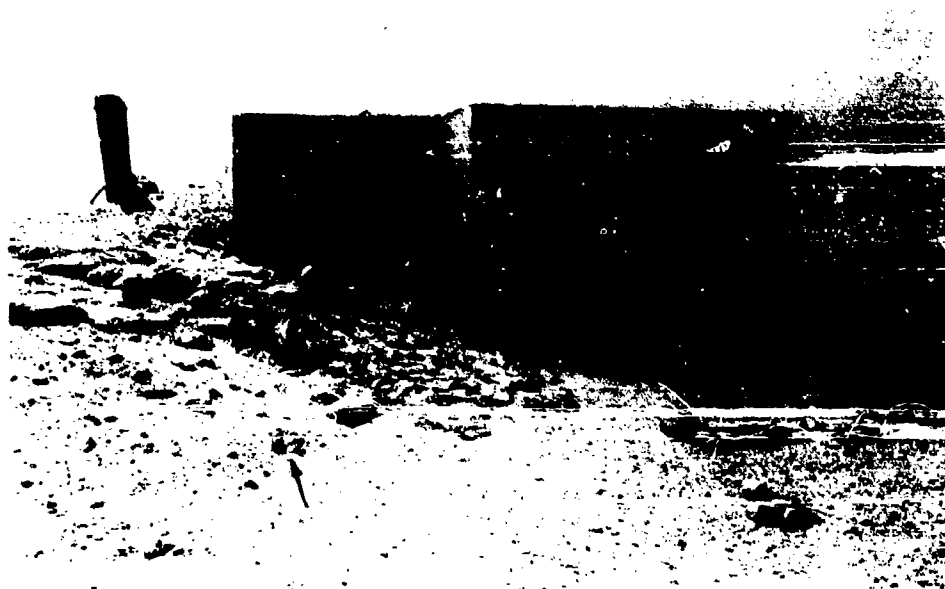


Figure 4.80 Postshot, (Item 31) Station 1130, entrance.
Pressure level: Cactus, 450 psi; Eutternut, 20 cal/cm².



Figure 4.81 Preshot, (Item 31) Station 1130, side-tunnel entrance, Site Yucca.



Figure 4.82 Post-Cactus, (Item 31) Station 1130, side-tunnel entrance. Pressure level: Cactus, 450 psi; 650 cal/cm².

4.3.2 Item 32, Station 1220.01. A steel cubicle mounted on a structural-steel platform was erected during Operation Hardtack. This station was located in the 450-psi air-overpressure range for Shot Cactus and was destroyed; only the legs of the structure survived. Preshot and postshot views are shown in Figures 4.84 and 4.86, respectively.

4.3.3 Item 33, Station 1216. A reinforced-concrete terminal for a pipeline was constructed during Operation Hardtack (1958).

This station was located in the 450-psi air-overpressure range for Shot Cactus and apparently undamaged. A preshot picture is shown in Figure 4.85 and a post-Cactus view in Figure 4.86.

4.3.4 Item 34, Station 1612. A reinforced-concrete recording station with a timber entrance tunnel and reinforced-concrete retaining wall was constructed during Operation Hardtack (1958). The plans for the station with details for the retaining wall only are shown in Figure 4.87.

This station was located in the 1,600-psi air-overpressure range for Shot Cactus. As a result of the surcharge from this overpressure the timber entrance tunnel was filled in with sand and the adjoining retaining wall cracked and tilted outward 2 to 3 feet. A preshot view of the retaining wall is shown in Figure 4.88 and a post-Cactus view showing both the retaining wall and the entrance to the station is shown in Figure 4.89.

The damaged, sand-filled timber tunnel was removed by the use of a bulldozer and the interior of the detector station was investigated for structural damage. It was observed that the rear wall (wall away from ground zero) was damaged at the junctures with both the ceiling and floor (Figure 4.90). Apparently air blast entered the collimator pipes and tended to blow out the rear wall. The rear wall was 1 foot thick, the floor and ceiling both were 2 feet thick, and the steel reinforcement for all three elements consisted of No. 7 bars at 12 inches on center, both ways, and in each face.

4.3.5 Item 35, Stations 1523.01 to 1523.04. Four steel-pipe towers encased by a plywood covering were constructed for Operation Hardtack (1958). A corrugated-metal pipe (48 inches in diameter) mounded with sand led from each station to ground zero. A preshot picture of this station is shown as Figure 4.91.

The stations were located in the 450-psi air-overpressure zone for Shot Cactus and were destroyed by that shot. All that remained was the foundations for the towers and remnants of the corrugated pipe.

The air-blast wave smashed the far wall of each tower foundation, as shown in Figure 4.92. A typical failure pattern for the 48-inch, round, corrugated-metal pipe leading to ground zero is shown in Figure 4.93.

4.3.6 Item 36, Station 1310. A massive, reinforced-concrete structure was constructed and undamaged during Operation Redwing (1956). A new reinforced-concrete room was added on the roof and the entire structure mounded over with earth for Operation Hardtack (1958).

This station received a maximum, estimated overpressure of 16 psi from Shot Magnolia and experienced no structural damage from any of the shots. A preshot view of this station is shown in Figure 4.94 and post-Rose view showing loss of earth cover is shown in Figure 4.95.

4.3.7 Item 37, Water Tank. A 21,000-gallon tank constructed of $\frac{1}{8}$ -inch steel plates with $\frac{1}{2}$ -inch round bolts spaced at 2 inches on center, and having a radius of 10 feet 10 inches and a height of 8 feet, was damaged during Hardtack (1958).

The tank was located in the 1.5-, 6.5-, 2.4-, 7.0-, 2.5-, 3.4-, 2.3-, and 3.4-psi air-overpressure zones for Shots Cactus, Butternut, Holly, Magnolia, Rose, Linden, Sequoia, and Pisonia. The tank was not affected by Shot Cactus but was damaged by Shot Butternut as shown in Figure 4.96. The tank was half full of water at that time. Shot Holly had no additional effects. The tank was damaged additionally by Shot Magnolia as seen by the local buckling failure around the top perimeter and the dishing of the roof as shown in Figure 4.97. No additional damage from the remain-



Figure 4.83 Post-Cactus, (Item 31) Station 1130, crack at intersection of tunnel and main structure. Pressure level: Cactus, 450 psi.

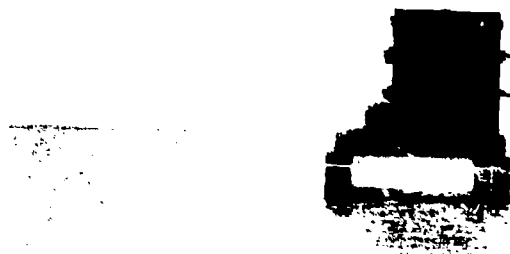


Figure 4.84 Preshot, (Item 32) Station 1220.01, cubicle, Site Yvonne.



Figure 4.85 Preshot, (Item 33) Station 1216, Site Yvonne.



Figure 4.86 Post-Cactus, (Items 32 and 33) Stations 1220.01 and 1216. Pressure level: Cactus, 450 psi.

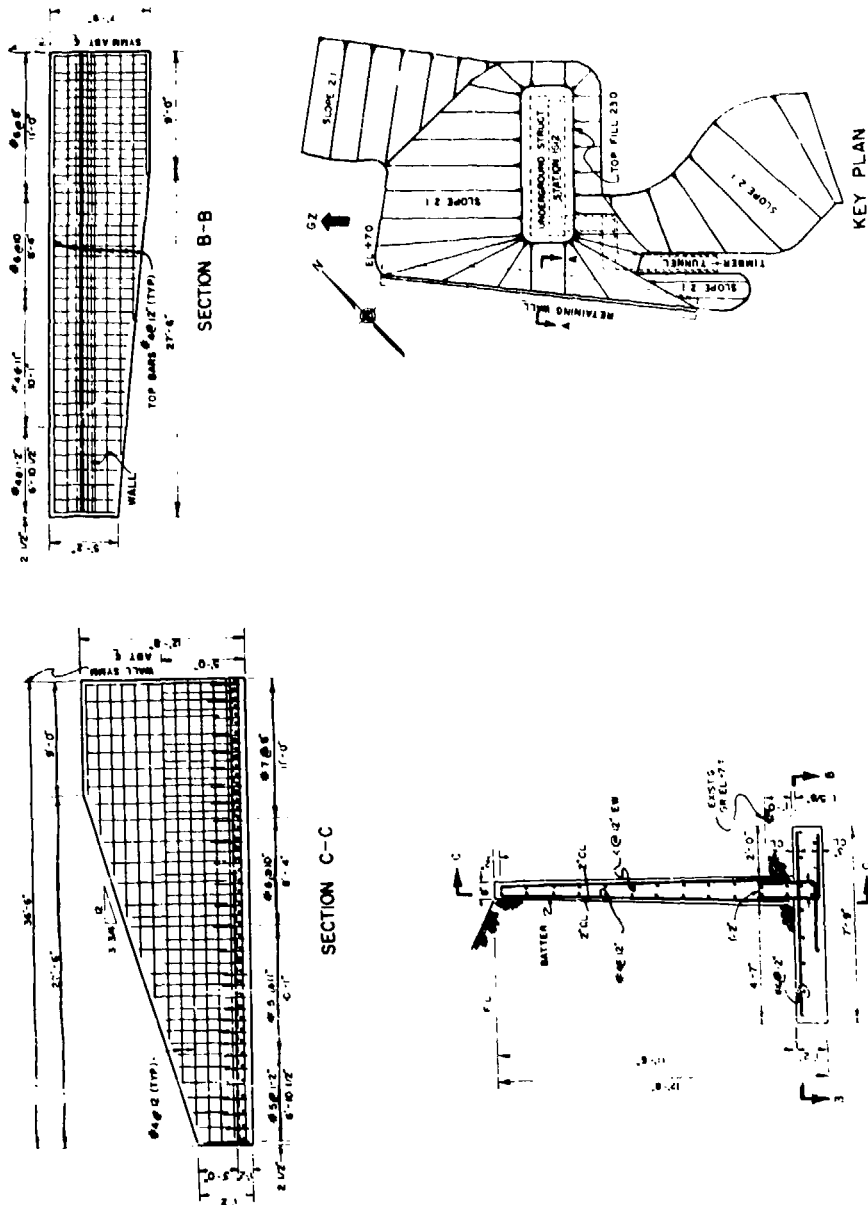


Figure 4.87 Plan and elevation for (Item 34) Station 1612, Site Yvonne.

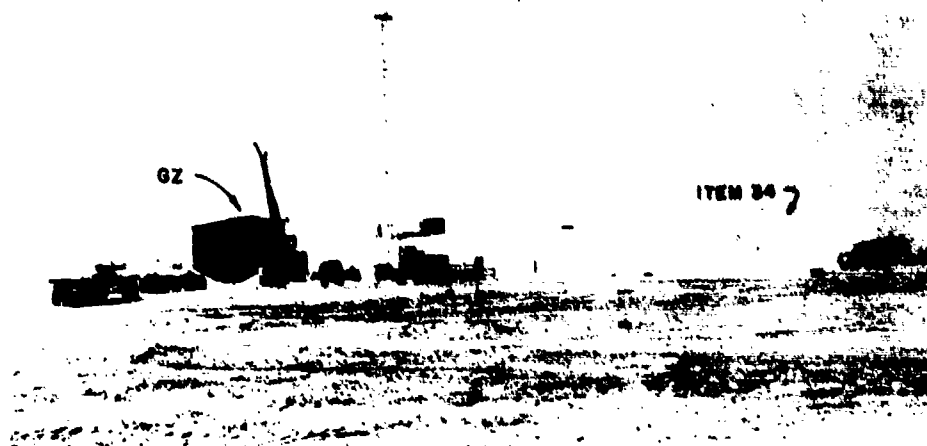


Figure 4.88 Preshot, (Item 34) Station 1612, retaining wall, Site Yvonne.



Figure 4.89 Post-Cactus, (Item 34) Station 1612, retaining wall and entrance to station. Pressure level: Cactus, 1,600 psi.



COLLIMATOR
PIPES

Figure 4.90 Post-Cactus, (Item 34) Station 1612, interior view.
Pressure level: Cactus, 1,600 psi.

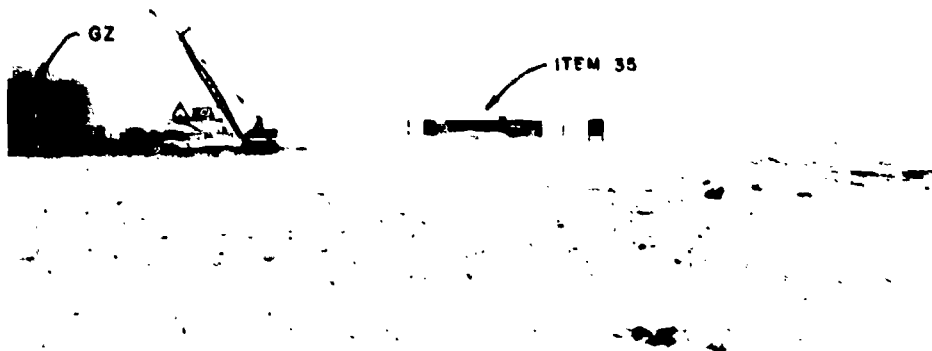


Figure 4.91 Preshot, (Item 35) Stations 1523.01 to 1523.04, Site Yvonne.



Figure 4.92 Post-Cactus, (Item 35) Stations 1523.01 to 1523.04, foundation pit for towers. Pressure level: Cactus, 450 psi.

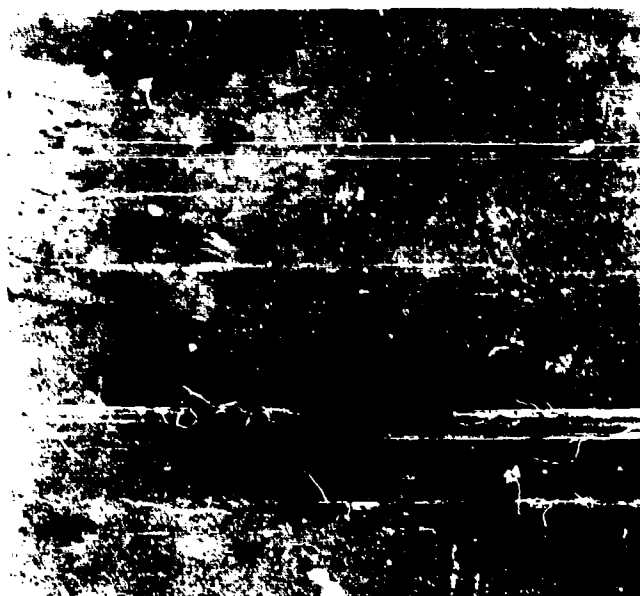


Figure 4.93 Post-Cactus, (Item 35) Stations 1523.01 to 1523.04, 48-inch metal corrugated pipe leading to ground zero. Pressure level: Cactus, 450 psi.

SZ ← (Except Cactus)



Figure 4.94 Preshot, (Item 36) Station 1310, concrete, earth-covered station, Site Yvonne.

SZ ← (Except Cactus)



Figure 4.95 Post-Rose, (Item 36) Station 1310, concrete, earth-covered station. Pressure levels: Cactus, 4.5 psi; Rutternut, 12 psi; Holly, 7.6 psi; Magnolia, 16 psi; and Rose, 4.2 psi.

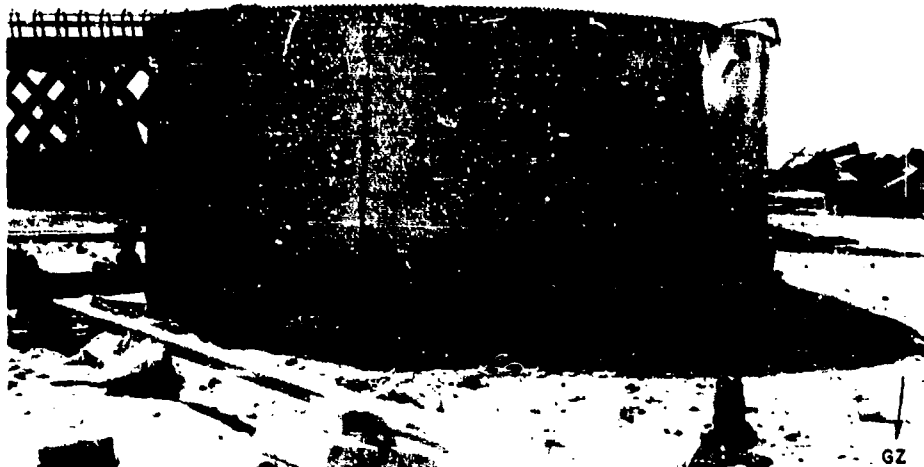


Figure 4.96 Post-Butternut, (Item 37) 21,000-gallon water tank.
Pressure level: Butternut, 6.5 psi.

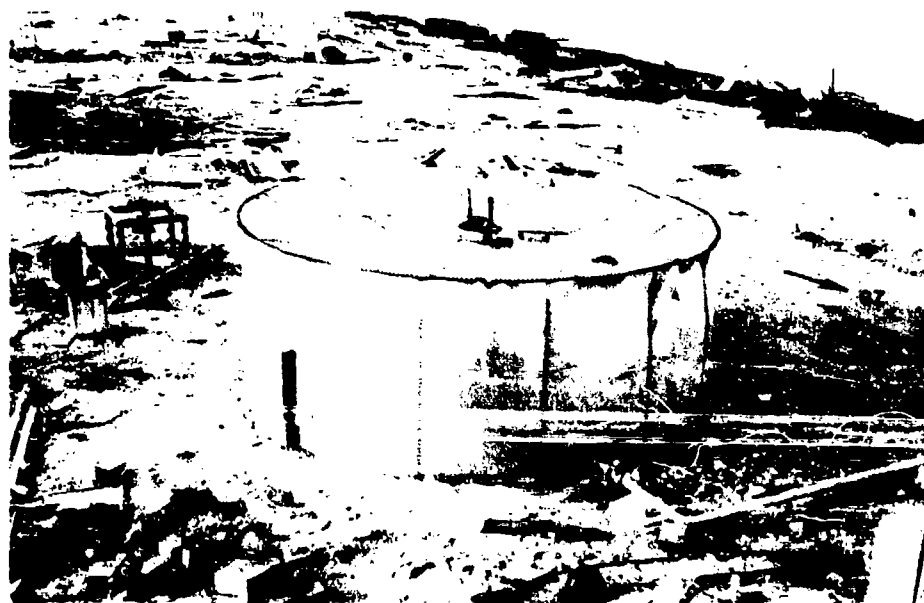


Figure 4.97 Post-Magnolia, (Item 37) 21,000-gallon water tank and
Yvonne Camp area. Pressure level: Magnolia, 7.0 psi.

ing shots was observed. Even though the tank was badly dented near the upper rim none of the bolts or bolt holes showed signs of incipient failure, and it appeared that the tank with some minor repairs could easily be placed in use again. The above-ground connections of 4-inch and 2-inch water pipes and the exposed 4-inch, rising-stem, gate valves (125-psi rated) were undamaged.

4.3.8 Yvonne Camp. The camp located at the south end of Site Yvonne (Figure 4.77) was damaged severely. Damage resulting from the various shots to several types of construction and miscellaneous items is described as follows:

Timber Buildings and Tents. Light temporary timber buildings were severely damaged from the 1.5- to 2.0-psi air overpressure from Shot Cactus. The first two rows of



Figure 4.98 Post-Cactus, camp damage, tents. Pressure level: Cactus, 2.0 psi.

tents (closest to ground zero) were not only collapsed but moved away from ground zero a distance of 6 to 8 feet (Figure 4.98). The remaining tents did not experience this movement but were partially collapsed. The light-plywood-covered buildings were severely damaged, the smaller buildings being damaged the least. The frames of many structures were collapsed to varying degrees and the plywood siding of many was blown off (Figure 4.99). The latrine which was the closest camp building to ground zero was not only damaged but moved 6 inches away from ground zero. The blast that entered this building apparently exerted a greater pressure than the external pressure, as indicated by the outward bulging of the roof and side walls as shown in Figure 4.100. None of the buildings or tents were charred from the thermal pulse from Shot Cactus. The estimated pressure level of 5.8 to 8.2 psi from Shot Butternut completely destroyed all the tents and timber buildings.

Telephone Poles. Wood telephone poles located in an estimated 2.5-psi pressure range for Shot Cactus were undamaged. The same poles located in the 12-psi air-overpressure for Shot Butternut were bent and one was broken at the base as shown in Figure 4.101; the bent pole



Figure 4.99 Post-Cactus, camp damage, light timber construction.
Pressure level: Cactus, 1.5 psi.

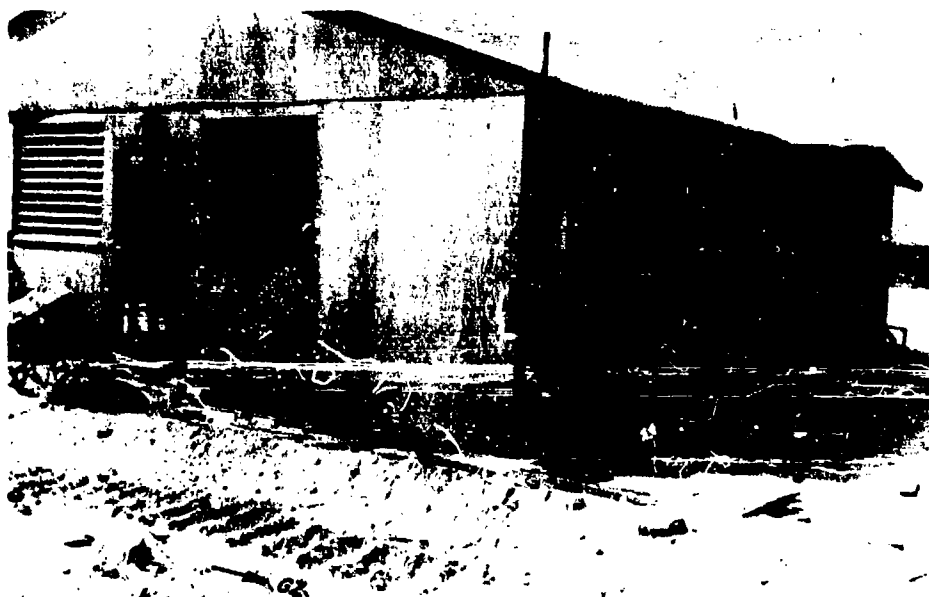


Figure 4.100 Post-Cactus, camp damage, latrine. Pressure
level: Cactus, 2.0 psi.

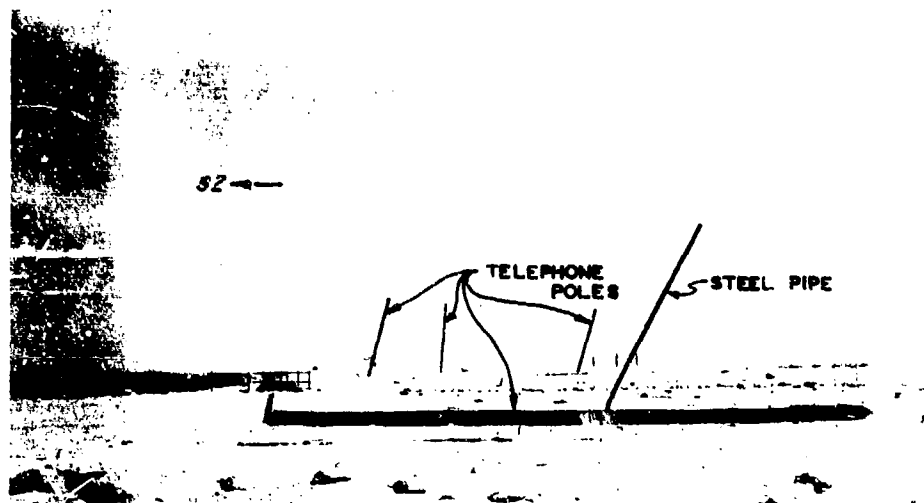


Figure 4.101 Post-Butternut, telephone poles. Pressure level: Butternut, 12 psi.



Figure 4.102 Post-Butternut, radar reflector. Pressure level: Butternut, 5.8 psi.

→ SZ

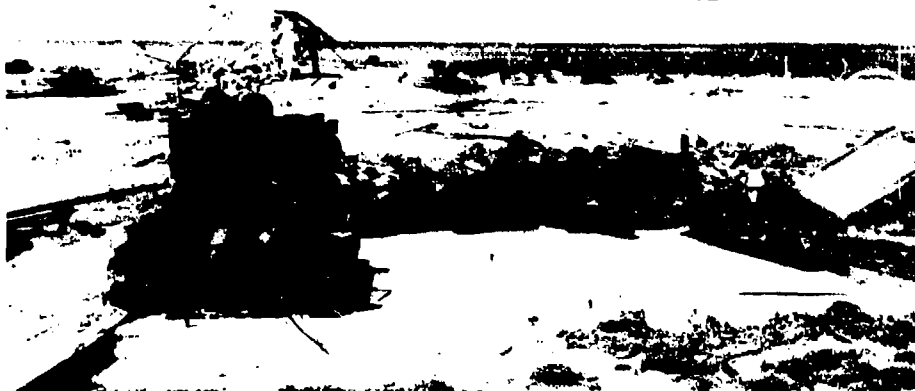


Figure 4.103 Post-Butternut, helium bottles. Pressure level: Butternut, 5.8 psi.



Figure 4.104 Post-Magnolia, helium bottles. Pressure level: Magnolia, 6 psi.

in the right foreground is a 3-inch, round, steel pipe. The same poles were located in an estimated 16-psi range for Shot Magnolia and were snapped off at the base.

Radar Reflector. A multiunit, radar reflector, undamaged from the effects of Shot Cactus, was ripped from its concrete foundation and thrown 50 feet from the effects of Shot Butternut. A view of this station, which was located in the estimated 5.8-psi range from Shot Butternut, is shown in Figure 4.102.

Helium Bottles. Helium bottles stored in the camp area were undamaged but snifted



Figure 4.105 Postshot, fire hydrant. Pressure levels: Cactus, 2.0 psi; Butternut, 8.2 psi; Holly, 3.1 psi; Magnolia, 9.0 psi; Rose, 3.1 psi; Linden, 4.7 psi; Sequoia, 3.0 psi; and Pisonia, 2.8 psi.

slightly from some of the shots. This movement can be compared by viewing Figure 4.103 (post-Butternut, 5.8 psi) and Figure 4.104 (post-Magnolia, 6 psi). The remaining shots had no additional effects.

Fire Hydrant. A typical view of a fire hydrant located in the 2.0-, 8.2-, 3.1-, 9-, 3.1-, 4.7-, 3.0-, and 2.8-psi air-overpressure range for Shots Cactus, Butternut, Holly, Magnolia, Rose, Linden, Sequoia, and Pisonia, respectively, is shown in Figure 4.105. The hydrant was not damaged by any of the shots.

Chapter 5

DISCUSSION

The discussion of results is divided into three general categories: prediction curves, radiation and water waves, and damage-distance relationships.

5.1 PREDICTION CURVES

5.1.1 Air Overpressure. Observed pressure-distance data, reduced to a 1-kt surface burst, have been plotted in Figure 5.1, where the solid curve is identical to the 1-kt plot shown in Figure 2.3, which was used for predicting the ground-surface air overpressure for each of the various stations that were investigated and summarized in this report. The points in the high-pressure zone, as plotted in Figure 5.1, represent data (References 12 and 13) from Shots Cactus (17 kt) and Koa (1.38 Mt), thus covering a low-yield and a high-yield shot.

In the very-low-pressure range, the plotted points represent data (Reference 12) from Shots Cactus, Koa, Butternut (80 kt), Magnolia (57 kt), and Yellowwood (340 kt). The data, as plotted, have not been corrected for wind, temperature, or any of the other meteorological conditions that can have marked effects on the properties of a blast wave in the ranges of very-low air overpressures.

The plotted points agree closely with the prediction curve, thus establishing a satisfactory level of confidence for the predicted air-overpressure values for the other shots investigated during the operation.

5.1.2 Floor-Slab Acceleration. Limited acceleration data are available, and only a few points (References 12 and 13) were plotted on the acceleration-prediction curve (Figure 2.5), as shown in Figure 5.2. The points represent data from Shots Koa and Cactus. The data are not sufficient to determine the overall reliability of results obtained from using the curve; however, it appears that a reasonable value can be determined.

5.2 RADIATION AND WATER WAVES

5.2.1 Nuclear Radiation. Methods for predicting radiation within structures were not available at the time of this operation except for the slant-thickness method which, as shown by this report, is not reliable. The path-of-least-resistance method for predicting radiation within structures was therefore developed and is described in Appendix A. The measured and predicted values using this method were in reasonably close agreement. See Section A.6 for a detailed discussion.

5.2.2 Thermal Radiation Damage. Primary thermal radiation has seldom been a governing factor in damage to structures. However, it is quite important to know thermal levels when designing protective structures for very-high-overpressure regions.

The predominant effect of thermal irradiation is the heating of exposed surfaces of structures. The effect of moderate irradiation on steel is simply to heat the surface; however, thin sections can lose strength. The effect of moderate irradiation on concrete results only in surface spalling.

Observation of structures during this operation showed no case where thermal radiation was a governing factor in structural damage. Observations included steel exposed to 1,400 cal/cm² (Item 10) and concrete exposed to 650 cal/cm² (Item 31).

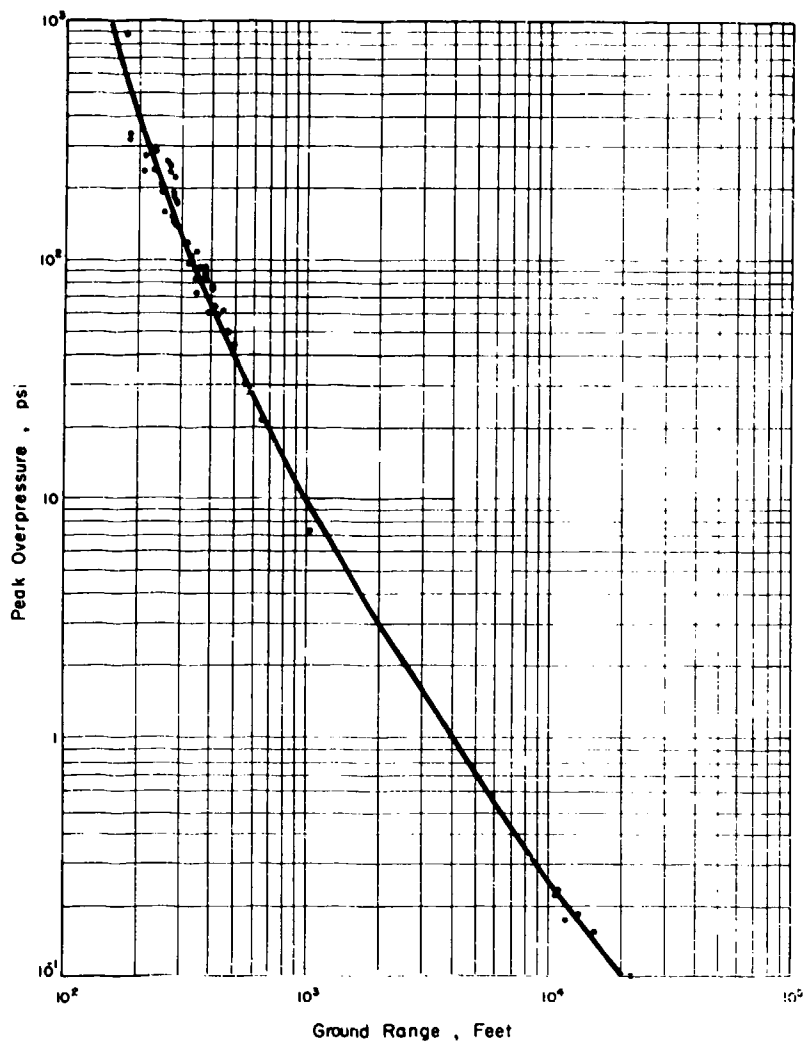


Figure 5.1 Peak air overpressure for a 1-kt surface burst, with observed points.

5.2.3 Water Waves. Blast-generated water waves were instrumental in removing considerable quantities of loose material from earth mounds and earth berms. Observations of wave damage in this and past operations indicate that close-in structures surviving the effect of air blast will undoubtedly survive the force of water waves. See Section D.5, Appendix D, for a detailed discussion.

5.3 DAMAGE-DISTANCE RELATIONSHIPS

Damage to certain common facilities and installations, such as camp sites, generators, and storage tanks, has been observed and reported during several previous operations. For these items, the past damage data, as well as that obtained during Operation Hardtack, have been studied for the purpose of determining damage-distance relationships. Where possible, the damage has been compared with the curves of TM 23-200 (Reference 8).

Damage classification, namely, severe, moderate, and light (Reference 8), has been used throughout this report in describing the degree of damage to the various stations. In the following sections a detailed description of damage classifications pertaining to specific items is given.

5.3.1 Camp and Wood-Frame Structures. The light wood-frame buildings for camp sites were constructed to provide temporary facilities for messing, storage, maintenance, and administration. Typical construction for these buildings consisted of 2-by-4-inch studs 2 feet on center, trussed rafters 2 feet on center, $\frac{1}{2}$ -inch exterior plywood siding, and corrugated aluminum roofing.

The damage-distance relationship shown in Figure 5.3 represents the results of observations of damage made during Operations Ivy, Castle, Redwing, (Section 1.2.1 and References 1 and 2), and Hardtack. The following descriptions define the damage levels for the curves shown:

Severe Damage. Frame shattered so that the structure is for the most part collapsed.

Moderate Damage. Wall framing cracked. Roof badly damaged. Interior partitions blown down.

Light Damage. Windows and doors blown in. Interior partitions cracked.

Distances shown for severe damage are those for which the probability of the damage occurring is 50 percent, the 2.0-psi level. The spread of the data in the severe-damage range supports the methods of obtaining 10-percent and 90-percent probability given in Reference 8. For 90-percent probability, use is made of the distance for a weapon of half the desired yield. For 10-percent probability, use is made of the distance for a weapon of twice the desired yield.

The moderate-damage level (1.0 psi) was determined by using the distance for a weapon of four times the desired yield, as in Reference 8. The light-damage curve (0.75 psi) is intended to represent the upper limit of nuisance damage and the threshold of light damage. The severe-damage curve (50-percent probability) for wood-frame buildings, one- or two-story house type, as given in Reference 8, is also shown in Figure 5.3.

Damage to several types of heavy-wood-framed structures has been observed, but insufficient data make it impossible to determine damage-distance relationships for such variable structures. However, it has been demonstrated that small, essentially windowless, wood-frame structures can be designed to withstand overpressures up to 4.5 psi (Reference 1), if a moderate degree of damage is acceptable.

5.3.2 Storage Tanks. Damage curves (Reference 8) show that large oil storage tanks (30 feet in height, 50 feet in diameter) are primarily diffraction structures and, therefore, overpressure sensitive. Damage levels for large oil tanks are described as follows:

Severe Damage. Large distortion of sides, seams split, so that most of the contents are lost (approximately 11-psi level).

Moderate Damage. Roof collapsed, sides above liquid buckled, some distortion below liquid level (approximately 5-psi level).

Light Damage. Roof badly damaged (approximately 1-psi level).

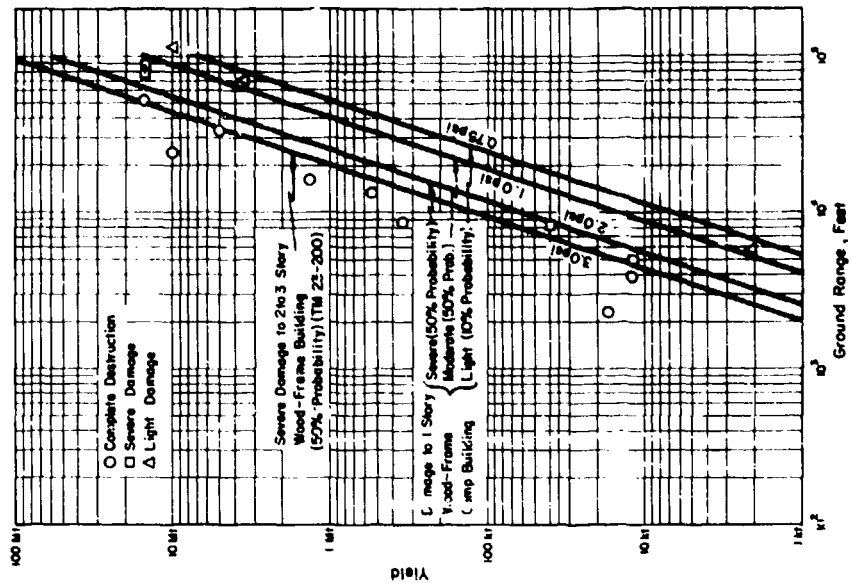


Figure 5.3 Damage to wood-frame camp structures for a surface burst.

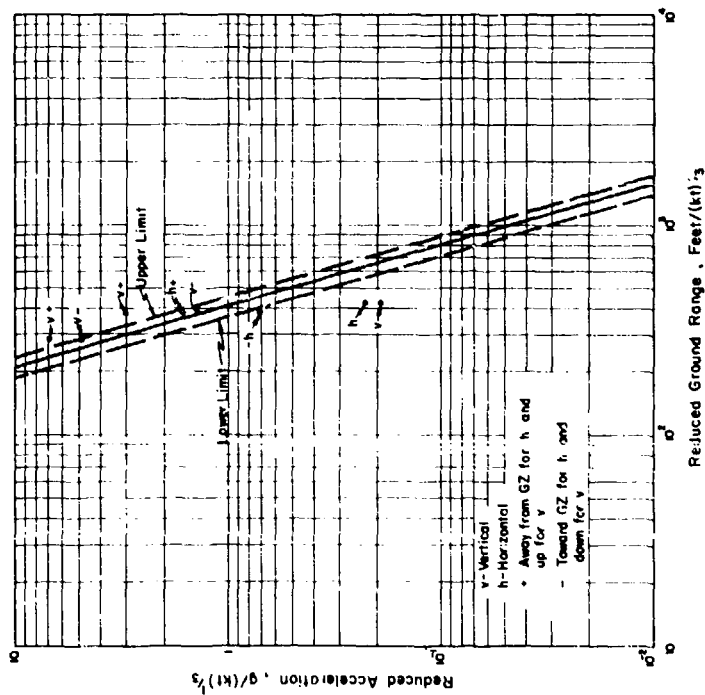


Figure 5.2 Reduced vertical ground acceleration 10 feet below ground surface for a 1-kt surface burst, with observed points.

A 21,000-gallon water tank (Item 37) directly exposed to 6.5 and 7.0 psi of air overpressures received light damage. The roof was dished in, and there was a small amount of buckling of the sides above the level of liquid in the tank. In addition, it was noted that there was no damage to the exterior connecting piping.

Similar tanks exposed during previous operations (Section 1.2.1) confirm the observation that these smaller tanks are considerably less vulnerable to damage at a given pressure level than large oil-storage tanks. There is insufficient data to plot a damage-distance relationship for tanks of the type investigated in this report. However, examination of the data indicates that light damage is to be expected between air overpressures of 3 and 10 psi.

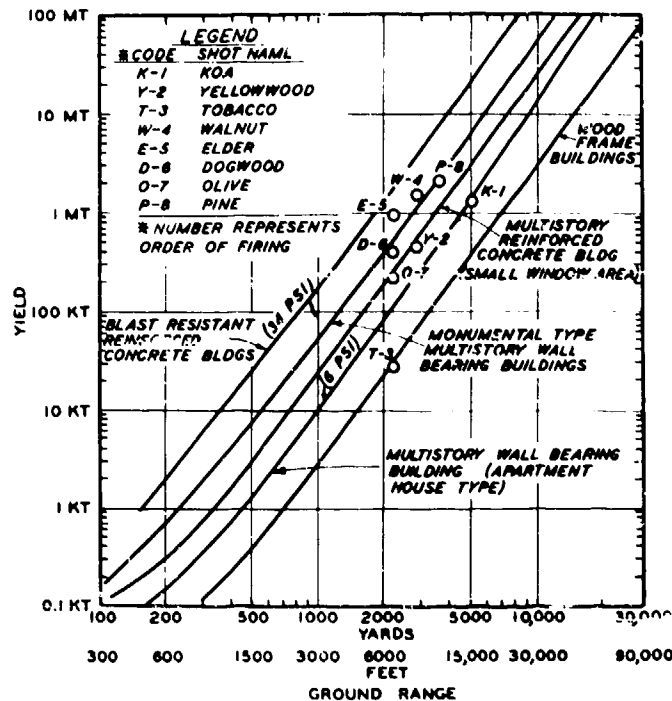


Figure 5.4 Data for Structure 3.1.1 plotted on curves entitled "Severe Damage to Various Structures Primarily Overpressure-Sensitive by Surface Burst of Various Yields" from Reference 8.

5.3.3 Station 3.1.1 (Item 26, Three-story Blast-Resistant Buildings). The response of this structure allowed a limited comparison of observed with predicted damage. However, predicted damage is based on the effects from single shots while the structures in question were subjected to many shots. The severe-damage curve labeled "Blast Resistant, Reinforced-Concrete Buildings" shown on Page 7-45 of Reference 8 was used for comparing predicted with observed response. This comparison can be seen in Figure 5.4. Here the observed responses for the various shots are plotted on the prediction curve. The curve labeled "Blast Resistant Reinforced Concrete Bldgs" has an indicated 34 psi at its lower end. The upper end, although not labeled, decreases to 32 psi for the greater yields and ranges.

The curve predicted something less than severe damage for Shots Walnut and Elder alone. Severe damage is defined as the collapse of the first floor columns of the building. Shot Walnut caused the columns of the first floor of Building No. 5 (the concrete structure with windows) to

displace laterally about one foot, thereby greatly weakening the structure. It can be assumed that a slight additional load would have caused collapse of the columns. Shot Elder, which had about the same input pressure as Walnut, provided the force necessary to cause collapse of the first floor columns.

Since none of the blast-resistant steel buildings, the concrete building without windows, and the shear-wall building underwent severe damage, the damage curve as used also appears reasonable for predicting the response of these structural types.

Although the roof of the shear-wall building collapsed, the frame and walls were only slightly distressed and the building was not considered to be severely damaged. The roof failure shows the need for careful consideration of roof designs. For example, it was observed that the line of failure for roofs occurred at locations where main stress steel had been terminated; had these bars been continued, these failures may not have occurred.

5.3.4 Station 1312 (Item 25, One-story, Reinforced-Concrete Building). This structure provided the opportunity to record blast-diffraction measurements from four different shots. It was observed that the predicted and recorded pressures on the front and rear faces of the station were in close agreement. The observed and the predicted pressure curves along the roof were in rather poor agreement, especially after the arrival of the vortex. See Section B.2, Appendix B, for a detailed discussion.

5.3.5 Gage Piers (Item 28). Since several of the piers failed from air-blast effects and one did not, an opportunity was afforded to compare predicted response with observed response for diffraction targets oriented at various angles of incidence with surface zero. Even though the analysis was made assuming both the strength properties of the materials and the air-overpressure values for the stations investigated, the predicted and the observed response were in close agreement. See Section C.4, Appendix C, for a detailed discussion.

5.3.6 Miscellaneous Damage. The many support-type structures located at the various sites were exposed to a wide range of overpressure. The heavily reinforced-concrete structures located at the end of Site Tare were subjected to pressures over 1,000 psi from low-yield kt devices without being damaged. An unmounded, reinforced structure (Item 2) located on Site Able was subjected to an estimated 1,200 psi from a 9.3-Mt device and was completely destroyed.

Generators (Item 23), located behind the station complex (earth-mounded station) and exposed to an overpressure of 35 psi, suffered severe damage. However, of particular interest was the striking evidence of the protection afforded objects sheltered from the air blast by an obstruction. The fully sheltered generator moved only 2 feet, whereas the least sheltered generator was thrown 60 feet.

Chapter 6

CONCLUSIONS and RECOMMENDATIONS

6.1 CONCLUSIONS

The objective of recording damage from air blast, radiation, and blast-generated water waves was attained. Detailed conclusions are presented in Appendixes A, B, C, and D. The general conclusions are that:

1. The peak air-overpressure curve (Figure 5.1) is reliable for scaled air overpressures from 0.1 to 350 psi.
2. The peak-ground-acceleration curve (Figure 5.2) gave reasonable predictions of floor-slab accelerations. However, the overall reliability of the curve is uncertain, inasmuch as limited data were obtained.
3. Radiation levels inside shelters discussed in this report were adequately predicted by using a path-of-least-resistance method (see Appendix A).
4. Radiation levels inside shelters were not realistically predicted using the least-slant-distance concept.
5. Thermal radiation was not a governing factor in structural damage for exposures up to 1,400 cal/cm² for steel.
6. Total thermal radiation of up to 650 cal/cm² caused only minor surface spalling of directly exposed concrete.
7. Structural effects due to water waves may be neglected for close-in structures designed to withstand air blast.
8. At greater distances, where air blast is of no great consequence, water waves must be considered in structural design and planning.
9. Light wood-frame structures (camp buildings) suffered severe damage from air overpressures ranging from 1.4 to 3.0 psi.
10. Bolted-steel, ground-surface storage tanks (27,000 to 30,000 gallons in capacity), full of liquid, suffered only light damage from overpressures less than 10 psi.
11. The damage-prediction curve entitled "Blast Resistant, Reinforced-Concrete Buildings," Reference 8, appears adequate for predicting damage to three-story, blast-resistant structures of the Station 3.1.1 type, i.e., reinforced-concrete building, with and without windows; structural steel, with and without windows; and a reinforced-concrete, shear-wall building.
12. Reinforcing steel in roofs of blast-resistant structures should be designed to provide more uniformity of strength. At least one half (but preferably all), the area of positive reinforcement required within a continuous or restrained section of roof should extend beyond the face of the support for a distance of 30 bar diameters. At least one half the reinforcement provided for negative moment at the support should be extended beyond the point of inflection a distance sufficient to develop the allowable stress in such bars or a distance equal to the depth of the member, whichever distance is greater. By this procedure, abrupt changes in the strength of a member would be minimized. Local failures, thus, would not cause the failure of a whole roof section before other portions (of that section) were overstressed.
13. Heavily reinforced concrete structures (earth-mounded and having 5- to 6-foot-thick walls and roof with clear spans up to 5 feet) survived air overpressures of 1,000 psi without damage.
14. Objects located close behind earth mounds within a distance approximately equal to the

height of the mound received considerable protection from dynamic pressures at overpressures of 35 psi and lower.

15. Exposed standard 2-inch and 4-inch water pipes, including standard rising-stem valves, survived pressures up to 8 psi without sign of damage.

16. For structures oriented so that a line drawn through ground zero is normal to the front face of the structure (zero angle of incidence), it was found that the method used in predicting loading on the front and back walls of diffraction-type structures provided results sufficiently realistic for design or analysis purposes.

17. The predicted shape of the overpressure curve for the roof of diffraction-type targets was not in close agreement with measured results.

18. The method used for predicting pressures on the front and rear faces of diffraction targets at various angles of incidence with ground zero is satisfactory for design but not for analysis purposes.

6.2 RECOMMENDATIONS

1. It is recommended that the path-of-least-resistance method (Appendix A) be adopted for use in predicting radiation within structures.

2. The present method available for predicting pressures on the front and rear faces of diffraction targets oriented at a zero angle of incidence is adequate and is recommended for design and analysis purposes. The present method of predicting roof pressure should be used until a better method is determined.

3. Additional high explosive and/or shock-tube experiments should be performed to: (1) determine a more realistic overpressure distribution along roofs of diffraction-type targets; and (2) determine the pressure distribution on the front and back faces of these targets when oriented at various angles of incidence with ground zero.

4. Continuous beams, slabs, or walls of blast-resistant structures should be designed for greater uniformity of strength throughout their span. Any abrupt changes in the strength of a member invite local failure which can cause the whole member to fail before other portions of the member are seriously distressed.

Appendix A

NUCLEAR RADIATION

By Edwin S. Townsley, Captain, Corps of Engineers, U.S. Army Engineer
Waterways Experiment Station, Vicksburg, Mississippi

A.1 INTRODUCTION

Film-badge dosimeters were installed in four structures to obtain additional information on shielding against nuclear radiation. The effectiveness of shielding is determined primarily by the following factors taken from Reference 8: (1) distribution of the energy of radiation, (2) intensity of the incident radiation, (3) angle of incidence of the radiation, (4) mass of the shielding material, and (5) geometry of the shielding.

The first three of these are functions of the radiation itself while the last two are functions of the protective shelter. Therefore, to better understand the problem of shielding, a brief review of what is known about radiation and how the structure affects radiation will be given.

A.2 THEORY OF RADIATION

Since the purpose of this discussion is to point out the uncertainties involved in making computations of shielding against radiation, the discussion will center primarily on initial gamma radiation. The uncertainties arising in considering neutron and residual radiation are no less formidable. The following definition of flux as pertains to nuclear radiation is taken from Reference 14:

"The flux of any type of radiation is the total number of particles per unit area and per unit time arriving at a particular point from all directions and at all energies. The unscattered flux is that portion of the total flux which arrives directly at the point in question from the source, without having suffered any previous collisions. The unscattered flux is mono-directional if the source of radiation is a point."

It is possible to write an equation for the unscattered flux at a target in terms of the intensity of the (point) source, distance between source and target and the mean free path in the uniform homogeneous medium in which both the target and source are assumed to be located. This equation becomes less accurate as approximations are added to account for the contribution of scattered flux, size and distribution of energy in the source, and the lack of uniformity and homogeneity in the medium (including both the hydrodynamic

effect and the air-earth interface). Therefore, it is obvious that there are considerable uncertainties not only as to the intensity of radiation, but also as to the distribution of the energy and the angle of incidence of the radiation at the exterior surface of the structure.

A.3 STRUCTURAL SHIELDING

As was noted in Section A.1, both the mass and geometry of the structure must be considered. In determining the attenuation of radiation with thickness for various materials, the normal procedure is to direct a known radiation perpendicularly against a specimen of the material in question and measure the amount of radiation on the other side of the specimen. Therefore the geometry of the material is assumed to be an infinite plane of given thickness, and the radiation is monodirectional, assumed to be monoenergetic, and normal to the surface of the specimen.

Thus the normal procedure for computing the attenuation to be obtained in a structure is to assume that a monoenergetic and monodirectional radiation strikes the surface of the structure at an angle determined by the line of sight between the source and the structure. The slant thickness of the structural material measured along this line of sight is used in determining attenuation. Work by the National Bureau of Standards (Reference 15) indicates that the shielding computed in this way may be much greater than actually exists for concrete walls of more than five inches thickness and angles of incidence greater than thirty-five degrees. Therefore, the problem of predicting shielding involves the dual problems of determining what radiation exists at the outside of the structure and of computing how much of that radiation passes through the walls of the structure to its interior, or, to quote Reference 14:

"No generalized treatment of the military gamma shielding problem, either theoretically or experimentally based, can be presented at this time. The geometrical configuration of a structure bears importantly on its shielding effectiveness; the geometry of the most practical structures and of the topography in which they are located cannot be simply described in a mathematical sense. It is extremely difficult therefore to compute the shielding effectiveness of a given

structure with any reasonable accuracy. The computational problem is compounded by the general lack of information of the distribution of radiation at the receiver in intensity, energy, and angle. Generalizations based on experimental measurements are equally difficult because the data are limited and distributed over a variety of structural types, and often lack internal consistency.

"Under these circumstances it is felt that, at present, the best way to determine the shielding effectiveness of a given configuration of materials is to estimate it from experimentally measured values for similar structures under similar conditions."

It was because of this statement that radiation measurements were taken in a variety of structures. But this method of determining the shielding is not adequate for the engineer who faces the problem of designing a structure to protect its contents from all weapon effects. Accordingly, for purposes of predicting the shielding offered by a structure, a somewhat different approach was taken.

A.4 PREDICTION METHODS

A.4.1 Slant Thickness. The conventional method of computing shielding is to determine the thickness of the material of the structure along the line of sight to the source. These thicknesses can be transformed into attenuation factors by reference to numerous available charts. In this study the charts in TM 23-200 (Reference 8) were used.

A.4.2 Path of Least Resistance. Generally, it has been observed that radiation inside structures is greater than could be explained on the basis of slant-thickness computation. It has long been recognized that the radiation inside a structure may be much higher than anticipated due to the admittance of radiation through the entranceway. To make some estimate of this effect, and to attempt to account for the weakness of the slant-thickness method found by the National Bureau of Standards, the following assumptions and approximations were made:

1. In regions of high flux, where shielding is a problem, radiation is assumed to be essentially directional along the line of sight in its properties. (An indication of the validity of this assumption will be found in Section A.6.)

2. Where this directional radiation must turn approximately 90 degrees to enter the shelter, the flux is reduced to $\frac{1}{15}$ of its line-of-sight intensity. (This figure was arrived at by observing that radiation intensities in foxholes, where essentially a right-angle turn of radiation is required, vary from $\frac{1}{10}$ to $\frac{1}{20}$ of the line-of-sight intensity.) If two right angles or 180 degrees must be turned, the intensity is $\frac{1}{200}$ the line-of-sight intensity (approximately $\frac{1}{15^2}$).

3. Since the foxhole is a box structure with one side open as a "window" to radiation, radiation through

more than one side or "window" is assumed to be additive.

4. Where two different shieldings are offered, such as when a steel door occupies a portion of a wall, the attenuations of radiation through the two are computed separately, and their contributions to the interior dose are assumed to be in proportion to their areas. This, in turn, assumes that the solid angle subtended by these areas at the point of interest is proportional to their areas. Steel doors located to one side of a wall do not satisfy this assumption, but the effect of the door is overestimated and the prediction is on the safe side.

These predictions are assumed to be valid up to a distance from the "window" equal to $1\frac{1}{2}$ times the largest dimension of the "window."

A.5 RESULTS

Internal radiation predictions were made for four structures (Stations 560.01, 78.01, Station Complex, and 3.4) using values of external doses determined from Reference 8 and shown in Tables 3.1 and 4.1. The attenuation factors for materials, i.e., concrete, steel, soil, etc., were also determined by using Reference 8. However, these attenuation factors are applicable for yields below 100 kt and therefore the factors used in this report will be somewhat conservative since the yields of most of the weapons in question exceed 100 kt. Both the slant-thickness and path-of-least-resistance prediction methods were used. In the following computations the attenuation factors are first determined and the resulting attenuated radiation values which are the product of the attenuation factor and the predicted external dose are presented in Tables A.1 through A.4.

A.5.1 Station 560.01 (Item 2). This was a rectangular box structure with interior dimensions of 25 by 10 by 9 feet with 4-foot-thick walls and roof (Figure 3.5). The wall facing surface zero for all shots of interest was shielded by an earth berm which was three feet higher than the structure (Figure 3.6). The berm was six feet thick at the top with a vertical surface adjacent to the structure and a two-on-one slope facing surface zero. This berm was partially eroded by wave action during Shot Fir.

Since the distance from surface zero was the same for Shots Fir, Sycamore, and Aspen, the shielding computations are the same for all three shots. The erosion of the berm was not surveyed and has not been taken into account, thus the ratio of observed to predicted interior doses may be slightly higher for the last two shots. The computations are as follows:

Slant-Thickness Method:

Geometry: 20 feet of earth and 4 feet of concrete.

Attenuation Factor (AF) for:

20 ft of soil = 10^{-5}

4 ft of concrete = 1.1×10^{-3}

Total AF: $(a \times b) = 1.1 \times 10^{-8}$, essentially zero.

TABLE A.1 PREDICTED AND RECORDED RADIATION VALUES FOR STATION 560.01

See Section A.5.1 for determination of attenuation factors (AF).

Shot	Predicted Exterior Dose	Dose Behind Door				Average Interior Dose					
		Predicted Method I *		Predicted Method II †		Recorded	Predicted Method I *		Predicted Method II †		Recorded
		AF	Dose	AF	Dose		AF	Dose	AF	Dose	
r	r	r	r	r	r	r	r	r	r		
Fir	7,000	0	0	7×10^{-3}	49	24.5	0	0	8.68×10^{-4}	6.1	3.0
Sycamore	210	0	0	7×10^{-3}	1.56	0.6	0	0	8.68×10^{-4}	0.18	0.1
Aspen	1,000	0	0	7×10^{-3}	7.0	21.0	0	0	8.68×10^{-4}	8.68	2.5

* Slant-thickness method.

† Path-of-least-resistance method.

TABLE A.2 PREDICTED AND RECORDED RADIATION VALUES FOR STATION 78.01

See Section A.5.2 for determination of attenuation factors (AF).

Shot	Predicted Exterior Dose	Dose Behind Door				Average Interior Dose				
		Predicted Method I *		Predicted Method II †		Recorded	Predicted Method I *		Predicted Method II †	
		AF	Dose	AF	Dose		AF	Dose	AF	Dose
r	r	r	r	r	r	r	r			
Fir	10,500	—	—	—	—	—	0	9.8×10^{-4}	9.8	3.0
Sycamore	320	—	—	—	—	—	0	9.8×10^{-4}	0.31	0
Aspen	1,500	0	0	3.5×10^{-3}	5.25	23.0	0	9.8×10^{-4}	1.47	1.3
Maple	—	—	—	—	—	—	—	—	—	1.2†

* Slant-thickness method.

† Path-of-least-resistance method.

‡ Radiation due to fallout.

TABLE A.3 PREDICTED AND RECORDED RADIATION VALUES FOR STATION COMPLEX

See Section A.5.3 for determination of attenuation factors (AF).

Shot	Predicted Exterior Dose	Dose in Entranceway				Recorded	Dose Beyond 90-Degree Turn				Recorded
		Predicted Method I *		Predicted Method II †			Predicted Method I *		Predicted Method II †		
		AF	Dose	AF	Dose		AF	Dose	AF	Dose	
r	r	r	r	r	r	r	r	r	r		
Koa	13,000	0	0	4.1×10^{-3}	53.0	70.0	0	0	2.73×10^{-4}	3.5	4.9
Yellowwood	600	0.82	480	0.82	480.0	130.0	0	0	5.46×10^{-2}	32.0	5.0
Walnut	4,100	0.82	3,370	0.82	3,370.0	875.0	0	0	5.46×10^{-2}	225.0	130.0
Elder	4,100	0.82	3,370	0.82	3,370.0	700.0	0	0	5.46×10^{-2}	225.0	44.0

* Slant-thickness method.

† Path-of-least-resistance method.

TABLE A.4 PREDICTED AND RECORDED RADIATION VALUES FOR STATION 3.4

See Section A.5.4 for determination of attenuation factors (AF).

Shot	Predicted Exterior Dose	Dose Under Hatch Cover					Average Interior Dose				
		Predicted Method I *		Predicted Method II †		Recorded	Predicted Method I *		Predicted Method II †		Recorded
		AF	Dose	AF	Dose		AF	Dose	AF	Dose	
	r		r		r	r		r		r	r
Koa	7,000	—	—	—	—	—	0	0	1.06×10^{-2}	74.0	7.3
Yellowwood	1,000	0	0	5.46×10^{-2}	54.6	6.3	0	0	1.06×10^{-2}	10.6	0.9
Walnut	6,700	0	0	5.46×10^{-2}	366.0	375.0	0	0	1.06×10^{-2}	71.0	41.0
Elder	6,700	0	0	5.46×10^{-2}	366.0	460.0	0	0	1.06×10^{-2}	71.0	38.0

* Slant-thickness method.

† Path-of-least-resistance method.

Path-of-Least-Resistance Method:

AF for one side wall and roof:
4 ft of concrete = $1.1 \times 10^{-3} \times 2$
1 90-degree turn = $\frac{1}{15} \times 2$

AF for rear wall:

4 ft of concrete = 1.1×10^{-3}
1 180-degree turn = $\frac{1}{200}$

Subtotal AF ($1 \times 2 + 3 \times 4$) = 2.98×10^{-4}

AF for side wall with door: (This wall is not only at slightly more than 90 degrees to the line of sight but is also in a radiation shadow caused by the berm. Thus the radiation must turn an angle somewhere between 90 and 180 degrees. A 135-degree factor of $\frac{1}{100}$ is used here although the full 180-degree factor of $\frac{1}{200}$ was used in the ITR.)

Four feet of concrete = 1.1×10^{-3}

Wall-area factor $\frac{(25 \times 9) - (6 \times 3)}{25 \times 9} = 0.92$

$\frac{3}{4}$ -inch steel door = 0.7

Door-area factor $\frac{(6 \times 3)}{(25 \times 9)} = 0.08$

135-degree turn = $\frac{1}{100}$

Subtotal AF ($1 \times 2 \times 5 + 3 \times 4 \times 5$) = 5.7×10^{-4}

Total AF for structure = 8.68×10^{-4}

Total AF just behind the door (3×5) = 7×10^{-3}

See Table A.1 for a comparison of the predicted with the measured radiation doses.

A.5.2 Station 78.01. This was a buried concrete structure. The earth cover over the roof, along the side, and the surface-zero side of the structure had been eroded since construction and were of unknown but appreciable thickness (Figure 3.18 and 3.19). However, since the walls and roof of the structure were so thick, it is believed that no significant radiation entered the structure except through the wall and door located at the back side of the structure. The rear wall was $5\frac{1}{2}$ feet thick, $9\frac{1}{2}$ feet high, and 13 feet wide with a $\frac{3}{4}$ -inch steel door 8 feet $2\frac{1}{2}$ inches high and 4 feet $2\frac{1}{2}$ inches wide.

Since the distances to surface zero were the same for all shots except Maple, the shielding calculations are the same for all conditions except Maple. For Maple, the radiation was due to fallout and no calculations have been made. The computations are as follows:

Slant-Thickness Method:

Since the slant thickness was so great, the attenuation factor determined by this method predicted that no significant radiation reached the interior of the structure, hence an AF of zero.

Path-of-Least-Resistance Method:

AF for wall and door:

$5\frac{1}{2}$ feet of concrete = 10^{-4}

Wall area factor = 0.721

$\frac{3}{4}$ -inch steel door = 0.7

Door area factor $\frac{4.2 \times 8.2}{9.5 \times 13} = 0.279$

180-degree turn = 5×10^{-3}

Total AF ($a \times b \times c + c \times d \times e$) = 9.8×10^{-4}

Total AF behind door ($c \times e$) = 3.5×10^{-3}

See Table A.2 for a comparison of the predicted with the measured radiation doses.

A.5.3 Station Complex. This was a buried, reinforced-concrete structure consisting of many components (Figure 4.3). The thickness of cover and layout of the structure were such that the only significant radiation was found in the entrance tunnel which had a $\frac{1}{2}$ -inch steel door the full height and width of the tunnel. The tunnel made a 90-degree turn, within a distance equal to one and one-half times the height of the door.

For Shot Koa, ground zero was located on the far side of the structure, and the door was completely in the shadow of the structure, thus requiring two 90-degree turns of radiation. For all other shots of interest, the door faced surface zero and thus the computations for slant-thickness and path-of-least-resistance methods were identical. The computations are as follows:

Slant-Thickness Method:

The slant thickness for the Shot Koa geometry resulted in an attenuation factor that predicted no significant radiation within the station.

For the other shots, the AF for the entrance was the same as that determined by the path-of-least-resistance method while the AF for the area beyond the 90-degree turn was negligible.

Path-of-Least-Resistance Method:

AF for Koa only, Entranceway:

$\frac{1}{2}$ -inch steel door = 0.82

180-degree turn = 5×10^{-3}

Total AF ($a \times b$) = 4.1×10^{-3}

Area beyond 90-degree turn:

90-degree turn = $\frac{1}{15}$

Total AF ($a \times b \times c$) = 2.73×10^{-4}

AF for all other shots, Entranceway:

Total AF (a) = 0.92

Area beyond 90-degree turn:

Total AF ($a \times c$) = 5.46×10^{-2}

See Table A.3 for a comparison of the predicted with the measured radiation doses.

A.5.4 Station 3.4. This was a reinforced-concrete, box-type structure mounded with earth, the roof being flush with the top of the mound. The roof was 30 inches thick and 7 by 7 feet in plan with a steel hatch cover $\frac{1}{2}$ inch by 3 feet by 3 feet located in one corner (Figure 4.24).

Since the "radiation window" for this structure was the roof, the location of ground zero or surface zero had no effect on the AF determined by either method. The computations are as follows:

Slant-Thickness Method:

Since the slant thickness was so great, the attenuation factor determined by this method predicted that no significant radiation reached the

interior of the structure, hence an AF of zero.

Path-of-Least-Resistance Method:

AF for roof:

30 inches of concrete = 10^{-2}

Roof-area factor $\frac{(7 \times 7) - (3 \times 3)}{7 \times 7} = 0.816$

$\frac{1}{2}$ inch steel hatch = 0.82

Hatch-area factor = 0.184

90-degree turn = $\frac{1}{16}$

Total AF ($a \times b \times e + c \times d \times e$) = 1.06×10^{-2}

AF under hatch:

Total AF ($c \times e$) = 5.46×10^{-2}

See Table A.4 for a comparison of the predicted with measured radiation doses.

A.6 DISCUSSION AND CONCLUSIONS

Comparison of the predictions shows that the path-of-least-resistance predictions gave a more realistic appraisal of interior dosages. The location and recorded values of the film badges used for the structures is shown in Tables 3.2, 3.3, 4.2, and 4.3. The following observations were made from a study of the referenced tables:

- (1) In Structure 560.01, Film-badge F, which is on the wall opposite the door, showed higher doses for all shots than any other interior badge.
- (2) In Structure 78.01, Film-badge J, also located on the wall opposite the door, showed the highest dose for Shot Aspen.
- (3) In Station 78.01, for Shot Maple, where the source of radiation was fallout, the film-badge recordings for all badges were very uniform.
- (4) In the Station Complex, the predicted doses using the path-of-least-resistance method are all too high. However, two points should be noted: first, the attenuation around the 90-degree turn inside the structure is of the right order of magnitude; and second, all devices were shielded with 180-degree concrete shields or 10-foot water shields. The effect of these shields on dose rates is not known to the author.
- (5) In Station 3.4, Film-badge B, which is the closest interior film badge to the door, showed the highest dose, and Film-badge A in the hatchway showed even higher doses.
- (6) The predictions for Station 3.4 from Shots Yellowwood, Walnut, and Elder were more nearly in agreement with observed doses than predictions for the same shots for the Station Complex.

Observations (1), (3), and (5) above tend to confirm the assumption that radiation follows the line of sight through a radiation window.

Observation (4) and the generally fair predictions for all structures tend to confirm the assumption of

attenuation for 90-degree turns.

Observation (6) may be explained by noting that the radiation window for Station 3.4 is horizontal so that fallout and residual radiations may contribute more significantly to the observations than they do in the Station Complex.

Observation (3) indicates that the 90-degree attenuation is not valid for residual-radiation predictions.

It should be noted that doses were recorded in the same location by several mutually perpendicular film badges. The effect of film-badge orientation was small. These film badges are sensitive to both gamma and neutron radiations, and to both initial and residual radiations. It is not possible to determine how much each of these contributed to the doses reported. Since the weapons considered and the range at which observations were taken were relatively large, it is assumed that neutron radiation is not a large percentage of the total, less than 20 percent. None of the structures were in regions of high fallout except as noted for Station 78.01.

The path-of-least-resistance method contains a number of approximations for which greater refinements are possible. Among these is the assumption that all the radiation is monodirectional along the line of sight, and therefore all radiation must turn the 90-degree angle. The actual distribution of radiation at various ranges from the source has been the subject of such studies as that reported in Reference 16. Another is the assumption that the parts of a window contribute to the total radiation in proportion to their area. It is stated in Reference 17 that the effective contribution of each portion of the window is taken as proportional to the solid angle subtended at the point of interest by the portion of the window being considered. It is believed that refinements such as these do not add sufficiently to the accuracy of the prediction to warrant their inclusion in a prediction procedure that an engineer would use in designing a structure.

A.7 RECOMMENDATIONS

It is recommended that the path-of-least-resistance method be used by engineers to predict initial radiation when designing structures to resist the effects of nuclear weapons and for determining structural and/or construction requirements to provide adequate radiation protection. When designing protective structures for which the point of burst is unknown (which will generally be true except at the Nevada and Entiwetok Proving Grounds), it should be assumed that the radiation window faces the point of burst.

Appendix B

DIFFRACTION LOADING of STATION 1312

Station 1312, a massive, reinforced-concrete structure, shown in Figure 4.32, made an excellent target for a blast-diffraction study. Consequently, five self-recording, air-blast gages were installed by personnel from BRL. The gages were placed flush with the front face, the roof, and the rear face of the station. Pressures were recorded for Shots Yellowwood, Tobacco, Walnut, and Elder. The gage geometry, including the plan and elevation for the station, is shown in Figure B.1.

B.1 PREDICTION METHODS

The general methods set forth in Reference 18 (which were derived mainly from shock-tube studies) were used in predicting the pressure on the front face, roof, and back face of the structure. However, pressure-decay curves both for side-on and dynamic pressures as presented in Reference 8 (TM 23-200) were used in predicting pressure-time relationships.

The free-field overpressure and duration measurements from Station 174.28, located adjacent to Station 1312, were used in predicting the diffracted pressures on the structure. In this manner a more reliable input value of pressure was obtained since the predicted values shown in Table 4.1 were slightly lower than the measured free-field values. The free-field pressure measurements are presented in Table 4.4. Where duration values were not available, the predicted values were used. Since the time of the preparation of this appendix, the value for the free-field overpressure for Shot Elder at Station 174.28 has been revised and is now 71 psi (see Table 4.4) rather than the 65 psi as used in the calculations for the diffraction study. Since the difference is slight, the values in Figure B.5 have not been changed to reflect the increase in measured pressure.

B.2 RESULTS AND DISCUSSION

The recorded and predicted pressure plots for the various gage locations for Shots Yellowwood, Tobacco, Walnut, and Elder are shown in Figures B.2, 3, 4, and 5, respectively.

The predicted arrival time of pressure at the various gages was in close agreement with the measured values where a comparison of these values was possible.

It was observed that the predicted and recorded

pressures on the front face of the structure were in close agreement; however, the predicted pressures were slightly greater.

The peak values for the recorded pressures on the roof were very close to the predicted values except for Record 5-C, Shot Walnut. It was also observed that the vortex-action effect on the measured pressure did not cause as great a decrease in pressure as the predicted plot implies; but the recorded duration shows that the vortex lasted for a longer period of time. It was also observed that the greater the pressure, the greater the strength, and the longer the duration of the vortex.

The predicted and the recorded pressures on the back face of the structure were in close agreement; the predicted pressure values were consistently slightly lower.

The predicted durations for the free-field overpressures were in very close agreement with the measured values.

B.3 CONCLUSIONS

The methods used in predicting the load on the front and back walls of diffraction-type structures oriented at a zero angle of incidence provided results sufficiently realistic for design or analysis purposes. The predicted front-wall pressures were higher and the predicted back-wall pressures were lower than the measured values, resulting in the prediction of a conservative, net-lateral load which is greater than the measured load.

The predicted pressures on the roof were in least agreement with the recorded results. The records indicate that the vortex action lasted for a longer period of time than predicted and that the maximum pressure decay was not as great as predicted. It was also observed that the vortex action is extremely sensitive to pressure level. These few records indicate that additional shock-tube study is needed for the purpose of revising prediction methods for determining pressures on the roof of diffraction structures. However, the present prediction method for determining roof overpressure, even though conservative, is satisfactory for design purposes until a better method is devised.

The wide range of pressure values presented in this study should enable designers to proceed with a reasonable degree of confidence when designing blast-resistant, diffraction-type structures.

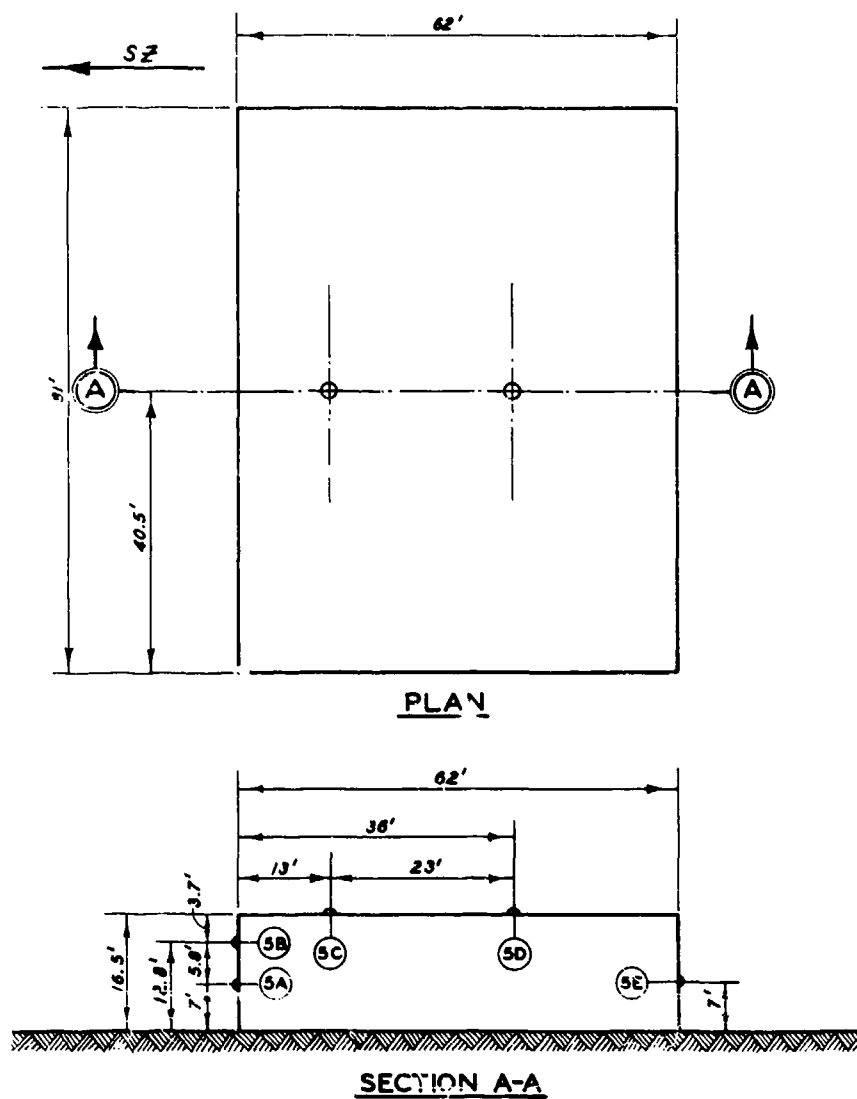


Figure B.1 Plan, elevation, and gage geometry for Station 1312, Site Janet.

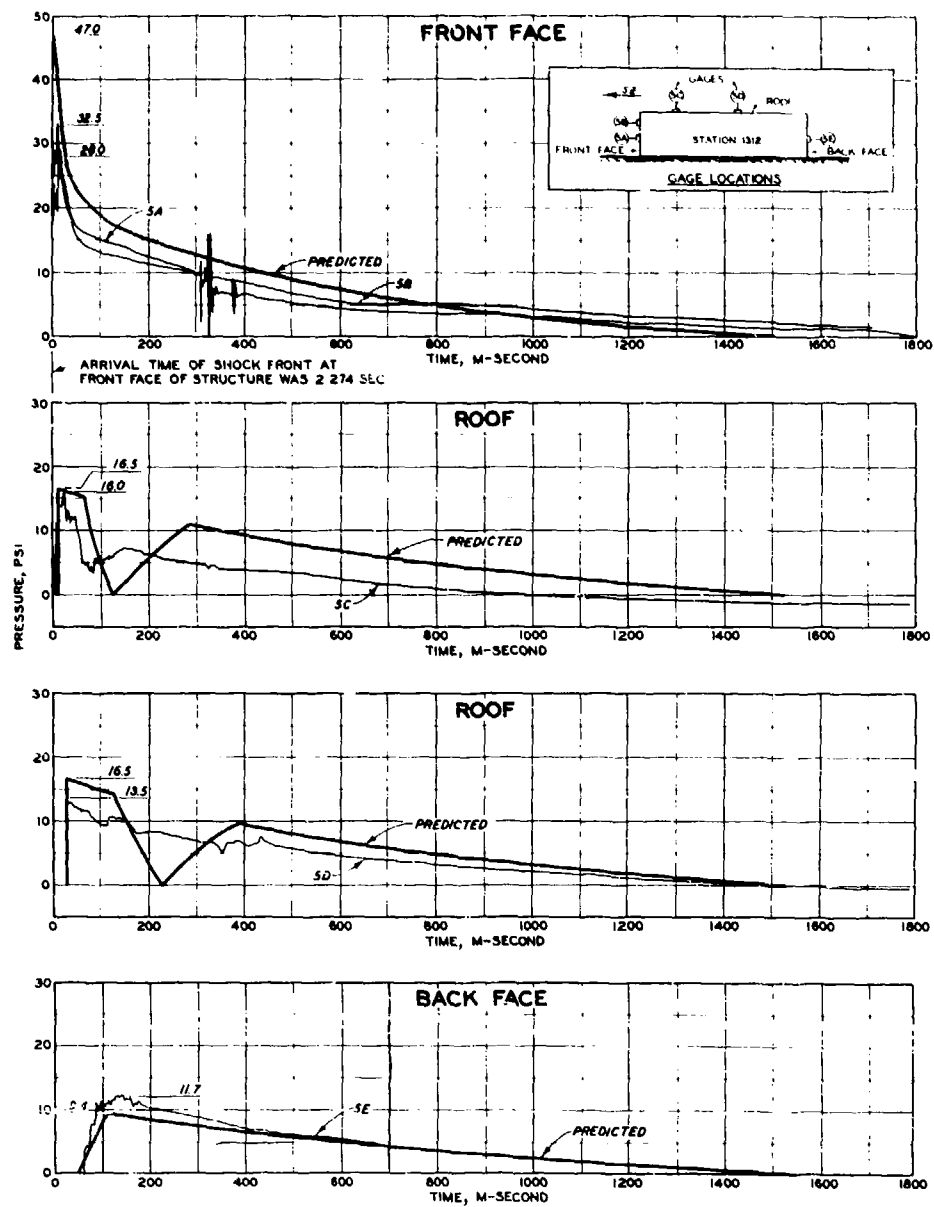


Figure B.2 Measured and predicted pressures for Station 1312, Shot Yellowwood.

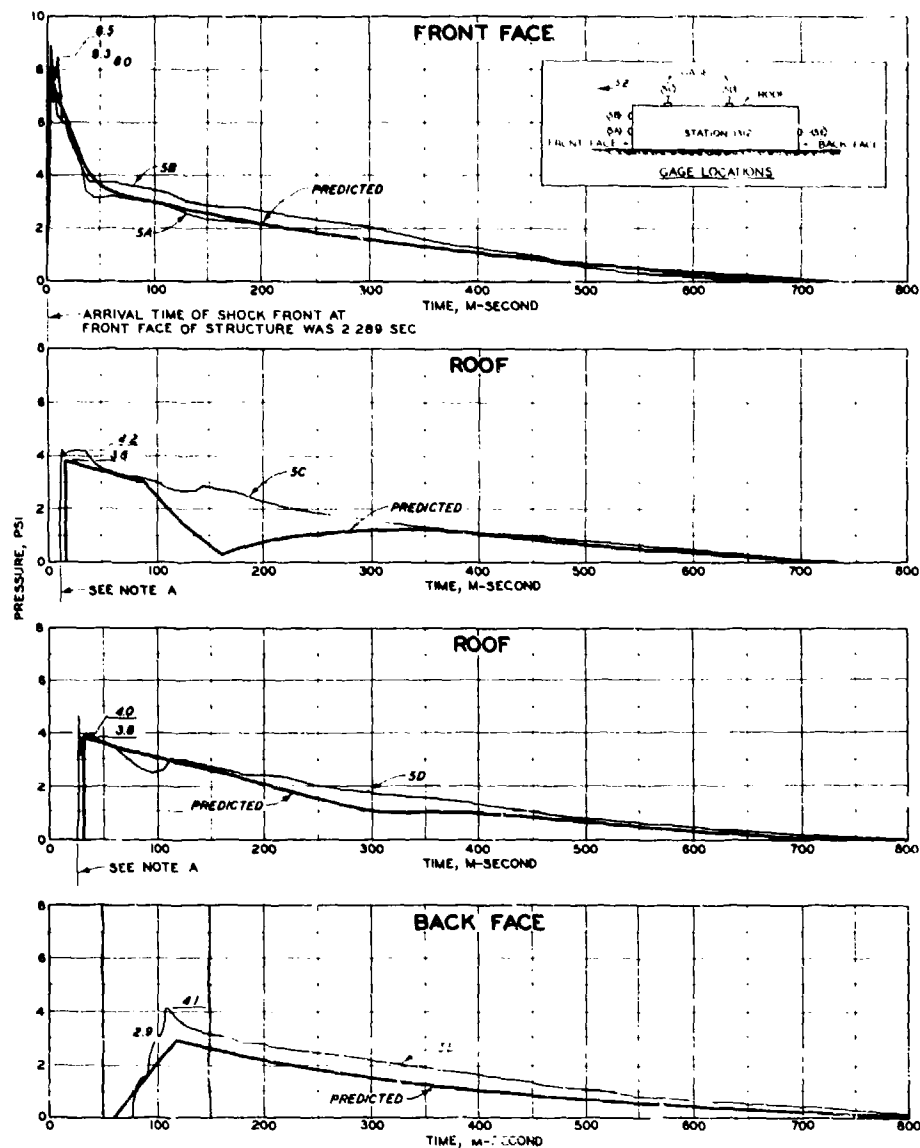


Figure 2.3 Measured and predicted pressures for Station 1312, Shot Tobacco.

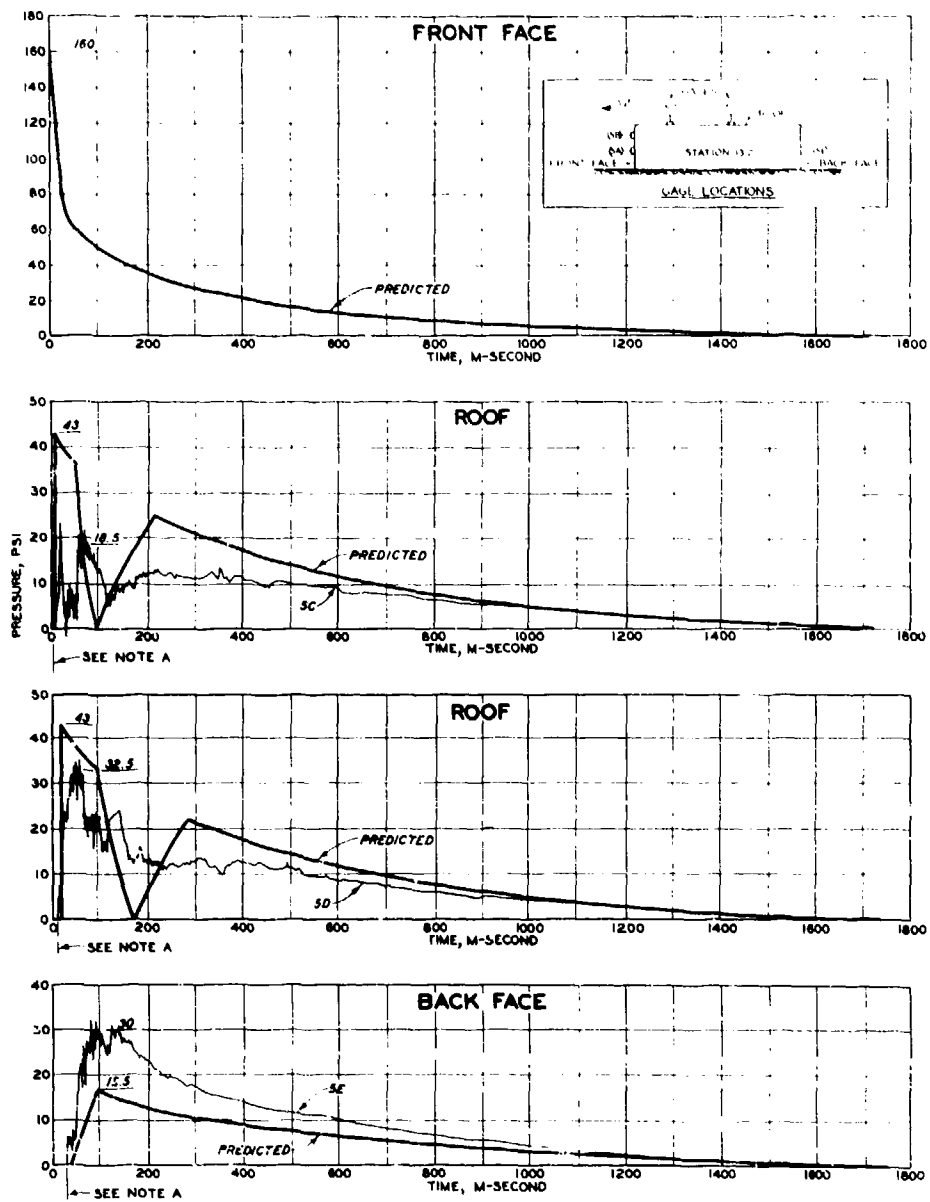


Figure B.4 Measured and predicted pressures for Station 1312, Shot Walnut.

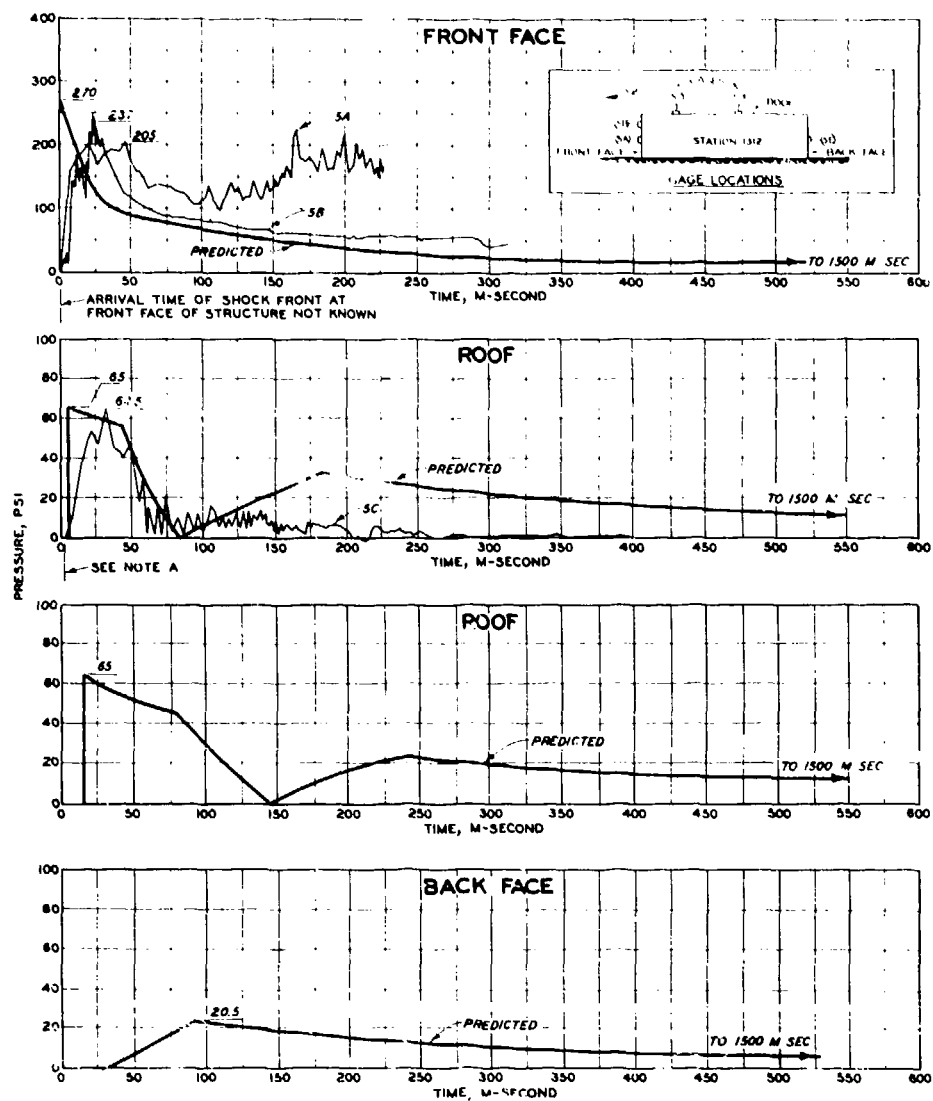


Figure B.5 Measured and predicted pressures for Station 1312, Shot Elder.

Appendix C

RESPONSE of GAGE PIERS to BLAST LOADS

Stations 20-B, C, D, and F on Site Janet offered an opportunity to compare predicted with observed response of reinforced-concrete gage piers, hereinafter also called beams, oriented at various angles of incidence with surface zero and located at various pressure levels. Stations 20-B, C, and F were cracked through at the base (see Figure 4.71) by the air blast from Shot Walnut; however, neither Shot Walnut nor Elder damaged Station 20-F. Since the length of the pier was greater than 5 feet it was analyzed as a diffraction target according to Reference 18. A typical pier and structural details can be seen in Figure 4.69. The estimated pressures received by the four stations at the various angles of incidence from ground zero are shown in Table C.1. The angle of incidence is the angle formed by the intersection of a line from ground zero and the normal to the front face of the structure.

Since information on the strength properties of material is necessary in predicting structural response, the stress-strain relations for steel and concrete used in the gage piers have been assumed and are shown in Figures C.1 and C.2, respectively. The compressive stress for the concrete was specified as 2,000 psi when the pier was constructed; however, it is assumed that age has increased the strength to at least 3,000 psi. The reinforcing steel was of intermediate grade and a typical curve has been drawn to represent the stress-strain relation of the $\frac{3}{4}$ -inch bars used in the piers. To account for the rapid loading by the blast forces, the curves have been increased by 30 percent as shown by the dotted lines. The first of the following analyses uses design strengths of materials under static conditions while the second considers the ultimate capacity of the system under dynamic conditions. Notations as used are listed at the end of this appendix.

C.1 STRUCTURAL ANALYSIS USING DESIGN STRENGTHS

The static design analysis, including definitions for symbols, was made according to practices set forth in Reference 19 (ACI Code). A 1-foot-wide section was assumed and the load causing reactions to the cantilever sections was assumed uniform and normal to the beam, see Figure C.3. The stress relation for the design condition is shown in Figure C.4. The following calculations predict the net lateral pressure (w) that can be applied to the beam as limited by moment, diagonal tension, bearing, and bond. The values listed were used in the computations.

$$A_g = A_g^* = 0.44 \text{ in}^2/\text{foot}$$

$$b = 12 \text{ in.}$$

$$d = 9 \text{ in.}$$

$$f_c = 1,350 \text{ psi}$$

$$f_c' = 3,000 \text{ psi}$$

$$f_s = 20,000 \text{ psi}$$

$$f_y = 47,000 \text{ psi}$$

$$n = 10$$

$$p = p' = 0.004$$

$$s_b = 750 \text{ psi}$$

$$u = 300 \text{ psi}$$

$$v = 90 \text{ psi}$$

$$\Sigma_0 = 2.4 \text{ in.}$$

Determination of Neutral Axis (NA):

Take moment of area about NA. See Figure C.4 for section geometry.

$$6X^2 - (3 - X)(4.4) - (9 - X)(4.4) = 0$$

$$X^2 + 1.47X = 8.8$$

$$X = 2.32 \text{ in.}$$

Determine if moment is limited by compression or tension. From Figure C.4,

$$f_s = \frac{n f_c (d - X)}{X}$$

when

$$f_c = 1,350 \text{ psi (design stress)}$$

then

$$f_s = \frac{10 (1,350) (6.68)}{2.32}$$

$$f_s = 39,000 \text{ psi} > 20,000 \text{ psi.}$$

Therefore the moment is limited by tension.

Determine f_c when $f_s = 20,000 \text{ psi}$

$$f_c = \frac{X f_s}{n (d - X)} = \frac{(2.32) (20,000)}{10 (6.68)}$$

$$f_c = 695 \text{ psi}$$

Use this value when computing moment.

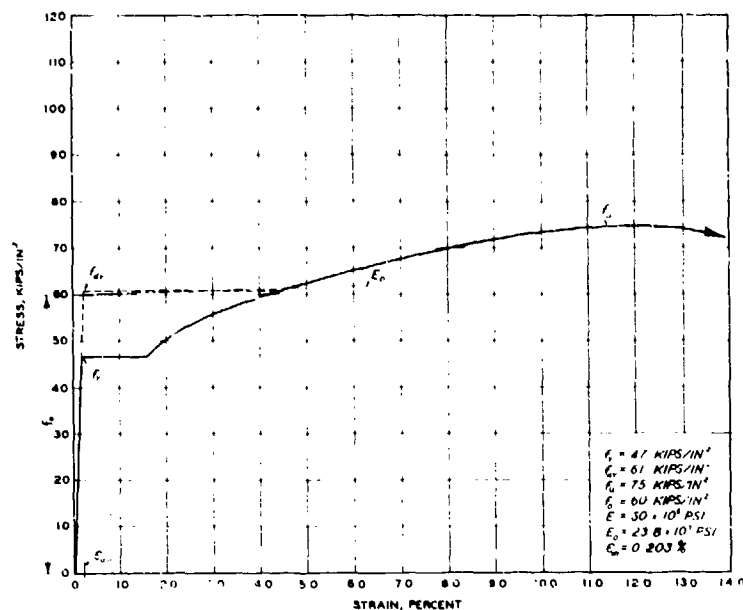


Figure C.1 Stress-strain curve for reinforcing steel.

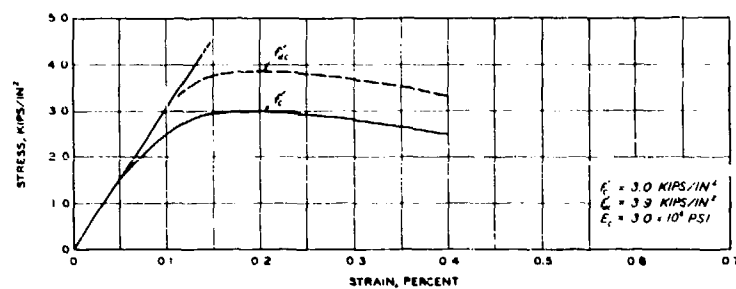


Figure C.2 Stress-strain curve for concrete.

TABLE C.1 PREDICTED PRESSURES AND DURATIONS FOR STATIONS 20-A TO 20-F

Station	Shot	Yield	Ground Range	Angle of Incidence	Overpressure	Reflected Pressure	Positive Duration	Remarks
			ft	deg	psi	psi	sec	
20-A	Walnut	1.45 Mt	6,600	24	26	80	—	*
20-B	Walnut	1.45 Mt	6,930	26	25	76	—	Failed
20-C	Walnut	1.45 Mt	7,125	29	23.5	70	—	Failed
20-D	Walnut	1.45 Mt	7,440	33	21	61	2.1	Failed
20-E	Walnut	1.45 Mt	8,160	40	18	54	—	*
20-F	Walnut	1.45 Mt	8,665	44	16	51	2.2	No damage
20-F	Elder	940 kt	7,105	53	18	43	1.9	No damage

* Destroyed during previous operation.

Moment:

From Figure C.4,

$$M = f'_s A'_s (3 - X/3) + f_s A_s (9 - X/3)$$

since

$$f'_s = \frac{n f_c (d - X - 6)}{X}$$

$$f_s = \frac{n f_c (d - X)}{X}$$

Assume a 1-foot section for the beam

SHEAR:

$$v = 60 \text{ in} \times 12 \text{ in} \times w$$

$$v = 720 w \text{ (lb/ft)}$$

MOMENT:

$$M = 12w \times 60^2 \times \frac{1}{2}$$

$$M = 21,600w \text{ (in-lb/ft)}$$

Determine the maximum shear (V_t) on the section as governed by allowable shearing stress (v).

$$V_t = (v) (b) (jd), \text{ where } jd \text{ in this case is } 8.23$$

$$V_t = (90) (12) (8.23)$$

$$V_t = 8,890 \text{ lb}$$

Determine lateral pressure (w) as governed by the maximum allowable shear of 8,890 lb. From Figure C.3,

$$w = \frac{V_t}{720}$$

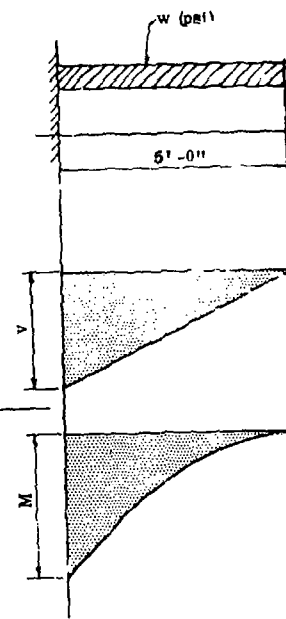


Figure C.3 Assumed loading geometry for typical pier.

then

$$M = 106.87 f_c$$

when

$$f_c = 696 \text{ psi}$$

then

$$M = 74,300 \text{ in-lb}$$

Determine lateral pressure (w) as governed by maximum allowable moment of 74,300 in-lb. From Figure C.3,

$$w = \frac{M}{21,600}$$

then

$$w = 3.4 \text{ psi}$$

Diagonal tension:

then

$$w = 12.3 \text{ psi}$$

Bearing:

Since a 3-inch keyway was used, assume the effective bearing area as 3 by 12 inches (36 square inches) and 750 psi (s_b) as the design stress in bearing

$$V_b = s_b (36)$$

$$V_b = 27,000 \text{ lb}$$

Determine lateral pressure (w) as governed by the maximum allowable bearing load of 27,000 at the keyway.

$$w = \frac{V_b}{720}$$

$$w = 38 \text{ psi}$$

Bond:

Determine the maximum shear (V_u) on the section as governed by allowable bond stress (u).

$$V_u = \Sigma \phi (j d) (u)$$

$$V_u = (2.4) (8.2) (300)$$

$$V_u = 5,900 \text{ lb}$$

Determine lateral pressure (w) as governed by the maximum allowable shear of 5,900 pounds.

$$w = \frac{V_u}{720}$$

then

$$w = 8.2 \text{ psi}$$

From the preceding calculations it is observed that moment controls the load for the piers and therefore, the design load (w) for the piers is 3.4 psi.

$$\frac{(1 - k' - K)d}{Kd} = \frac{\epsilon'_s}{\epsilon_c} \quad (C.2)$$

$$\frac{(1 - k' - K)d}{(1 - K)d} = \frac{\epsilon'_s}{\epsilon_g} \quad (C.3)$$

Stress Relation:

$$C = T_1 + T_2 \quad (C.4)$$

$$\frac{1}{2} f_c K b d = p' b d f'_s + p b d f_g \quad (C.5)$$

$$M_y = b d^2 p' (1 - k' - K/3) f'_s + b d^2 p (1 - K/3) f_g \quad (C.6)$$

From Figure C.1 the following stress-strain relation for steel was determined when f_g is less than f_{dy} :

$$f_g = \epsilon_g E \quad (C.7)$$

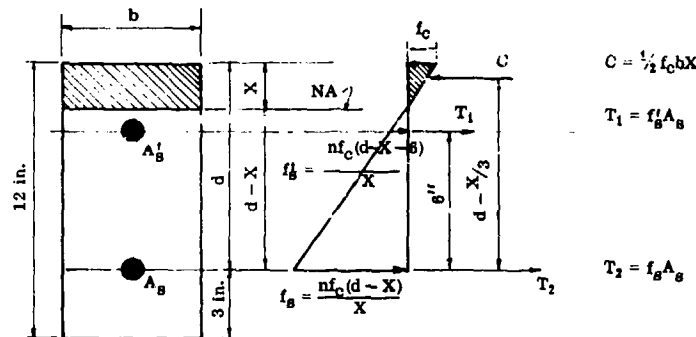


Figure C.4 Stress relationship for concrete section at design strength.

C.2 BEHAVIOR OF CONCRETE SECTION UNDER DYNAMIC LOADS

The analyses were made according to the general procedures set forth in Reference 20 except that dynamic values were used in place of static-strength values for each material. The behavior of the beam (gauge pier) was first determined at the yield strength and secondly at the ultimate strength capacity of the section. From the values of moment at yield and ultimate, an idealized resistance curve for the typical beam was determined.

C.2.1 Flexural Behavior at Yield. The following geometric relations were determined from the stress-strain relation for the concrete section at yield as shown in Figure C.5.

Strain Relation:

$$\frac{Kd}{d} = \frac{\epsilon_c}{\epsilon_c + \epsilon_s} \quad (C.1)$$

$$f'_s = \epsilon'_s E \quad (C.8)$$

From Figure C.2 the following stress-strain relation for concrete was determined when f_c is less than 3,000 psi:

$$f_c = \epsilon_c E_c \quad (C.9)$$

Determination of Moment at Yield (M_y). The general moment equation (6) was used to solve M_y by letting f_g equal f_{dy} and by determining values for K and f'_s . By solving Equation C.5 with the aid of Equations C.1, C.3, C.7, C.8, and C.9, K was determined. Once K was solved, f'_s was found by solving Equations C.3 and C.8. The results are as follows:

$$K = \frac{\sqrt{2p'n(1 - K') + 2pn + n^2(p' + p)^2 - n(p' + p)}}{2(p' + p)} \quad (C.10)$$

when

$$p = p' = 0.004$$

$$k' = 0.67$$

$$n = 10$$

then

$$K = 0.256$$

$$f'_s = \epsilon_s E \left(1 - \frac{k'}{1-K} \right) \quad (C.11)$$

when

$$\epsilon_s = 0.00203 \text{ (see Figure C.1)}$$

$$E = 30 \times 10^6 \text{ psi}$$

$$k' = 0.67$$

then

$$f'_s = 6,040 \text{ psi}$$

Solve f_c to make certain that it is less than 3,000 psi, the upper limit of Equation C.9.

$$\Delta_y = \frac{\phi_y L^2}{4} \quad (C.16)$$

Where: $L = 60 \text{ in}$

$$\Delta_y = 0.256 \text{ in}$$

C.2.2 Flexural Behavior at Ultimate. At the ultimate capacity of the section several conditions of steel stress could exist. The first possibility that was investigated assumed that f_s was greater than f_{dy} and that f'_s was less than f_{dy} when f_c was at ultimate strength. The assumption proved erroneous since the strain value for f'_s exceeded the strain at yield. It was next assumed that both f_s and f'_s were greater than f_{dy} . However, for this condition, the strain values showed that both stress values were in the yield

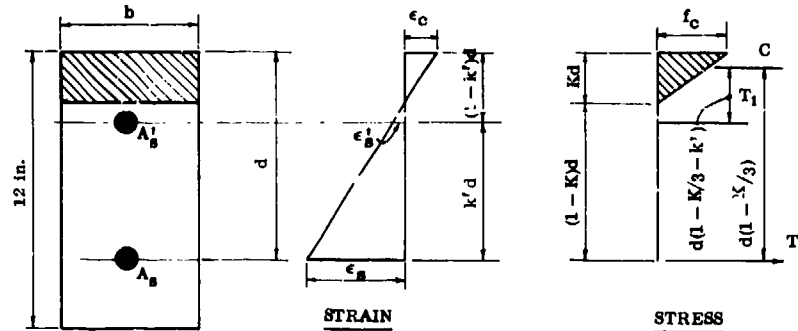


Figure C.5 Stress and strain relationships for concrete section at yield strength.

$$\epsilon_c = \frac{\epsilon_s K}{1-K} = 0.0007 \quad (C.12)$$

$$f_c = \epsilon_c E_c = 2,100.0 \text{ psi} \quad (C.13)$$

By substituting the appropriate values into Equation C.6, M_y was determined.

$$M_y = 223,000 \text{ in-lb} \quad (C.14)$$

Determination of Maximum Curvature (ϕ_y) of Beam. The maximum curvature of the beam when the moment is equal to M_y was found by solving the following expressions:

$$\phi_y = \frac{M_y}{E_c I_y} \quad (C.15)$$

Where: $I_y = b(kd)^3 + pnb d^3(1-K)^2 + p'nbd^3(1-k'-K)^2$

$$I_y = 251.1 \text{ in}^4$$

$$\phi_y = 2.85 \times 10^{-4} \text{ in}^{-1}$$

Determination of Maximum Deflection (Δ_y) at Yield. The maximum deflection of the beam at yield was found by solving the following expression:

range for steel. It was evident that both f_s and f'_s were equal to f_{dy} but it was also evident that the quantity "a" shown in Figure C.6 must be calculated carefully since this value controlled the compressive area of concrete as well as the length of moment arms. Therefore, an idealized stress-strain curve ($f_y = 60,000 \text{ psi}$; and $E_s = 23,800 \text{ psi}$) as shown in Figure C.1 (which closely approximates the actual curve) was assumed. The stress-strain relation for the concrete section at ultimate capacity is shown in Figure C.6, and the following geometric relations were determined:

Strain Relation:

$$\frac{a}{d} = \frac{\epsilon_u}{\epsilon_u + \epsilon_s} \quad (C.17)$$

$$\frac{a}{d(1-k')} = \frac{\epsilon_u}{\epsilon_u + \epsilon'_s} \quad (C.18)$$

$$\frac{\epsilon'_s}{\epsilon_s} = \frac{d(1-k') - a}{d - a} \quad (C.19)$$

Stress Relation:

$$C = T_1 + T_2 \quad (C.20)$$

$$K_1 K_3 f_c' b a = f_s' p' b d + f_s p b d \quad (C.21)$$

$$M_u = (d - K_2 a) (A_s f_s) + d(1 - k') - K_2 a A_s' f_s' \quad (C.22)$$

From the idealized portion of the stress-strain curve shown in Figure C.1, the following expressions were determined:

$$f_s = f_0 + \epsilon_s E_0 \quad (C.23)$$

$$f_s' = f_0 + \epsilon_s' E_0 \quad (C.24)$$

Determination of Moment at Ultimate (M_u). The ultimate moment for the beam was found

$$E_0 = 23,800 \text{ psi}$$

then

$$f_s = 60,650 \text{ psi}$$

Solve ϵ_s from Equation C.23,

$$\epsilon_s = 0.0273 \quad (C.26)$$

Solve a by using Equation C.17,

$$a = 1.15 \text{ in.} \quad (C.27)$$

Solve ϵ_s' by using Equation C.19 which ascertains that the strain was in the yield range.

$$\epsilon_s' = 0.0063 \quad (C.28)$$

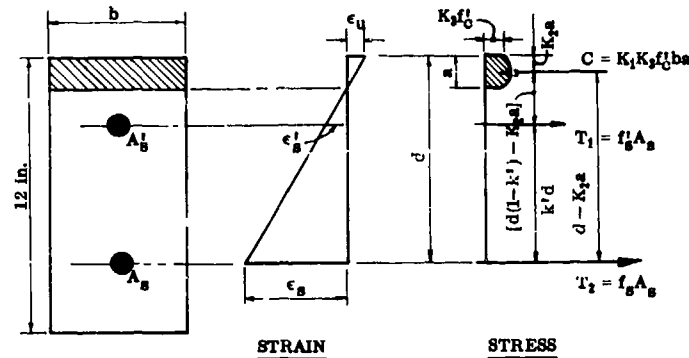


Figure C.6 Stress and strain relationships for concrete section at ultimate strength.

by solving Equation C.21; however, the quantities f_s , f_s' , and a were first determined while f_c was assumed equal to its ultimate value. The quantity f_s was first determined by solving Equation C.21 with the aid of Equations C.17, C.18, C.19, C.23, and C.24. Once f_s was found, a was determined by solving Equation C.17, and f_s' was found by solving Equation C.24. The results are as follows:

$$f_s = \sqrt{\frac{K_1 K_3 f_c' \epsilon_u E_0}{p \beta} + \frac{p' k'}{p \beta} \left(f_0^2 - 2 f_0 \epsilon_u E_0 + \epsilon_u E_0^2 \right) + \frac{C^2}{4} - \frac{C}{2}} \quad (C.25)$$

where

$$C = \frac{(\epsilon_u E_0 - f_0) (1 + p/p' - 2p'k'/p)}{\beta}$$

$$\beta = \left(1 + \frac{p'}{p} - \frac{p'}{p} k' \right)$$

when

$$f_c' = 3,900 \text{ psi}$$

$$\epsilon_u = 0.004$$

$$p = p' = 0.004$$

$$k' = 0.67$$

$$f_0 = 60,000 \text{ psi}$$

By substituting the appropriate values into Equation C.22, M_u was determined.

$$M_u = 290,000 \text{ in-lb} \quad (C.29)$$

Determination of Maximum Curvature (ϕ_u) of Beam. The maximum curvature of the beam when the moment is equal to M_u was found by solving the following expression:

$$\phi_u = \frac{\epsilon_s + \epsilon_u}{d} \quad (C.30)$$

$$\phi_u = 3.48 \times 10^{-3} \text{ in}^{-1}$$

Determination of Maximum Deflection (Δ_u) at Ultimate. The maximum deflection was found by taking statical moments of the beam loaded with angle changer which is illustrated in Figure C.7.

when

$$M = M_u, w = 13.4 \text{ psi} \quad (C.31)$$

Find the section on the beam where the moment is equal to M_y .

$$X = 52.6 \text{ inches} \quad (C.32)$$

Determine deflection at end of beam.

$$\Delta_u = c_y(10X + 500) + \phi_u(1,200 + 10X - X^2/6)$$

$$\Delta_u = 1.062 \text{ inches} \quad (\text{C.33})$$

C.2.3 Moment-Curvature Relation. The moment-curvature relation ($M - \phi$) is shown in Figure C.8. The idealized curve as shown by the dotted line was drawn to establish the idealistic resistance function of the beam. The resistance (r) of the beam was determined by using the idealized moment and found as follows:

$$M_p = \frac{M_y + M_u}{2} \quad (\text{C.34})$$

$$M_p = 261,500 \text{ in-lb}$$

$$w = r = \frac{M_p}{21,600} \quad (\text{Figure C.3}) \quad (\text{C.35})$$

$$r = 12.1 \text{ psi (Resistance of Beam)}$$

C.2.4 Shear-Compression Mode. The moment required to produce failure in the shear-compression mode was determined as shown in Reference 18 and presented as follows:

$$M_s = bd^2 \left[f'_c (k + np') \left(0.57 - \frac{4.5f'_c}{10^4} \right) \right] \quad (\text{C.36})$$

where

$$k = \sqrt{[n(p + p')]^2 + 2n(p + p' - p'k') - n(p + p')}$$

$$M_s = 440,000 \text{ in-lb}$$

Since this moment is greater than the moment determined for flexural failure, it may be assumed that the critical mode is in flexure and not in shear compression.

C.3 DYNAMIC ANALYSIS

Since no measured pressures for any of the piers were taken, the incident pressures were predicted along with reflected pressures for the particular angles of incidence. The positive durations for pressure were also predicted and are shown along with the other values in Table C.1. From the table it was obvious that it was necessary to construct only two pressure diagrams, namely for Stations 20-D and 20-F for Shot Walnut. The pressure diagram for 20-D gave the minimum observed pressure that caused failure while the diagram for Station 20-E showed the maximum observed pressure that did not cause failure. After the pressure curves were determined the piers were analyzed to compare predicted response with observed response.

C.3.1 Determination of Load on Piers. The procedure presented in Reference 18 was used in predicting the pressure-load curves for Stations 20-D and 20-F. A method for accurately determining the pressure on the rear face of diffraction targets when the incident pressure is at an angle of incidence greater

than zero is not described. However, for design purposes the reference recommends that the method described for determining the pressure on the back face for the zero-angle-of-incidence condition also be used for conditions when the angle of incidence is greater than zero. This obviously results in a conservative estimate for the net lateral pressure. The pressure and duration values shown in Table C.1 were used in computing the curves shown in Figures C.9 and C.10. The figures show the pressure on the front and back faces of the pier, the net lateral pressure, and the net idealized lateral pressure which was used in the dynamic analysis. A detailed plot of the reflected pressures for both cases is presented in Figure C.11.

C.3.2 Natural Period of Vibration. The following equation from Reference 21 was used to determine the natural period of the beam for the fundamental mode.

$$T_n = \frac{2\pi}{\omega_n} \sqrt{\frac{W}{gF_c I}} \quad (\text{C.37})$$

where

$$(n_1 L)^2 = 3.52 \text{ (first mode)}$$

$$n^2 = 9.78 \times 10^{-4}$$

when

$$g = 387 \text{ in/sec}^2$$

$$E_c = 3 \times 10^6 \text{ psi}$$

$$I = 332 \text{ in}^4$$

$$W = 12.5 \text{ lb/in of beam}$$

$$L = 60 \text{ in}$$

then

$$T_n = 36.6 \text{ msec}$$

C.3.3 Dynamic Analysis of Pier. Since the durations of the pressure spikes in Figure C.11 were significant when compared to the natural period of vibration of the beam, the piers were analyzed for both the effects from the spike and the regular net lateral pressure. A chart entitled "Maximum Response of Single-Degree-of-Freedom System to Initial Peak Triangular Force Pulse," in Reference 22, was used in determining P_m , the maximum transient pressure that the beam can withstand.

Station 20-D:

Spike alone:

$$t = 0.016 \text{ sec (Figure C.11)}$$

$$P = 61 \text{ psi (Figure C.11)}$$

$$T_n = 0.0366 \text{ sec}$$

$$\Delta_y = 0.256 \text{ in (Equation C.16)}$$

$$\Delta_u = 0.062 \text{ (Equation C.33)}$$

Find "w" when $M = M_u$

$$w = \frac{M_u}{21,600} \quad (\text{see Figure C.3})$$

Find section on beam where moment is equal to M_y

$$M_y = 6wX^2$$

$$\therefore X = \sqrt{\frac{3,600 M_y}{M_u}}$$

Determine maximum deflection (Δ_u)

Take statical moments of angle changes about "O"

$$\phi_1 : \frac{2X}{3} \cdot \phi_y \cdot \frac{X}{2}$$

$$= \frac{\phi_y X^2}{3}$$

$$\phi_2 : \left(\frac{X}{2} + 30\right) \cdot \phi_y \cdot (60 - X)$$

$$= \phi_y \left(1,800 - \frac{X^2}{2}\right)$$

$$\phi_3 : \left(\frac{X}{3} + 40\right) (\phi_u - \phi_y) \cdot \frac{1}{2} \cdot (60 - X) = (\phi_u - \phi_y) \left(1,200 - 10X - \frac{X^2}{6}\right)$$

$$\Delta_u = \Sigma = \phi_y (10X + 600) + \phi_u \left(1,200 - 10X - \frac{X^2}{6}\right)$$

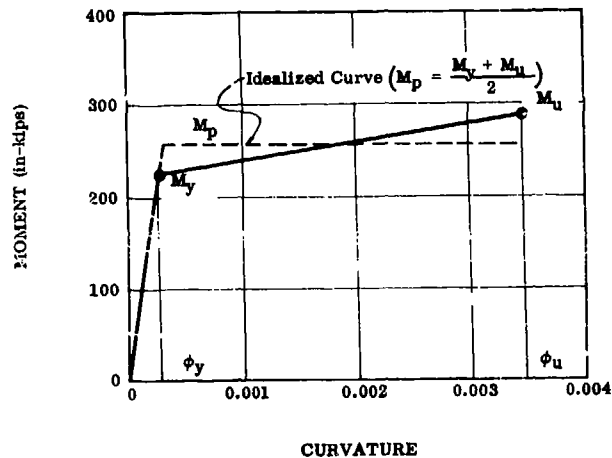
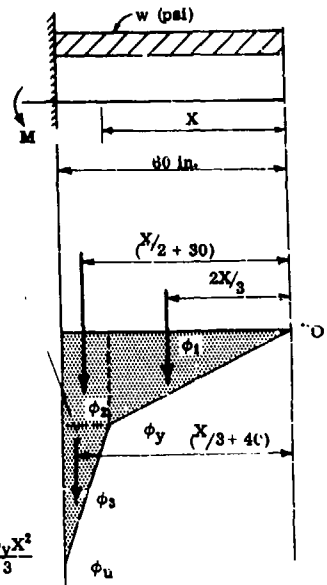


Figure C.8 Moment-curvature diagram for beam.

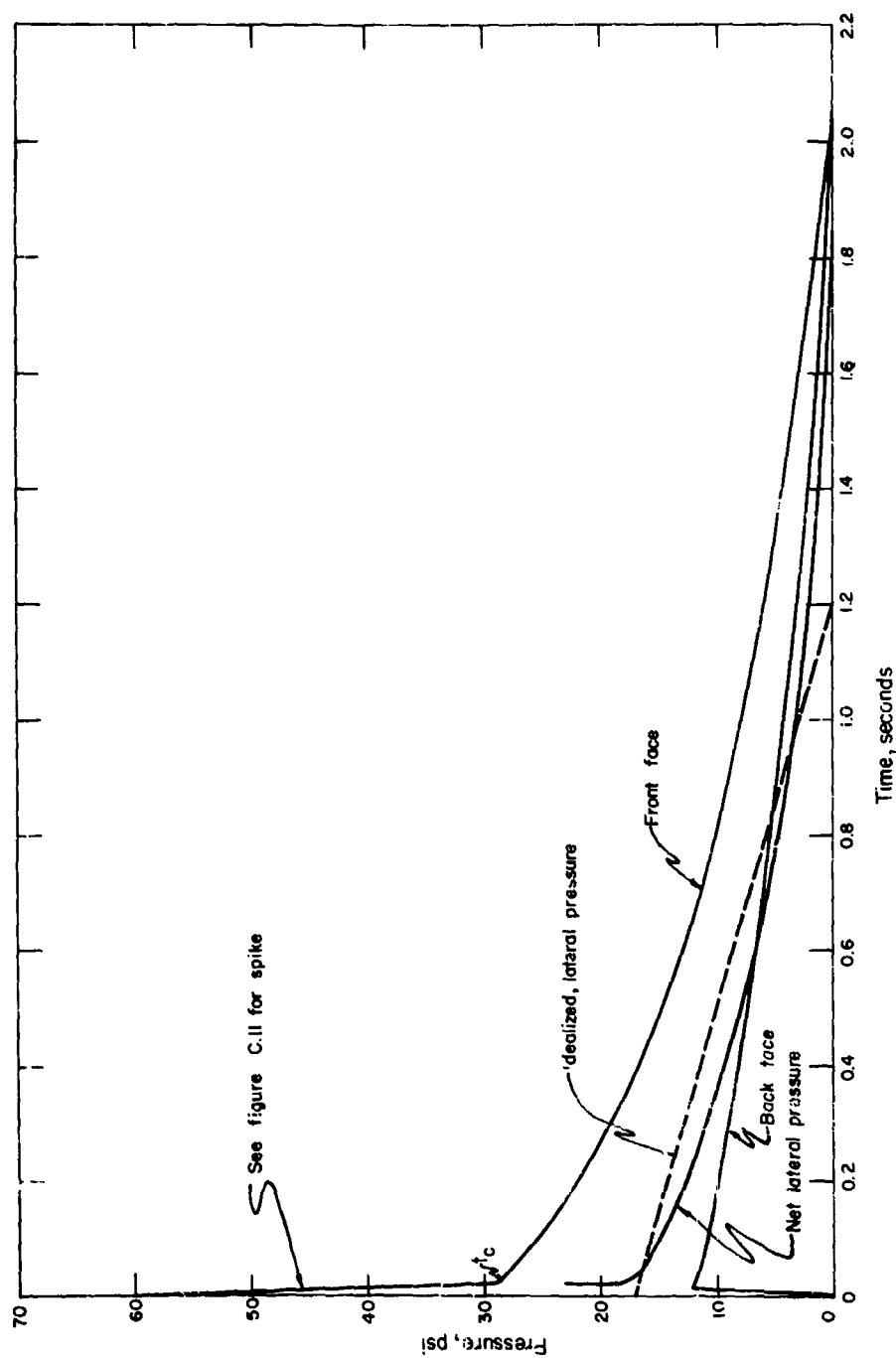


Figure C.9 Effective blast pressure on Station 20-D.

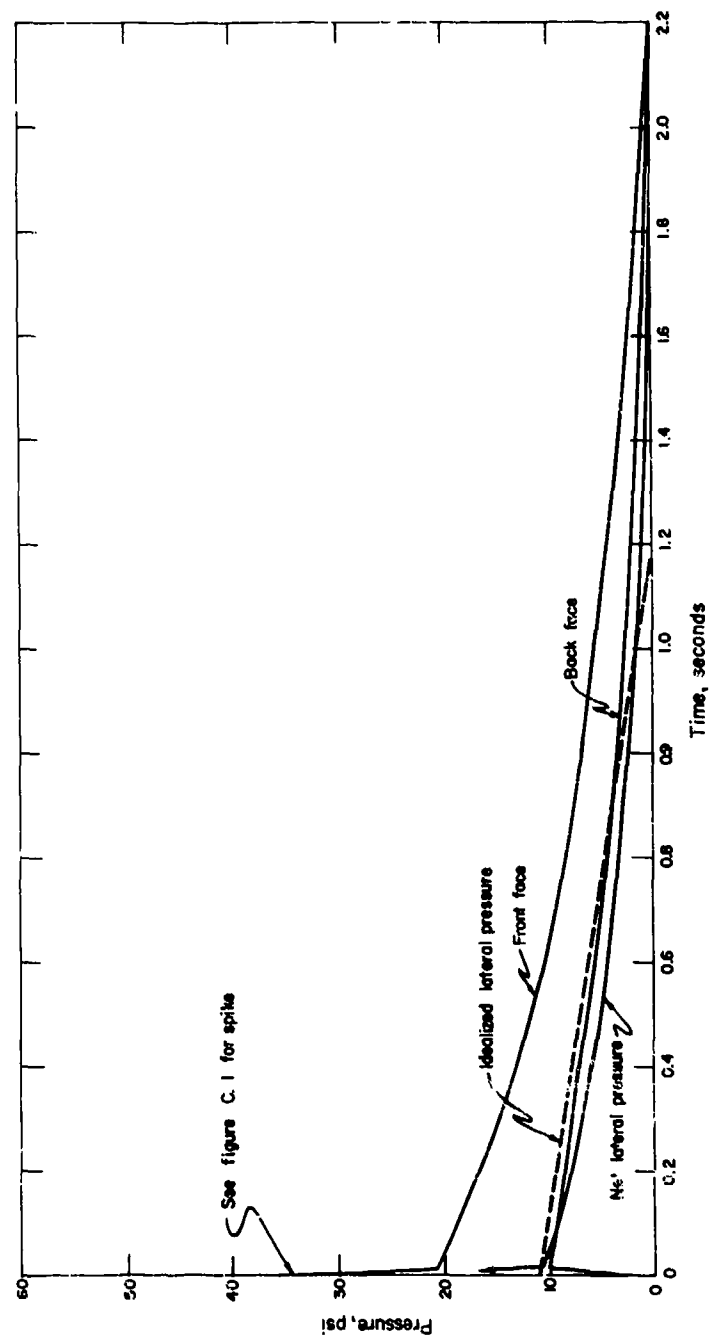


Figure C.10 Effective blast pressure on Station 20-F.

SECRET

162

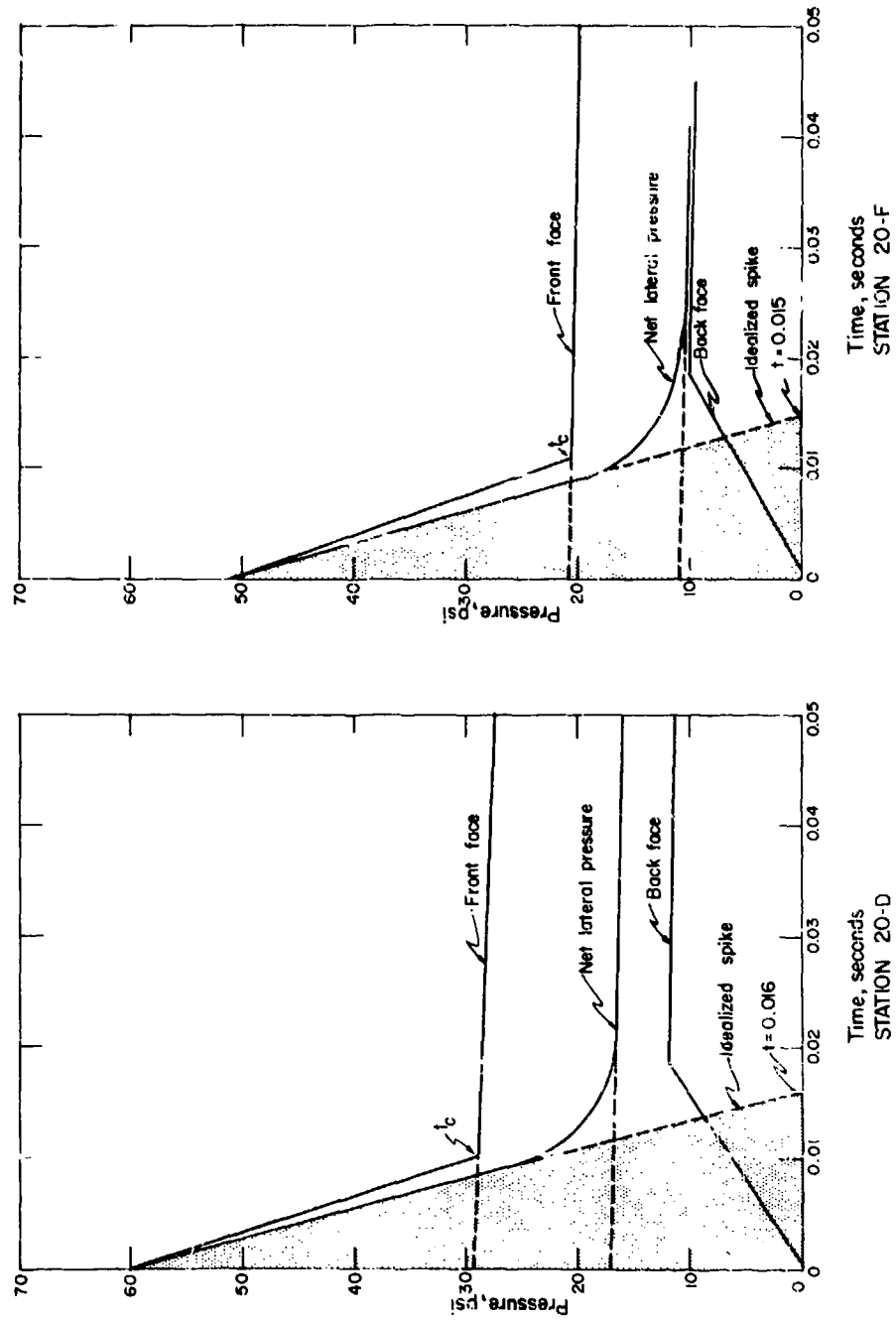


Figure C.1. Reflected pressures for Stations 20-D and 20-F.

$$r = w = 12.1 \text{ psi (Section C.2.3)}$$

$$\text{Then: } \sqrt{t/T_n} = \frac{0.016}{0.0366} = 0.437$$

$$\Delta u / \Delta y = \frac{1.062}{0.256} = 4.2$$

From Chart, Reference 22:

$$P_m/r = 2.4$$

$$P_m = 2.4(12.1) = 29 \text{ psi} < 61 \text{ psi}$$

Since the net predicted pressure to cause failure was 29 psi and the actual pressure was 61 psi, the beam should have failed from the spike load alone. Idealized lateral pressure (without the spike load):

$$t = 1.2 \text{ sec (Figure C.9)}$$

$$P = 17 \text{ psi (Figure C.9)}$$

$$\text{Then: } t/T_n = 33$$

$$\frac{\Delta u}{\Delta y} = 4.2$$

From Chart, Reference 22:

$$P_m/r = 0.9$$

$$P_m = 0.9 \times 12.1 = 10.9 \text{ psi} < 17 \text{ psi}$$

The pressure of 17 psi was sufficient to cause failure of the beam.

Station 20-F:

Spike alone:

$$t = 0.015 \text{ sec (Figure C.11)}$$

$$P = 51.0 \text{ psi (Figure C.11)}$$

then

$$t/T_n = 0.410$$

$$\frac{\Delta u}{\Delta y} = 4.2$$

From Chart, Reference 22:

$$P_m/r = 2.5$$

$$P_m = 2.5 \times 12.1 = 30.2 \text{ psi} < 51 \text{ psi}$$

Since the actual pressure was 51 psi the beam should have failed according to the above calculations; however, the beam did not fail.

Idealized lateral pressure:

$$t = 1.2 \text{ (Figure C.10)}$$

$$P = 11.0 \text{ psi (Figure C.10)}$$

then

$$t/T_n = 33$$

$$\frac{\Delta u}{\Delta y} = 4.2$$

From Chart, Reference 22:

$$P_m/r = 0.9$$

$$P_m = 0.9 \times 12.1 = 10.9 \text{ psi} < 11.0 \text{ psi}$$

The net predicted pressure of 11.0 psi and the minimum pressure of 10.9 psi to cause failure are very close, and it can be assumed that due to this loading the beam

was very close to failure.

C.4 DISCUSSION AND CONCLUSIONS

Even though the analysis was made assuming both the strength properties of the materials and the air-overpressure values for the two stations investigated, the predicted and the observed response are in fairly close agreement.

However, there exists a lack of data for use in determining reflected front-wall pressures as the angle of incidence deviates from zero. There is even less data concerning pressures on the rear faces of such structures. Shock-tube studies and/or high-explosive tests should be conducted to establish the relation of pressure on the front and back faces of diffraction targets at various angles of incidence.

If the spikes are neglected, the analysis predicts that Station 20-D would fail, which it did. The analysis for Station 20-F predicts that the pier was at the threshold of failure; however, the pier did not fail. The analysis predicts that both piers should fail from the spike loads alone.

It can be observed that the ultimate bending capacity of the beam under dynamic conditions is approximately four times greater than the bending capacity under standard design strength conditions.

For design purposes the method used was satisfactory; however, for analysis purposes refinement is needed.

C.5 NOTATIONS

a, depth of stress block in concrete at maximum load-carrying capacity

A_s , area of tension reinforcement

A'_s , area of compression reinforcement

b, width of rectangular flexure member

C, total compressive force in concrete

d, effective depth of beam which is the distance from the compression face of the concrete to the centroid of the tension steel

E_c , modulus of elasticity of concrete in the elastic region

E_0 , idealized slope of stress-strain curve for reinforcing steel in yield region

f_c , stress for concrete in compression

f'_c , ultimate compressive strength of concrete as determined by standard test cylinders

f'_{dc} , dynamic ultimate compressive strength of concrete

f_s , stress for steel in tension

f_y , yield point of steel in tension

f_{dy} , dynamic yield of steel

f_0 , defined in Figure C.1

I_y , moment of inertia of beam cross section transformed to concrete

j, ratio of distance (jd) between resultants of compressive and tensile stresses to effective depth

jd, lever arm of resisting couple

k' , a factor when multiplied by d gives the distance between tension and compression reinforcement

k , a factor when multiplied by d gives the distance from the compressive face to the neutral axis of transformed section (straight-line theory)
 K_1, K_2 , coefficients defining the magnitude and position of the internal compressive force in concrete
 k_c , ratio of maximum compressive strength of concrete in beam to compressive strength of standard test cylinders, f'_c
 M , any bending moment
 M_p , idealized bending moment
 M_s , bending moment for shear-compression mode
 M_u , bending moment at ultimate
 M_y , bending moment at yield point
 n , E_s/E_c , modular ratio
 p , A_s/bd
 p' , A'_s/bd
 P_m , maximum transit pressure the beam can withstand
 r , equivalent static resistance required in a member to resist imposed transient load
 s_b , allowable bearing unit stress
 t , duration of triangular force pulse
 T_1 , total tensile force in upper reinforcement
 T_2 , total tensile force in lower reinforcement
 T_n , natural period of vibration
 u , allowable bond stress per unit of surface area of bar
 v , allowable shearing unit stress
 V_b , shear governed by allowable bearing unit stress (S_b)
 V_t , shear governed by allowable shearing unit stress (v)
 V_u , shear governed by allowable bond stress (u)
 w , uniformly distributed load per unit of length of beam
 X , depth of neutral axis from edge of compression end
 Δ_u , maximum deflection at end of beam at ultimate
 Δ_y , maximum deflection at end of beam at yield
 ϵ_c , strain in concrete
 ϵ_{dy} , strain in steel at dynamic yield point
 ϵ_u , ultimate strain in concrete
 ϵ_s , strain in tensile reinforcement
 ϵ'_s , strain in compression reinforcement
 Σ_0 , sum of perimeters of bars
 ϕ_y , curvature of beam at yield point, in region of constant moment
 ϕ_u , curvature of beam at maximum load-carrying capacity, in region of constant moment.

Appendix D

WATER-WAVE DAMAGE

D.1 INTRODUCTION

Water waves (produced by surface or subsurface bursts) striking shore installations may cause serious damage to the components of such installations. There are many variables; the interrelationships involved in predicting damage from wave action are complex and not well understood at this time. The following discussion, in accordance with this project's objectives, is intended to point out certain salient features concerning wave damage in this operation. A much more comprehensive study devoted to water-wave terminal effects was made in Operation Hardtack by Project 50.1 (Reference 23) to provide more-adequate design data on wave run-up and overtopping of shore structures.

D.2 BACKGROUND

Shot Baker of Operation Crossroads caused waves which reached a maximum height of 7 feet on shore at a distance of about $3\frac{1}{2}$ miles from the target center. In the process of eroding the beach, the waves displaced large slabs of beach rock several feet; these slabs measured up to 9 by 5 by 1 foot in size, Reference 24.

Wave damage on shore had seldom been reported in detail; however, numerous photographs and observations were made by Holmes and Narver during Operation Castle (1954) and Operation Redwing (1956). See Section 1.2.1 concerning previous wave-damage surveys. The following summaries set forth some of the major wave damage.

D.2.1 Operation Castle. There were numerous instances of wave damage during Operation Castle, both at close-in stations and those at great distances. Shot geometries of Operation Castle are shown in Figures 1.1 and 1.2 for Bikini and Eniwetok, respectively. Table D.1 summarizes this damage. It should also be noted that at many close-in stations the entrances, on the lee side from the blast, were blocked by sand and debris left by the inundating wave.

D.2.2 Operation Redwing. In Operation Redwing there were fewer large surface shots on water and therefore much less wave damage than in Operation Castle. Shot geometries for Operation Redwing are shown in Figures 1.3 and 1.4. Only one close-in sta-

tion was observed, Station 1320, Site Dog, previously used in Operation Castle as Station 1210. In this operation, the protective mound of sand was covered by a layer of asphaltic mixture a few inches thick. Air blast and waves from Shots Flathead, Dakota, and Navajo broke up the asphaltic layer but only about 2 feet of cover was removed from the top of the station in the three events.

Shot Navajo was a good wave producer. At Site Nan, 15 miles away, there was no indication of any air-blast damage; however, the camp area was inundated causing considerable damage. Frame structures on the lagoon (DUKW repair shop, rigging loft, H&N Marine Department headquarters) were demolished. POL tanks were undermined and slightly moved; a small dynamite storage house was displaced 75 feet; some of the large latrines were displaced 10 to 15 feet; and there were numerous examples of lesser damage.

D.3 THEORY

Wave damage to shore installations according to Reference 8 may result from the following three effects: (1) impact and hydrostatic force; (2) drag force; and (3) inundation. Impact from a front of advancing water or a breaking wave, in addition to the hydrostatic pressure due to the depth of water, is sufficient to damage most onshore structures with the exception of hardened structures such as those which are built at the proving ground. Drag forces may displace medium sized structures or move relatively large objects into collision with a structure, thus causing damage. The third effect, inundation, is due to the long duration of blast-generated waves; the water may reach a considerable distance inland and large areas are covered with water for the period of time until the water recedes.

Generally speaking, it is not economically feasible to build protective sea walls so high that they will never be overtopped by waves. The wave phenomena are complex; however, experience at the proving ground has shown that adequate protection for test structures and facilities can be provided (see D.2.1 and D.2.2). Approximate maximum wave heights can be predicted from Reference 8. However, estimates based on Reference 8 are for constant depth of water, i.e., a bottom slope of zero. A more general treat-

TABLE D 1 OBSERVATIONS OF WAVE DAMAGE, OPERATION CASTLE

Description	Site	Shot	Code Name	Damage	Range, feet
Close-in Stations:					
Station 131: Reinforced-concrete gage pier, 12 feet long, 4 feet wide, and 4 feet deep.	George	4	Union	Pier exposed by erosion of sand.	15,430
		5	Yankee	Pier displaced approximately 100 feet.	15,660
Station 130.07: Reinforced-concrete gage pier, 4 by 4 by 4 feet.	George	4	Union	Pier exposed by erosion of sand.	15,430
		5	Yankee	Pier displaced approximately 500 feet.	15,500 *
Stations 1403.07 to 1403.14: Reinforced-concrete detector stations approximately 7 feet long, 5 feet wide, and 3 feet deep.	Dog	5	Yankee	All stations displaced considerable distances.	6,890
					7,100 *
					7,470
					7,700 *
					8,090
					8,280
Station 3.1: Reinforced-concrete submarine terminal pit (similar to Item 22, Chapter 4).	Charlie	2	Romeo	Protective mound washed away and footings undermined; left structure tilted.	8,980
					8,600 *
Station 3.2: Reinforced-concrete submarine terminal pit (similar to Item 22, Chapter 4).	Dog	4	Union	Protective mound eroded completely.	7,200 *
		5	Yankee	Completely destroyed; no traces left.	7,400 *
Station 3.3: Reinforced-concrete submarine terminal pit (similar to Item 22, Chapter 4).	George	4	Union	Protective mound severely eroded.	15,660
Station 1342: Reinforced-concrete, three-story instrument shelter, above ground unmounted (similar to Item 1, Chapter 3).	George	4	Union	Sand eroded from around foundation, very little undermining.	15,920
		5	Yankee		16,130
Station 101: Reinforced-concrete instrument shelter, mounded.	George	4	Union	Protective mound severely eroded.	15,680
Stations 1210, 1211: Large reinforced-concrete diagnostic station, mounded with approximately 10 feet of cover.	Dog	4	Union	Mounding partially eroded leaving corners of the building exposed.	6,900
		4	Union	Mounding completely eroded; water damage to equipment inside the station; water stood 24 inches deep inside.	6,900
Distant Sites:					
Station 70: Reinforced-concrete timing station.	Nan	5	Yankee	Water stood 2 inches deep inside the station.	84,050
Station 7400: Reinforced-concrete homing beacon shelter.	Nan	5	Yankee	Major damage to scientific equipment by 4 feet of water inside the station.	83,800 *
Tare Complex: Sites Obos, Peter, Roger, Sugar, Tare.	Tare Complex	2	Romeo	An 11-foot wave washed over the complex causing damage to causeways and protective berms; 500 feet of coaxial cable were exposed; one small structure was undermined and knocked out of alignment.	80,000 *
		4	Union	Causeways were seriously damaged; there was severe erosion around several structures.	59,000 *
Tare Complex: Sites Obos, Peter, Roger, Sugar, Tare.	Tare Complex	5	Yankee	Causeways washed out; one small unmounted concrete block house (5 by 7 ft high) was displaced approximately 400 feet.	59,200 *
Construction Camp:	Nan	4	Union	Water reached most of the camp area and caused damage to several of the light frame buildings.	83,000 *
		5	Yankee	Camp was wrecked.	83,000 *

* Approximately.

ment of wave-height prediction is given in Reference 23 where bottom slope, reefs, and shore lines at close-in ranges are all considered.

D.4 WAVE DAMAGE IN OPERATION HARDTACK

Wave damage in Operation Hardtack was not extensive. This was due to the relatively low yields of the shots and the care taken to prevent extensive damage from waves. The wave damage that occurred as reported in Chapters 3 and 4 will only be summarized here.

Close-in stations were affected as follows:

1. Station Redwing 560.01, Site Able (Item 2): a reinforced-concrete shelter surrounded by a circular, sandbagged berm 9 feet high. The water wave (and air blast) from Shot Fir passing over the island removed about 2 feet of earth from the berm.

2. Station Redwing 1519, Site Able (Item 4): a reinforced concrete photographic station approximately 24 feet long, 9 feet wide, and 7 feet high, weighing an estimated 50 tons was displaced approximately 11 feet by Shot Fir.

3. Station 78.01, Site Charlie (Item 5): a well-mounded timing station was undamaged but had its entrance blocked by sand and debris as a result of Shot Fir. This effect tended to be repeated in later events.

4. Station Complex, Site Irene (Item 18) and Station 1525 (Item 19): there was some deep erosion around these stations but no structural damage resulted.

5. Station 3.4, Site Irene (Item 22): a submarine terminal pit had nearly all of its protective mound eroded.

6. Station 1312, Site Janet (Item 25): a very large, unrounded, concrete structure was not damaged or undermined although some sand was eroded from around the foundation.

7. Landing pier, Site Janet (Item 30): several of its large 6-foot concrete cubes were washed on shore by waves from Shots Walnut and Elder. The pre-Yellowwood condition of the pier is shown in Figure 4.73; post-Walnut is shown in Figure 4.74; and the final state, post-Elder, is shown in Figure 4.75. This last figure also indicates the extent of inundation on Janet due to Shot Elder.

Distant sites received very little wave action. This was mainly due to firing the larger-yield shots at low tides and in shallow water. The only notable wave damage was at Site Elmer due to Shot Oak. The main damage was to the personnel pier and a pipeline discharging into the lagoon. One of the later waves from Shot Oak is shown striking the pier in Figure D.1. Damage could have been much more extensive if protective berms had not been placed around shore-side installations.

The protection offered by a sandbag berm is illustrated in Figures D.2, 3, 4, and 5. The equipment

shown in these figures was a vital link in the electrical distribution system for Sites Elmer and Fred.

D.5 DISCUSSION

Two facts observed in past operations at the proving grounds were once again demonstrated during Operation Hardtack:

1. Generally, close-in structures which survived air-blast effects received no appreciable damage from water waves; however, erosion was sometimes extensive.

2. Distant sites (several miles) suffered wave action from the larger-yield devices at ranges where air-blast damage was small or negligible.

Close-in structures which are designed to survive high blast pressures are not susceptible to wave damage since close-in air blast is much more severe than water-wave impact and drag forces. In designing for air blast, the prevention of flooding of a station during inundation should be considered. The only close-in effect from waves on large structures seems to be erosion and this only becomes a serious concern after several events, particularly when there is no opportunity between shots to replace protective cover.

As distance from ground zero increases, the peak overpressure attenuates very rapidly. For pressures in the range of 1 to 1,000 psi, pressure is inversely proportional to the $\frac{1}{3}$ power of range.

$$P \sim \frac{10 W^{2/3}}{R^{1/3}}$$

Where: P = peak side-on pressure, psi

W = yield, kilotons

R = range, kilofeet

Water waves, however, scale in a different fashion. For a wave moving in open water, the crest height (height above tide stage) is inversely proportional to the range. For shallow water conditions, the relationship of the variables can be expressed approximately by:

$$H_c \sim K \frac{W^{1/2} d^{1/2}}{R}$$

Where: H_c = crest height, feet

K = a constant generally less than 1

W = yield, kilotons

d = depth at surface zero, feet

R = range, kilofeet

The major characteristic of the blast-generated water waves that reach intermediate range and distant sites is their long period. The height of these waves is not large, in fact, storm waves are often higher. However, the long period of these waves causes water to continue to "pile up" at the shore



Figure D.1 Wave action at the personnel pier from Shot Oak, Site Elmer.



Figure D.2 Transformer station prior to wave arrival. Shot Oak, Site Elmer.



Figure D.3 Transformer station, first wave striking the lagoon shore. Shot Oak, Site Elmer.

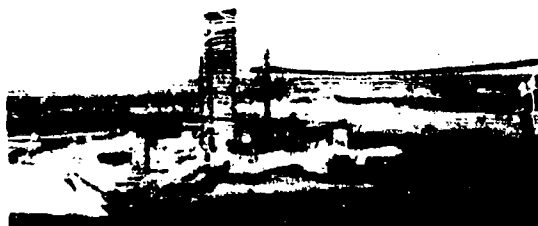


Figure D.4 Transformer station, first wave moving onshore; the start of inundation. Shot Oak, Site Elmer.

line so that water runs inland to great distances. Protective works can dissipate much of the energy of the water on shore but flooding of large land areas cannot be prevented.

works offer reasonably adequate protection against impact and drag effects by dissipating wave energy. The long period of blast-generated waves makes protection from inundation very difficult. Inundation and



Figure D.5 Transformer station after wave action ceased and water subsided. Shot Oak, Site Elmer.

D.6 CONCLUSIONS AND RECOMMENDATIONS

Structural effects due to water waves may be neglected for close-in structures designed to withstand air blast.

At greater distances, where air blast is of no great consequence, water waves must be considered in structural planning. The standard shore-protection

flooding that cannot be prevented may be provided for in design of facilities by waterproofing vital equipment and by making doors seal tightly. One structural feature that has shown its usefulness is the provision of proper drainage for a station, i.e., eliminating sunken floors and sills that trap water, and having floors slope toward the entrance, so that any water that gets into the station can be readily drained out.

REFERENCES

1. J. S. Archer and E. A. Lawlor; "Damage Survey and Analysis of Structures"; Operation Ivy, WT--641, June 1954; Massachusetts Institute of Technology, Cambridge, Massachusetts; Secret Restricted Data.
2. W. J. Christensen; "Blast Effects on Miscellaneous Structures"; Project 3.5, Operation Castle, WT-901, July 1955; Armed Forces Special Weapons Project, Washington 25, D. C.; Secret Formerly Restricted Data.
3. J. J. Meszaros and C. N. Kingery; "Ground Surface Air Pressure Versus Distance from High Yield Detonations"; Project 1.2b, Operation Castle, WT-905, May 1957, page 46; Ballistics Research Laboratories, Aberdeen Proving Ground, Maryland; Secret Formerly Restricted Data.
4. C. D. Broyles; "Blast Measurements on a Medium-Yield Surface Burst"; Project 1.2, Operation Redwing, WT-1302, January 1960; Sandia Corporation, Albuquerque, New Mexico; Secret Formerly Restricted Data.
5. L. M. Swift, D. C. Sachs, and F. M. Sauer; "Ground Acceleration, Stress, and Strain at High Incident Overpressures"; Project 1.4, Operation Plumbbob, WT-1404, May 1960; Stanford Research Institute, Menlo Park, California; Secret Formerly Restricted Data.
6. J. W. Wistor and W. R. Perret; "Ground Motion Studies at High Incident Overpressure"; Project 1.5, Operation Plumbbob, ITR-1405, October 1957; Sandia Corporation, Albuquerque, New Mexico; Confidential Formerly Restricted Data.
7. W. J. Flathau, R. A. Breckenridge, and C. K. Wiehle; "Blast Loading and Response of Underground Concrete-Arch Protective Structures"; Project 3.1, Operation Plumbbob, WT-1420, June 1959; U. S. Army Engineer Waterways Experiment Station, Corps of Engineers, Vicksburg, Mississippi, and U. S. Naval Civil Engineering Laboratory, Port Hueneme, California; Confidential.
8. "Capabilities of Atomic Weapons"; TM 23-200, November 1957; Armed Forces Special Weapons Project, Washington, D. C.; Confidential.
9. "Scientific Director's Report of Atomic Weapon Tests at Eniwetok, 1951"; Annex 3.1, U. S. Army Structures, Appendix 11, Operation Greenhouse, WT-118, August 1957; Unclassified.
10. N. E. Kingsley and H. K. Gilbert; "Summary Report of the Commander, Task Unit 13"; Operation Castle, WT-934, January 1959; Field Command, Armed Forces Special Weapons Project, Albuquerque, New Mexico; Secret Restricted Data.
11. K. D. Coleman; "Summary Report of the Commander, Task Unit 3"; Operation Redwing, ITR-1344, November 1956; Field Command, Armed Forces Special Weapons Project, Albuquerque, New Mexico; Secret Restricted Data.
12. J. J. Meszaros and others; "Air-Blast Phenomena and Instrumentation of Structures"; Project 1.7, Operation Hardtack, ITR-1612-1, August 1958; Ballistics Research Laboratories, Aberdeen Proving Ground, Maryland; Secret Formerly Restricted Data.
13. L. M. Swift and others; "Ground Motion Produced by Nuclear Detonations"; Project 1.8, Operation Hardtack, ITR-1613, August 1958; Stanford Research Institute, Menlo Park, California; Secret Formerly Restricted Data.

14. "The Nuclear Radiation Handbook, 1957"; Armed Forces Special Weapons Project, Washington, D. C.; Secret.
15. F. S. Kirn, R. J. Kennedy, and H. O. Wyckoff; "The Attenuation of Gamma Rays at Oblique Incidence"; Radiology, Volume 63 No. 1, pages 99 - 104, July 1954.
16. G. S. Hurst, and R. H. Ritchie; "Radiation Dosimetry for Human Exposures"; Project 39.5, Operation Plumbbob, WT-1504, March 1958; Oak Ridge National Laboratory, Oak Ridge, Tennessee; Secret Restricted Data.
17. "U. S. Defense Study"; CDG Project Nr 373; United States Army Engineer School, Fort Belvoir, Virginia; Secret.
18. C. H. Norris, et al.; "Structural Design for Dynamic Loads"; 1959; McGraw-Hill Book Co., Inc., New York, New York; Unclassified.
19. "Building Code Requirements for Reinforced Concrete"; 1951; American Concrete Institute, Detroit, Michigan; Unclassified.
20. J. R. Gaston, C. P. Sless, and N. M. Newmark; "An Investigation of the Load-Deformation Characteristics of the Reinforced Concrete Beams Up to the Point of Failure"; Contract N6onr-07134, 1952; University of Illinois, Urbana, Illinois; Unclassified.
21. W. T. Thomson; "Mechanical Vibrations"; page 218; Second Edition, 1954; Prentice-Hall, Inc., New York, N. Y.; Unclassified.
22. J. L. Merritt and N. M. Newmark; "Design of Underground Structures to Resist Nuclear Blast"; page 87; Contract DA-49-129-eng-312, 1958; University of Illinois, Urbana, Illinois; Unclassified.
23. L. W. Kidd; "Special Study of Wave Terminal Effects"; Project 50.1, Operation Hardtack, WT-1638; Scripps Institution of Oceanography, La Jolla, California; Secret.
24. "Effects of Nuclear Weapons"; 1957; United States Department of Defense; Washington, D. C.; Unclassified.

DISTRIBUTION

Military Distribution Categories 28 and 32

ARMY ACTIVITIES		
1	Deputy Chief of Staff for Military Operations, D/A, Washington 25, D.C. ATTN: Dir. of SWAR	49- 50
2	Chief of Research and Development, D/A, Washington 25, D.C. ATTN: Atomic Div.	51- 52
3	Assistant Chief of Staff, Intelligence, D/A, Washington 25, D.C.	53- 54
4- 5	The Quartermaster General, D/A, Washington 25, D.C. ATTN: Research and Dev.	55
6- 7	Chief Chemical Officer, D/A, Washington 25, D.C.	56
8	Chief of Engineers, D/A, Washington 25, D.C. ATTN: ENGRS	57
9	Chief of Engineers, D/A, Washington 25, D.C. ATTN: ENGRS	58- 59
10	Chief of Engineers, D/A, Washington 25, D.C. ATTN: ENGRS	60
11- 12	Office, Chief of Ordnance, D/A, Washington 25, D.C. ATTN: ORDN	61
13	Chief Signal Officer, D/A, Research and Development Div., Washington 25, D.C. ATTN: SIGRD-4	62
14	Chief of Transportation, D/A, Office of Planning and Int., Washington 25, D.C.	63
15- 16	The Surgeon General, D/A, Washington 25, D.C. ATTN: MEDIC	64
17- 19	Commanding General, U.S. Continental Army Command, Ft. Monro, Va.	65
20	Director of Special Weapons Development Office, Headquarters COMAR, Ft. Bliss, Tex. ATTN: Capt. Chester I. Peterson	66
21	President, U.S. Army Artillery Board, Ft. Sill, Okla.	67
22	President, U.S. Army Infantry Board, Ft. Benning, Ga.	68
23	President, U.S. Army Air Defense Board, Ft. Bliss, Tex.	69
24	President, U.S. Army Aviation Board, Ft. Rucker, Ala. ATTN: ATBO-DC	70
25	Commanding General, First United States Army, Governor's Island, New York 4, N.Y.	71
26	Commanding General, Second U.S. Army, Ft. George G. Meade, Md.	72
27	Commanding General, Third United States Army, Ft. McPherson, Ga. ATTN: ACORF G-3	73
28	Commanding General, Fourth United States Army, Ft. Sam Houston, Tex. ATTN: G-3 Section	74
29	Commanding General, Fifth United States Army, 1660 E. Hyde Park Blvd., Chicago 15, Ill.	75
30	Commanding General, Sixth United States Army, Presidio of San Francisco, San Francisco, Calif. ATTN: AMOCT-4	76
31	Commandant, U.S. Army Command & General Staff College, Ft. Leavenworth, Kansas. ATTN: ARCHIVES	77
32	Commandant, U.S. Army Air Defense School, Ft. Bliss, Tex. ATTN: Command & Staff Dept.	
33	Commandant, U.S. Army Armored School, Ft. Knox, Ky.	
34	Commandant, U.S. Army Artillery and Missile School, Ft. Sill, Okla. ATTN: Combat Development Department	
35	Commandant, U.S. Army Aviation School, Ft. Rucker, Ala.	
36	Commandant, U.S. Army Infantry School, Ft. Benning, Ga. ATTN: C.D.S.	
37	The Superintendent, U.S. Military Academy, West Point, N.Y. ATTN: Prof. of Ordnance	
38	Commandant, The Quartermaster School U.S. Army, Ft. Lee, Va. ATTN: Chief, QM Library	
39	Commanding General, Chemical Corps Training Comd., Ft. McClellan, Ala.	
40	Commandant, USA Signal School, Ft. Monmouth, N.J.	
41	Commandant, USA Transport School, Ft. Eustis, Va. ATTN: Security and Info. Off.	
42	Commanding General, The Engineer Center, Ft. Belvoir, Va. ATTN: Asst. Chd., Engr. School	
43	Commanding General, Army Medical Service School, Brooke Army Medical Center, Ft. Sam Houston, Tex.	
44	Director, Armed Forces Institute of Pathology, Walter Reed Army Med. Center, 625 16th St., NW, Washington 25, D.C.	
45	Commanding Officer, U.S. Army Research Lab., Ft. Knox, Ky.	
46	Commandant, Walter Reed Army Inst. of Res., Walter Reed Army Medical Center, Washington 25, D.C.	
47- 48	Commanding General, QM R&D Comd., QM R&D Cntr., Natick, Mass. ATTN: CBR Liaison Officer	
	Commanding General, Qm. Research and Engr. Comd., USA, Natick, Mass.	
	Commanding General, U.S. Army Chemical Corps, Research and Development Comd., Washington 25, D.C.	
	Commanding Officer, Chemical Warfare Lab., Army Chemical Center, Md. ATTN: Tech. Library	
	Commanding General, Engineer Research and Dev. Lab., Ft. Belvoir, Va. ATTN: Chief, Tech. Support Branch	
	Director, Waterways Experiment Station, P.O. Box 631, Vicksburg, Miss. ATTN: Library	
	Commanding Officer, Diamond Ord. Fuse Labs., Washington 25, D.C. ATTN: Chief, Nuclear Vulnerability Br. (230)	
	Commanding General, Aberdeen Proving Grounds, Md. ATTN: Director, Ballistics Research Laboratory	
	Commanding Officer, Ord. Materials Research Off., Watertown Arsenal, Watertown 72, Mass. ATTN: Mr. Foster	
	Commanding General, Ordnance Tank Automotive Command, Detroit Arsenal, Centerline, Mich. ATTN: ORDMC-RO	
	Commanding General, Ordnance Ammunition Command, Joliet, Ill.	
	Commanding Officer, USA Signal R&D Laboratory, Ft. Monmouth, N.J.	
	Commanding General, U.S. Army Electronic Proving Ground, Ft. Huachuca, Ariz. ATTN: Tech. Library	
	Commanding General, USA Combat Surveillance Agency, 1124 W. Highland St., Arlington, Va.	
	Commanding Officer, USA, Signal R&D Laboratory, Ft. Monmouth, N.J. ATTN: Tech. Doc. Ctr., Evans Area	
	Commanding Officer, USA Transportation Combat Development Group, Ft. Rustis, Va.	
	Director, Operations Research Office, Johns Hopkins University, 6935 Arlington Rd., Bethesda 14, Md.	
	Commandant, U.S. Army Chemical Corps, CBR Weapons School, Dugway Proving Ground, Dugway, Utah.	
	Commander-in-Chief, U.S. Army Europe, APO 403, New York, N.Y. ATTN: Opt. Div., Weapons Br.	
	Commanding General, Southern European Task Force, APO 168, New York, N.Y. ATTN: ACORF G-3	
	Commanding General, Eighth U.S. Army, APO 301, San Francisco, Calif. ATTN: ACORF G-3	
	Commanding General, U.S. Army Alaska, APO 949, Seattle, Washington	
	Commanding General, U.S. Army Caribbean, Ft. Amador, Canal Zone. ATTN: Cal Office	
	Commander-in-Chief, U.S. Army Pacific, APO 976, San Francisco, Calif. ATTN: Ordnance Officer	
	Commanding General, USARFANT & MDP, Ft. Brooke, Puerto Rico	
	Commanding Officer, 9th Hospital Center, APO 180, New York, N.Y. ATTN: CO, US Army Nuclear Medicine Research Detachment, Europe	
NAVY ACTIVITIES		
78	Chief of Naval Operations, D/N, Washington 25, D.C. ATTN: OP-0380	
79	Chief of Naval Operations, D/N, Washington 25, D.C. ATTN: OP-0380	
80	Chief of Naval Operations, D/N, Washington 25, D.C. ATTN: OP-0380	
81	Chief of Naval Personnel, D/N, Washington 25, D.C.	
82- 83	Chief of Naval Research, D/N, Washington 25, D.C. ATTN: Code 811	
84	Chief, Bureau of Naval Weapons, D/N, Washington 25, D.C. ATTN: DLI-3	
85	Chief, Bureau of Medicine and Surgery, D/N, Washington 25, D.C. ATTN: Special Wms. Def. Div.	
86	Chief, Bureau of Ordnance, D/N, Washington 25, D.C.	
87	Chief, Bureau of Ships, D/N, Washington 25, D.C. ATTN: Code 423	
88	Chief, Bureau of Yards and Docks, D/N, Washington 25, D.C. ATTN: D-440	

SECRET

- 89 Director, U.S. Naval Research Laboratory, Washington 25, D.C. ATTN: Mrs. Katherine E. Cass
- 90-91 Commander, U.S. Naval Ordnance Laboratory, White Oak, Silver Spring 19, Md.
- 92 Director, Material Lab. (Code 900), New York Naval Shipyard, Brooklyn 1, N.Y.
- 93-96 Commanding Officer, U.S. Naval Radiological Defense Laboratory, San Francisco, Calif. ATTN: Tech. Info. Div.
- 97-98 Commanding Officer and Director, U.S. Naval Civil Engineering Laboratory, Port Hueneme, Calif. ATTN: Code L31
- 99 Superintendent, U.S. Naval Academy, Annapolis, Md.
- 100 Commanding Officer, U.S. Naval Schools Command, U.S. Naval Station, Treasure Island, San Francisco, Calif.
- 101 Superintendent, U.S. Naval Postgraduate School, Monterey, Calif.
- 102 Officer-in-Charge, U.S. Naval School, CEC Officers, U.S. Naval Construction Bn. Center, Port Hueneme, Calif.
- 103 Commanding Officer, Nuclear Weapons Training Center, Atlantic, U.S. Naval Base, Norfolk 11, Va. ATTN: Nuclear Warfare Dept.
- 104 Commanding Officer, Nuclear Weapons Training Center, Pacific, Naval Station, San Diego, Calif.
- 105 Commanding Officer, U.S. Naval Damage Control Tug. Center, Naval Base, Philadelphia 12, Pa. ATTN: ABC Defense Course
- 106 Commanding Officer, U.S. Naval Air Development Center, Johnsville, Pa. ATTN: NAS, Librarian
- 107 Commanding Officer, U.S. Naval Medical Research Institute, National Naval Medical Center, Bethesda, Md.
- 108 Commander, U.S. Naval Ordnance Test Station, China Lake, Calif.
- 109 Commanding Officer and Director, David W. Taylor Model Basin, Washington 7, D.C. ATTN: Library
- 110 Officer-in-Charge, U.S. Naval Supply Research and Development Facility, Naval Supply Center, Rayonne, N.J.
- 111 Commander, Norfolk Naval Shipyard, Portsmouth, Va. ATTN: Underwater Explosions Research Division
- 112 Commander-in-Chief, U.S. Atlantic Fleet, U.S. Naval Base, Norfolk 11, Va.
- 113 Commandant, U.S. Marine Corps, Washington 25, D.C. ATTN: Code A03H
- 114 Director, Marine Corps Landing Force, Development Center, MCB, Quantico, Va.
- 115 Chief, Bureau of Ships, D/N, Washington 25, D.C. ATTN: Code 372
- 116 Commanding Officer, U.S. Naval CIC School, U.S. Naval Air Station, Glynnco, Brunswick, Ga.
- 117 Chief of Naval Operations, Department of the Navy, Washington 25, D.C. ATTN: OP-02B5
- 118 Chief, Bureau of Naval Weapons, Navy Department, Washington 25, D.C. ATTN: WR12
- 119 Commander-in-Chief, U.S. Pacific Fleet, Fleet Post Office, San Francisco, Calif.
- AIR FORCE ACTIVITIES**
- 120 Deputy Chief of Staff, Operations, HQ USAF, Washington 25, D.C. ATTN: AFOP
- 121 HQ USAF, ATTN: Operations Analysis Office, Office, Vice Chief of Staff, Washington 25, D.C.
- 122 Director of Civil Engineering, HQ USAF, Washington 25, D.C. ATTN: AFOP-ES
- 123-133 Air Force Intelligence Center, HQ USAF, ACSI (AFICM-371) Washington 25, D.C.
- 134 Director of Research and Development, DCS/D, HQ USAF, Washington 25, D.C. ATTN: Guidance and Weapons Div.
- 135 The Surgeon General, HQ USAF, Washington 25, D.C. ATTN: Bio-Def. Pre. Med. Division
- 136 Commander, Tactical Air Command, Langley AFB, Va. ATTN: Doc. Security Branch
- 137 Commander, Air Defense Command, Ent AFB, Colorado. ATTN: Assistant for Atomic Energy, ADMC-A
- 138 Commander, HQ Air Research and Development Command, Andrews AFB, Washington 25, D.C. ATTN: SEMA
- 139 Commander, Air Force Ballistic Missile Div. HQ ARCC, Air Force Unit Post Office, Los Angeles 45, Calif. ATTN: MDSOT
- 140-141 Commander, AF Cambridge Research Center, L. G. Hanscom Field, Bedford, Mass. ATTN: CMST-2
- 142-146 Commander, Air Force Special Weapons Center, Kirtland AFB, Albuquerque, N. Mex. ATTN: Tech. Info. & Intel. Div.
- 147-148 Director, Air University Library, Maxwell AFB, Ala.
- 149 Commander, Lowry Technical Training Center (TW), Lowry AFB, Denver, Colorado.
- 150 Commandant, School of Aviation Medicine, USAF Aerospace Medical Center (ATC), Brooks Air Force Base, Tex. ATTN: Col. Garritt L. Hekhuis
- 151 Commander, 1009th Sp. Wpn. Squadron, HQ USAF, Washington 25, D.C.
- 152-154 Commander, Wright Air Development Center, Wright-Patterson AFB, Dayton, Ohio. ATTN: WCACT (For WCOSI)
- 155-156 Director, USAF Project RAND, VIA: USAF Liaison Office, The RAND Corp., 1700 Main St., Santa Monica, Calif.
- 157 Commander, Rome Air Development Center, ARDC, Griffiss AFB, N.Y. ATTN: Documents Library, RCBEL-1
- 158 Commander, Air Technical Intelligence Center, USAF, Wright-Patterson AFB, Ohio. ATTN: APCIN-HSLA, Library
- 159 Headquarters, 1st Missile Div., USAF, Vandenberg AFB, Calif. ATTN: Operations Analysis Office
- 160 Assistant Chief of Staff, Intelligence, HQ USAF, APO 953, New York, N.Y. ATTN: Directorate of Air Targets
- 161 Commander, Alaskan Air Command, APO 942, Seattle, Washington. ATTN: AAOV
- 162 Commander-in-Chief, Pacific Air Forces, APO 953, San Francisco, Calif. ATTN: PFCIN-PS, Base Recovery
- OTHER DEPARTMENT OF DEFENSE ACTIVITIES**
- 163 Director of Defense Research and Engineering, Washington 25, D.C. ATTN: Tech. Library
- 164 Chairman, Armed Services Explosives Safety Board, DOD, Building T-7, Gravelly Point, Washington 25, D.C.
- 165 Director, Weapons Systems Evaluation Group, Room 1E880, The Pentagon, Washington 25, D.C.
- 166 Commandant, The Industrial College of The Armed Forces, Ft. McMeir, Washington 25, D.C.
- 167 Commandant, Armed Forces Staff College, Norfolk 11, Va. ATTN: Library
- 168-171 Chief, Defense Atomic Support Agency, Washington 25, D.C. ATTN: Document Library
- 172 Commander, Field Command, DASA, Sandia Base, Albuquerque, N. Mex.
- 173 Commander, Field Command, DASA, Sandia Base. ATTN: FCMV
- 174-175 Commander, Field Command, DASA, Sandia Base, Albuquerque, N. Mex. ATTN: FCMV
- 176 Commander, JTF-7, Arlington Hall Station, Arlington 12, Va.
- 177 Administrator, National Aeronautics and Space Administration, 1200 "H" St., N.W., Washington 25, D.C. ATTN: Mr. R. V. Rhoads
- 178 Commander-in-Chief, Strategic Air Command, Offutt AFB, Neb. ATTN: OAMS
- 179 Commandant, US Coast Guard, 1300 E. St., F.W., Washington 25, D.C. ATTN: Cdr. B. E. Kolhorst
- 180 Commander-in-Chief, EUCOM, APO 128, New York, N.Y.
- 181 Commander-in-Chief, Pacific, c/o Fleet Post Office, San Francisco, Calif.
- 182 U.S. Documents Officer, Office of the United States National Military Representative - SHAPE, APO 35, New York, N.Y.
- ATOMIC ENERGY COMMISSION ACTIVITIES**
- 183-185 U.S. Atomic Energy Commission, Technical Library, Washington 25, D.C. ATTN: For IMA
- 186-187 Los Alamos Scientific Laboratory, Report Library, P.O. Box 1663, Los Alamos, N. Mex. ATTN: Helen Redman
- 188-192 Sandia Corporation, Classified Document Division, Sandia Base, Albuquerque, N. Mex. ATTN: H. J. Smyth, Jr.
- 193-202 University of California Lawrence Radiation Laboratory, P.O. Box 808, Livermore, Calif. ATTN: Clevio G. Craig
- 203 Weapon Data Section, Office of Technical Information Extension, Oak Ridge, Tenn.
- 204-235 Office of Technical Information Extension, Oak Ridge, Tenn. (Surplus)



Defense Special Weapons Agency
6801 Telegraph Road
Alexandria, Virginia 22310-3398

TRC

27 August 1998

MEMORANDUM TO DEFENSE TECHNICAL INFORMATION CENTER
ATTN: OCQ/Mr William Bush

SUBJECT: CLASSIFICATION CHANGES

The Defense Special Weapons Agency Security Office has reviewed and declassified the following documents and distribution statement A now applies:

WT-1631, AD-355505
WT-1619, AD-357951

Also WT-1619-EX should be withdrawn from the system.

Also WT-1637, AD-339275, has been downgraded to Confidential FRD.

Arldith Jarrett

ARDITH JARRETT
Chief, Technical Resource Center